

Sum rules for semi-leptonic $b \rightarrow c$ and $b \rightarrow u$ decays: accuracy checks and implications

Wen-Feng Duan,^a Syuhei Iguro,^{b,c,d} Xin-Qiang Li,^{a,e,1} Ryoutaro Watanabe,^{a,2}
and Ya-Dong Yang^{a,f}

^a*Institute of Particle Physics and Key Laboratory of Quark and Lepton Physics (MOE),
Central China Normal University, Wuhan, Hubei 430079, China*

^b*Institute for Advanced Research, Nagoya University, Nagoya 464-8601, Japan*

^c*Kobayashi-Maskawa Institute for the Origin of Particles and the Universe, Nagoya Uni-
versity, Nagoya 464-8601, Japan*

^d*KEK Theory Center, IPNS, KEK, Tsukuba 305-0801, Japan*

^e*Center for High Energy Physics, Peking University, Beijing 100871, China*

^f*Institute of Particle and Nuclear Physics, Henan Normal University, Xinxiang 453007,
China*

*E-mail: dufewe@mails.ccnu.edu.cn, igurosyuhei@gmail.com,
xqli@mail.ccnu.edu.cn, watanabe@ccnu.edu.cn, yangyd@ccnu.edu.cn*

ABSTRACT: The semi-leptonic $b \rightarrow c\ell\nu$ processes are receiving a lot of attention, as the lepton flavor universality (LFU) violation has been hinted by the measured ratios $R_{D^{(*)}} = \Gamma(B \rightarrow D^{(*)}\tau\nu)/\Gamma(B \rightarrow D^{(*)}\ell\nu)$ for $\ell = e, \mu$. Recently, it has also been pointed out that the baryonic counterpart, $R_{\Lambda_c} = \Gamma(\Lambda_b \rightarrow \Lambda_c\tau\nu)/\Gamma(\Lambda_b \rightarrow \Lambda_c\ell\nu)$, has a strong correlation with $R_{D^{(*)}}$, referred to as the R ratio sum rule in this paper. The correlation is almost independent of the new physics (NP) contributions and hence can predict R_{Λ_c} from the measured $R_{D^{(*)}}$. On the other hand, we have fewer measurements and/or theoretical studies of the semi-leptonic $b \rightarrow u\ell\nu$ processes, although the same arguments can be applied to the ratios R_π , R_ρ , and R_p as above. Since these processes are measurable at the ongoing LHCb run-3 and/or Belle II experiments, precise studies on them are important as well. In this paper, we obtain the semi-analytic formulae for all the aforementioned R_X ratios in the presence of model-independent NP contributions by using the available lattice QCD and/or light-cone sum rule fits to the form factors. Two novel points are highlighted: (i) We evaluate uncertainties of R_X including both the Standard Model (SM) and NP terms, inherited from the form factor fits, and discuss how the uncertainties affect the R ratio sum rules. (ii) We obtain the R ratio sum rule among the semi-leptonic $b \rightarrow u\ell\nu$ processes for the first time, which provides a complementary motivation for observing these processes. In addition, based on our model-independent results, we investigate how the different NP scenarios work in the $b \rightarrow c$ and $b \rightarrow u$ sectors and perform a combined study in the framework of SM effective field theory with specific flavor symmetries.

¹Corresponding author.

²Corresponding author.

Contents

1	Introduction	2
2	Sum rule formulae	5
2.1	General formula	5
2.2	Sum rule utility: a first look	6
3	Uncertainties from the form factor inputs	8
3.1	Decay rate descriptions	8
3.2	$B \rightarrow D$, $B \rightarrow D^*$, and $\Lambda_b \rightarrow \Lambda_c$ form factors	11
3.3	$B \rightarrow \pi$, $B \rightarrow \rho$, and $\Lambda_b \rightarrow p$ form factors	16
3.4	Numerical results	20
4	Phenomenological implications	23
4.1	The $b \rightarrow c$ mode	23
4.1.1	Sum rule predictions and shift factor	23
4.1.2	Relations to $R_{J/\psi}$ and R_{X_c}	24
4.2	The $b \rightarrow u$ mode	26
4.2.1	Correlations among R_X in the presence of NP	27
4.2.2	Sum rule predictions and shift factor	29
4.3	Combined study: SMEFT explanation	31
4.3.1	Brief description of SMEFT and $U(3)^5$ symmetry	31
4.3.2	Application to the semi-leptonic $b \rightarrow ql\nu$ processes	32
4.3.3	Third generation-philic interaction and $U(2)^5$ symmetry	34
4.3.4	Numerical analysis	36
5	Summary	38
A	Flavor symmetries for the semi-leptonic decays	40
A.1	MFV hypothesis	40
A.2	Third generation-philic flavor structure	42
B	Covariance tables for our results	45

1 Introduction

Testing the flavor structure of the Standard Model (SM) of particle physics has been performed with tremendous efforts since the CLEO, LEP, Tevatron, Belle, and BaBar experiments were established, and then it has been taken over by the LHCb and Belle II experiments with the advantage of higher luminosities. In particular, the determinations of the Cabibbo-Kobayashi-Maskawa (CKM) matrix elements $|V_{ub}|$ and $|V_{cb}|$ have been a significant task, as they are of fundamental importance for establishing the flavor structure of the SM. They have been studied in the semi-leptonic decays of bottom-flavored hadrons, and it is expected that some rare decays can also be used to test the flavor structure at the ongoing LHCb run-3 [1, 2] and Belle II [3, 4] experiments. The current status regarding these decays contains rich implications for both the precision tests of the SM and the indirect probes of new physics (NP) beyond the SM [5–9].

Regarding the semi-leptonic B -meson decays mediated by the quark-level $b \rightarrow c\ell\nu$ transition with $l = e, \mu, \tau$, we have the following observations:

- The exclusive processes $B \rightarrow D^{(*)}\ell\nu$ for $\ell = e, \mu$ have been measured to extract $|V_{cb}|$ by the Belle [10–12], Belle II [13] and BaBar [14, 15] collaborations. The experimental average is presently given as $|V_{cb}|^{\text{ex}} = (39.8 \pm 0.6) \times 10^{-3}$ [16], although it relies on the modeling of the $B \rightarrow D^{(*)}$ transition form factors. This value is then compared with $|V_{cb}|^{\text{in}} = (42.2 \pm 0.5) \times 10^{-3}$ [16] extracted from the inclusive $B \rightarrow X_c\ell\nu$ decays, which is analyzed based on the heavy quark expansion. Thus, we see a 3σ discrepancy between the values extracted with these two methods; see Refs. [9, 17] for a recent review.
- The semi-tauonic counterparts, $B \rightarrow D^{(*)}\tau\nu$, have been analyzed by using the ratios defined by $R_{D^{(*)}} = \Gamma(B \rightarrow D^{(*)}\tau\nu)/\Gamma(B \rightarrow D^{(*)}\ell\nu)$, so that their dependence on the CKM matrix element V_{cb} is cancelled out and the uncertainties due to the $B \rightarrow D^{(*)}$ transition form factors are reduced to a large extent. Thus, these ratios can be used to test the lepton flavor universality (LFU) of the SM. They have been measured by Belle [18–22], BaBar [23, 24], LHCb (*i.e.*, run-1 [25–29] and run-2 [30]), and Belle II [31] collaborations. The latest world average is reported in Ref. [32] as $R_D^{\text{exp}} = 0.342 \pm 0.026$ and $R_{D^*}^{\text{exp}} = 0.287 \pm 0.012$. A complementary probe of the LFU to $R_{D^{(*)}}$ can be seen in the inclusive ratio of $R_{X_c} = \Gamma(B \rightarrow X_c\tau\nu)/\Gamma(B \rightarrow X_c\ell\nu)$ [33], which has been recently measured by the Belle II experiment with $R_{X_c}^{\text{exp}} = 0.228 \pm 0.039$ [34].

On the other hand, we have the following situation for the $b \rightarrow u\ell\nu$ semi-leptonic B -meson decays:

- The exclusive $B \rightarrow \pi\ell\nu$ and inclusive $B \rightarrow X_u\ell\nu$ processes have been measured to obtain $|V_{ub}|$. The present official status is summarized as $|V_{ub}|^{\text{ex}} = (3.70 \pm$

$0.10 \pm 0.12) \times 10^{-3}$ and $|V_{ub}|^{\text{in}} = (4.13 \pm 0.12 \pm 0.13 \pm 0.18) \times 10^{-3}$ [16], consistent with each other within 2σ . A more recent measurement of $B^0 \rightarrow \pi^- \ell^+ \nu$ from Belle II [35] reduces the deviation in $|V_{ub}|$ to be within 1σ level. Although the other exclusive processes of $B \rightarrow \rho \ell \nu$ and $B \rightarrow \omega \ell \nu$ have been observed [35, 36] and theoretical studies for the $|V_{ub}|^{\text{ex}}$ extraction are available in Refs. [37, 38], it has not yet been included in the official world average [16, 36]. Notice that we have to rely on the light-cone sum rule (LCSR) calculations for the $B \rightarrow \rho, \omega$ form factors and the narrow-width approximation for the $|V_{ub}|^{\text{ex}}$ extraction, which results in lower values of $|V_{ub}|$ [37, 38].

- The semi-tauonic process $B \rightarrow \pi \tau \nu$ was first measured by the Belle collaboration [39], with a branching ratio of $\mathcal{B}(\bar{B}^0 \rightarrow \pi^+ \tau^- \nu) < 2.5 \times 10^{-4}$ at 90% confidence level (CL), or equivalently $\mathcal{B}(\bar{B}^0 \rightarrow \pi^+ \tau^- \nu) = (1.52 \pm 0.72 \pm 0.13) \times 10^{-4}$. Taking $\mathcal{B}(\bar{B}^0 \rightarrow \pi^+ \ell^- \nu) = (1.50 \pm 0.06) \times 10^{-4}$ [36], we find a value of $R_\pi^{\text{exp}} = \Gamma(B \rightarrow \pi \tau \nu) / \Gamma(B \rightarrow \pi \ell \nu) \approx 1.01 \pm 0.49$. On the other hand, the $B \rightarrow \rho \tau \nu$ and $B \rightarrow \omega \tau \nu$ decays have not been measured yet, but are expected to be measurable at the LHCb run-3 [1, 2] and Belle II [3, 4] experiments.

We also have other interesting processes relevant for $b \rightarrow (c, u) l \nu$, such as the semi-leptonic Λ_b and B_c decays. Their status can be summarized as below.

- The baryonic processes $\Lambda_b \rightarrow \Lambda_c \mu \nu$ and $\Lambda_b \rightarrow \Lambda_c \tau \nu$ have been measured by the DELPHI [40] and LHCb [41] collaborations, respectively. The latter also reports $R_{\Lambda_c}^{\text{exp}} = \Gamma(\Lambda_b \rightarrow \Lambda_c \tau \nu) / \Gamma(\Lambda_b \rightarrow \Lambda_c \mu \nu) = 0.242 \pm 0.026 \pm 0.040 \pm 0.059$. Normalizing the LHCb measurement to the SM prediction for $\Gamma(\Lambda_b \rightarrow \Lambda_c \mu \nu)$ instead of the DELPHI measurement, a modestly increased value of $R_{\Lambda_c}^{\text{exp}} = (0.04/|V_{cb}|)^2 (0.285 \pm 0.073)$ would be obtained [42]. Regarding $b \rightarrow u \mu \nu$, Ref. [43] observed $\Lambda_b \rightarrow p \mu \nu$ in terms of the ratio to $\Lambda_b \rightarrow \Lambda_c \mu \nu$ for limited q^2 ranges, with q^2 being the invariant mass squared of the lepton-neutrino system. It also gives a measurement of $|V_{ub}/V_{cb}| = 0.083 \pm 0.004 \pm 0.004$ and $\mathcal{B}(\Lambda_b \rightarrow p \mu \nu) = (4.1 \pm 1.0) \times 10^{-4}$ by extrapolating to the full q^2 range. However, the semi-tauonic mode $\Lambda_b \rightarrow p \tau \nu$ has not been measured yet.
- The semi-leptonic $B_c \rightarrow J/\psi l \nu$ decays arise from the same quark-level $b \rightarrow c l \nu$ transition as in the $B \rightarrow D^{(*)} l \nu$ and $\Lambda_b \rightarrow \Lambda_c l \nu$ processes, and thus they are on the same playground as R_D , R_{D^*} and R_{Λ_c} . Recently, the τ/μ ratio has been observed by the LHCb [44] and CMS [45, 46] collaborations, although these measurements are still plagued by large uncertainties. A naive average is given as $R_{J/\psi}^{\text{exp}} = \Gamma(B_c \rightarrow J/\psi \tau \nu) / \Gamma(B_c \rightarrow J/\psi \mu \nu) = 0.61 \pm 0.18$ [47].

As a matter of fact, both the electronic and muonic processes are used to extract the CKM matrix elements, in which the LFU between the first two generations is always assumed. On the other hand, as the experimental measurements have shown some

discrepancies from the SM predictions in the ratios $R_{D^{(*)}}$ since 2012, many theoretical studies have paid attention to NP possibilities in the tauonic modes, which will also be supposed in this paper. In this case, the ratios R_X/R_X^{SM} can be considered as optimal observables for testing the LFU, where R_X^{SM} stands for the SM prediction and R_X indicates both the SM and NP contributions in the tauonic processes.

Combining all these developments, the authors of Refs. [48–50] have found one significant relation among R_D , R_{D^*} and R_{Λ_c} . In particular,

$$\frac{R_{\Lambda_c}}{R_{\Lambda_c}^{\text{SM}}} \simeq 0.280 \frac{R_D}{R_D^{\text{SM}}} + 0.720 \frac{R_{D^*}}{R_{D^*}^{\text{SM}}}, \quad (1.1)$$

is obtained in the recent study of Ref. [50], which will be referred to as the R ratio sum rule in this paper. As pointed out in Ref. [50], this relation holds unless the NP contribution is large beyond the current bounds. Thus, it gives a complementary check for the experimental results of the R_X measurements, almost independent of the theoretical predictions. In case the three experimental measurements of R_D , R_{D^*} and R_{Λ_c} do not follow Eq. (1.1), it would imply that some of these measurements are questionable. Therefore, the R ratio sum rule gives a crucial feedback to the experimental measurements. This is an absolutely novel point, which cannot be provided by the individual R_X study.

Theoretical analyses of R_X and the R ratio sum rules rely on the modelling of the hadronic matrix elements for $b \rightarrow c$ and $b \rightarrow u$ transitions. Thus, it is crucial to see how Eq. (1.1) would be affected when theoretical uncertainties from the form factor inputs are taken into account. In this paper, we summarize the recent developments of the relevant form factors, and evaluate possible uncertainties on the R_X formulae and the R ratio sum rules, inherited from these inputs. With our updated numerical results, we then discuss whether the R ratio sum rule is predictable and usable for the consistency check among the three measurements. It should be especially noted that we obtain the R ratio sum rule in $b \rightarrow ul\nu$ decays for the first time. We also show the relations to the other observables, such as the inclusive ratio R_{X_c} and the semi-leptonic B_c decay ratio $R_{J/\psi}$. Based on our model-independent results, we also investigate how the different NP scenarios work in the $b \rightarrow cl\nu$ and $b \rightarrow ul\nu$ transitions, and perform a combined study of these processes in the framework of SM effective field theory (SMEFT) [51–54] with specific flavor symmetries [55, 56].

This paper is organized as follows. In Sec. 2, we will present the general formulae for R_X and our procedure to get the R ratio sum rules. Then, the recent form factor inputs are summarized, and the impacts of their uncertainties on R_X and the R ratio sum rules are discussed in Sec. 3. Phenomenological implications of the R ratio sum rules are discussed in Sec. 4, and then specific flavor structures are considered for a combined study in the SMEFT. Finally, our conclusion is made in Sec. 5. For convenience, details of the specific flavor symmetries we are considering are relegated in App. A, and the covariance tables for our results are presented in App. B.

2 Sum rule formulae

We describe the most general NP contributions to the quark-level $b \rightarrow ql\nu$ transitions for $q = c, u$ and $l = e, \mu, \tau$ in terms of the effective weak Hamiltonian,

$$\mathcal{H}_{\text{eff}} = 2\sqrt{2}G_F V_{qb} \left[\left(1 + C_{V_L}^{ql}\right) \mathcal{O}_{V_L}^{ql} + C_{V_R}^{ql} \mathcal{O}_{V_R}^{ql} + C_{S_L}^{ql} \mathcal{O}_{S_L}^{ql} + C_{S_R}^{ql} \mathcal{O}_{S_R}^{ql} + C_T^{ql} \mathcal{O}_T^{ql} \right], \quad (2.1)$$

with the four-fermion operators of our interest given by

$$\begin{aligned} \mathcal{O}_{V_L}^{ql} &= (\bar{q}\gamma^\mu P_L b)(\bar{l}\gamma_\mu P_L \nu_l), & \mathcal{O}_{V_R}^{ql} &= (\bar{q}\gamma^\mu P_R b)(\bar{l}\gamma_\mu P_L \nu_l), \\ \mathcal{O}_{S_L}^{ql} &= (\bar{q}P_L b)(\bar{l}P_L \nu_l), & \mathcal{O}_{S_R}^{ql} &= (\bar{q}P_R b)(\bar{l}P_L \nu_l), \\ \mathcal{O}_T^{ql} &= (\bar{q}\sigma^{\mu\nu} P_L b)(\bar{l}\sigma_{\mu\nu} P_L \nu_l), \end{aligned} \quad (2.2)$$

where $P_L = (1 - \gamma_5)/2$ and $P_R = (1 + \gamma_5)/2$. The NP contributions are encoded in the short-distance Wilson coefficients (WCs) C_i^{ql} with $i = V_L, V_R, S_L, S_R, T$, which have been normalized by the SM factor of $2\sqrt{2}G_F V_{qb}$. As stated in Sec. 1, we assume that the electronic and muonic processes are described by the SM, namely $C_i^{qe} = C_i^{q\mu} = 0$. It is also assumed that the light neutrino is always left-handed for simplicity. The case with right-handed neutrinos can be found, *e.g.*, in Refs. [57–62].

2.1 General formula

Depending on the spin properties of the hadrons involved in the semi-leptonic decays, we have specific forms of R_X in terms of the WCs $C_i^{q\tau}$ for each NP effective operator. Explicitly, we can obtain the following general formulae:

$$\begin{aligned} \frac{R_P}{R_P^{\text{SM}}} &= |1 + C_{V_L}^{q\tau} + C_{V_R}^{q\tau}|^2 + a_P^{SS} |C_{S_L}^{q\tau} + C_{S_R}^{q\tau}|^2 + a_P^{TT} |C_T^{q\tau}|^2 \\ &+ a_P^{VS} \text{Re} \left[(1 + C_{V_L}^{q\tau} + C_{V_R}^{q\tau}) (C_{S_L}^{q\tau*} + C_{S_R}^{q\tau*}) \right] + a_P^{VT} \text{Re} \left[(1 + C_{V_L}^{q\tau} + C_{V_R}^{q\tau}) C_T^{q\tau*} \right], \end{aligned} \quad (2.3)$$

$$\begin{aligned} \frac{R_V}{R_V^{\text{SM}}} &= |1 + C_{V_L}^{q\tau}|^2 + |C_{V_R}^{q\tau}|^2 + a_V^{SS} |C_{S_L}^{q\tau} - C_{S_R}^{q\tau}|^2 + a_V^{TT} |C_T^{q\tau}|^2 \\ &+ a_V^{V_L V_R} \text{Re} \left[(1 + C_{V_L}^{q\tau}) C_{V_R}^{q\tau*} \right] + a_V^{VS} \text{Re} \left[(1 + C_{V_L}^{q\tau} - C_{V_R}^{q\tau}) (C_{S_L}^{q\tau*} - C_{S_R}^{q\tau*}) \right] \\ &+ a_V^{V_L T} \text{Re} \left[(1 + C_{V_L}^{q\tau}) C_T^{q\tau*} \right] + a_V^{V_R T} \text{Re} \left[C_{V_R}^{q\tau} C_T^{q\tau*} \right], \end{aligned} \quad (2.4)$$

$$\begin{aligned} \frac{R_H}{R_H^{\text{SM}}} &= |1 + C_{V_L}^{q\tau}|^2 + |C_{V_R}^{q\tau}|^2 + a_H^{SS} [|C_{S_L}^{q\tau}|^2 + |C_{S_R}^{q\tau}|^2] + a_H^{TT} |C_T^{q\tau}|^2 \\ &+ a_H^{V_L V_R} \text{Re} \left[(1 + C_{V_L}^{q\tau}) C_{V_R}^{q\tau*} \right] + a_H^{S_1} \text{Re} \left[(1 + C_{V_L}^{q\tau}) C_{S_L}^{q\tau*} + C_{V_R}^{q\tau} C_{S_R}^{q\tau*} \right] \\ &+ a_H^{S_2} \text{Re} \left[(1 + C_{V_L}^{q\tau}) C_{S_R}^{q\tau*} + C_{V_R}^{q\tau} C_{S_L}^{q\tau*} \right] + a_H^{S_L S_R} \text{Re} \left[C_{S_L}^{q\tau} C_{S_R}^{q\tau*} \right] \\ &+ a_H^{V_L T} \text{Re} \left[(1 + C_{V_L}^{q\tau}) C_T^{q\tau*} \right] + a_H^{V_R T} \text{Re} \left[C_{V_R}^{q\tau} C_T^{q\tau*} \right], \end{aligned} \quad (2.5)$$

where $(P, V, H) = (D, D^*, \Lambda_c)$ for $q = c$ and $(P, V, H) = (\pi, \rho, p)$ for $q = u$. For each hadronic final state X , a_X^{ij} is denoted as the numerical coefficient associated with the product of the WCs, where ij represents the NP current structure of the corresponding term. Since some of these NP structures give identical coefficients, we have introduced the following abbreviations such that

$$\begin{aligned} a_P^{VS} &\equiv a_P^{V_L S_L} = a_P^{V_L S_R} = a_P^{V_R S_L} = a_P^{V_R S_R}, & a_P^{VT} &\equiv a_P^{V_L T} = a_P^{V_R T}, \\ a_V^{VS} &\equiv a_V^{V_L S_L} = -a_V^{V_L S_R} = -a_V^{V_R S_L} = a_V^{V_R S_R}, & & \\ a_H^{VS_1} &\equiv a_H^{V_L S_L} = a_H^{V_R S_R}, & a_H^{VS_2} &\equiv a_H^{V_L S_R} = a_H^{V_R S_L}, \end{aligned} \quad (2.6)$$

in Eqs. (2.3)–(2.5). In the next section, we will introduce our setup with a summary of the commonly adopted parametrizations of the form factors together with the latest fitting parameters, and obtain the numerical coefficients a_X^{ij} with uncertainties inherited from the form factor inputs. Then, we find that Eqs. (2.3)–(2.5) can be combined into a single relation

$$\frac{R_H}{R_H^{\text{SM}}} = b \frac{R_P}{R_P^{\text{SM}}} + c \frac{R_V}{R_V^{\text{SM}}} + \delta_H. \quad (2.7)$$

Here δ_H is some function of the WCs $C_i^{q\tau}$, and the two coefficients b and c are not unique but can be determined by setting a desired condition so that δ_H becomes small. In this paper, we follow Ref. [50] and set

$$b + c = 1, \quad a_P^{VS} b + a_V^{VS} c = a_H^{VS_1}, \quad (2.8)$$

so that the terms $|1 + C_{V_L}^{q\tau}|^2$ and $\text{Re}[(1 + C_{V_L}^{q\tau})C_{S_L}^{q\tau*}]$ in Eq. (2.7) vanish, respectively. The other terms are all contained in δ_H that would shift the R ratio sum rule if it is not negligible. For convenience, we call it the shift factor for the R ratio sum rule throughout this paper.

2.2 Sum rule utility: a first look

Before showing details on the form factor inputs and evaluating the resulting uncertainties of the R ratio sum rules, let us firstly summarize the current situation at the central values of the theoretical inputs. For the $b \rightarrow c$ case, we obtain

$$\frac{R_{\Lambda_c}}{R_{\Lambda_c}^{\text{SM}}} = 0.272 \frac{R_D}{R_D^{\text{SM}}} + 0.728 \frac{R_{D^*}}{R_{D^*}^{\text{SM}}} + \delta_{\Lambda_c}, \quad (2.9)$$

with

$$\begin{aligned} \delta_{\Lambda_c} = & -0.001 (|C_{S_L}^{c\tau}|^2 + |C_{S_R}^{c\tau}|^2) - 0.007 \text{Re} (C_{S_L}^{c\tau} C_{S_R}^{c\tau*}) - 2.681 |C_T^{c\tau}|^2 \\ & + \text{Re} [(1 + C_{V_L}^{c\tau}) (0.041 C_{V_R}^{c\tau*} + 0.594 C_T^{c\tau*})] - 0.561 \text{Re} (C_{V_R}^{c\tau} C_T^{c\tau*}) \\ & - 0.002 \text{Re} [(1 + C_{V_L}^{c\tau}) C_{S_R}^{c\tau*} + C_{S_L}^{c\tau} C_{V_R}^{c\tau*}]. \end{aligned} \quad (2.10)$$

This is consistent with the previous study where $C_{V_R}^{c\tau}$ has been omitted in Ref. [50].¹ One can observe potentially large contributions from the terms $\text{Re}[(1 + C_{V_L}^{c\tau}) C_T^{c\tau*}]$, $\text{Re}(C_{V_R}^{c\tau} C_T^{c\tau*})$ and $|C_T^{c\tau}|^2$, while all the other terms are completely negligible even for $|C_i^{c\tau}| \sim \mathcal{O}(1)$. Their effects can be further checked by looking at the collider bounds on $C_i^{c\tau}$ through the analysis of the $\tau + \text{missing}$ searches at ATLAS and CMS, as demonstrated in Refs. [65, 66]. It has turned out that the allowed range depends on the mediator mass, which is given as [65]

$$|C_T^{c\tau}| \lesssim 0.3 - 0.2, \quad (2.11)$$

for the tensor-type interaction, where 0.3 corresponds to a t -channel NP mediator with mass of 2 TeV and 0.2 indicates an effective-field-theory-limit case. Given the above bound, we find that the R ratio sum rule could be shifted by $\delta_{\Lambda_c} \approx -0.4 - -0.2$ at most. If this were the case, such a shift factor would be not negligible.

On the other hand, if we try to find a NP solution to the R_D and R_{D^*} anomalies by the tensor-type interaction, the best-fit point to the current experimental data is obtained as $C_T^{c\tau} \approx 0.02 \pm i0.13$ [47]. Taking this fit point as input leads to $\delta_{\Lambda_c} \approx -0.035$, which is sufficiently smaller than the current experimental resolutions for the R_X measurements, especially for the ratio R_{Λ_c} [41, 42]. Thus, the current situation of the $R_{D^{(*)}}$ anomalies tells us that the R ratio sum rule should be satisfied without the shift factor δ_{Λ_c} . The world average of the $R_{D^{(*)}}$ measurements, reported by the Heavy Flavor Averaging Group (HFLAV) for Moriond 2024 [32], reads

$$R_D^{\text{exp}} = 0.342 \pm 0.026, \quad R_{D^*}^{\text{exp}} = 0.287 \pm 0.012. \quad (2.12)$$

If we take the R ratio sum rule by neglecting the small shift factor δ_{Λ_c} that has been verified by the above discussion, we may *predict* a value of R_{Λ_c} from Eq. (2.9) as

$$R_{\Lambda_c}^{\text{SR}} = 0.372 \pm 0.017, \quad (2.13)$$

where R_X^{SM} is presented in Eq. (3.85), as we will evaluate later, and Eq. (2.12) is taken. This should be compared with the current LHCb measurement [41]

$$R_{\Lambda_c}^{\text{LHCb}} = 0.242 \pm 0.076. \quad (2.14)$$

Therefore, the R ratio sum rule looks violated for the moment, implying that

$$\delta_{\Lambda_c}^{\text{SR/LHCb}} = -0.39 \pm 0.23. \quad (2.15)$$

¹ The reason for omitting $C_{V_R}^{c\tau}$ is motivated by the observation that the LFU violating operator $\mathcal{O}_{V_R}^{ql}$ is firstly generated by the $SU(2)_L \otimes U(1)_Y$ invariant operators at dimension eight, and thus the corresponding WC $C_{V_R}^{cl}$ will have an additional suppression compared with that of the other operators generated from the dimension-six operators [63, 64].

This is, however, inconsistent with the shift of $\delta_{\Lambda_c} \approx -0.035$ (indicated by the $R_{D^{(*)}}$ best-fit point as demonstrated above) beyond the above error. We will get back to this point once we take the form factor uncertainties into account.

For the $b \rightarrow u$ case, we collect the recent updates for the form factor inputs (which will be detailed in the next section), and then obtain for the first time the following R ratio sum rule:

$$\frac{R_p}{R_p^{\text{SM}}} = 0.284 \frac{R_\pi}{R_\pi^{\text{SM}}} + 0.716 \frac{R_\rho}{R_\rho^{\text{SM}}} + \delta_p, \quad (2.16)$$

with

$$\begin{aligned} \delta_p = & -0.090 (|C_{S_L}^{u\tau}|^2 + |C_{S_R}^{u\tau}|^2) - 0.185 \text{Re} [C_{S_L}^{u\tau} C_{S_R}^{u\tau*}] - 0.913 |C_T^{u\tau}|^2 \\ & + \text{Re} [(1 + C_{V_L}^{u\tau}) (0.169 C_{V_R}^{u\tau*} + 0.370 C_T^{u\tau*})] - 0.203 \text{Re} (C_{V_R}^{u\tau} C_T^{u\tau*}) \\ & - 0.079 \text{Re} [(1 + C_{V_L}^{u\tau}) C_{S_R}^{u\tau*} + C_{S_L}^{u\tau} C_{V_R}^{u\tau*}]. \end{aligned} \quad (2.17)$$

From Eqs. (2.10) and (2.17), we see that the suppression of the numerical factors in δ_p is milder than those in δ_{Λ_c} for the scalar and vector terms. On the other hand, the terms involving the tensor contribution in δ_p are more suppressed than those in δ_{Λ_c} . Note that, to obtain the numerical coefficients involving $C_T^{u\tau}$, we need a prescription for the $\Lambda_b \rightarrow p$ tensor form factors, as will be discussed in the next section.

The collider bound on $|C_T^{u\tau}|$ obtained in Ref. [65] is roughly of $|C_T^{u\tau}| \lesssim 0.4$, which is rather milder than on $C_T^{c\tau}$. This is based on the observation that the net effect due to V_{ub} suppression and parton-distribution-function enhancement of $b\bar{u} \rightarrow \tau^-\bar{\nu}$, compared with the $b\bar{c} \rightarrow \tau^-\bar{\nu}$ case, results in a reduction of the production rate and hence less statistics of the process $pp \rightarrow \tau^\pm + \text{missing}$ from $b\bar{u} \rightarrow \tau^-\bar{\nu}$. Therefore, we obtain a milder upper bound on the NP contribution, and a shift factor of $\delta_p \approx -0.29$ may be possible for the moment. In any case, the R ratio sum rule provides us with a good motivation for measuring the semi-tauonic decays of $B \rightarrow \pi\tau\nu$, $B \rightarrow \rho\tau\nu$ and $\Lambda_b \rightarrow p\tau\nu$ at the ongoing LHCb run-3 [1, 2] and/or Belle II [3, 4] experiments.

3 Uncertainties from the form factor inputs

The numerical coefficients a_X^{ij} in Eqs. (2.3)–(2.5) rely on the form factor inputs that can be evaluated by several theoretical methods, such as the lattice QCD calculations and the LCSR evaluations. Our numerical results for a_X^{ij} will be shown in Sec. 3.4, but here we begin with summarizing recent developments on the form factor evaluations, and then give the explicit inputs we will use in our analysis.

3.1 Decay rate descriptions

Let us start with providing a general description for the decay rates of the semi-leptonic $B \rightarrow Pl\nu$, $B \rightarrow Vl\nu$, and $\Lambda_b \rightarrow Hl\nu$ processes for $P = (D, \pi)$, $V = (D^*, \rho)$,

and $H = (\Lambda_c, p)$ [37, 67–77]. By taking the usual notations of

$$N_B \equiv \frac{G_F^2 |V_{qb}|^2}{192\pi^3 m_B^3} \sqrt{Q_+^X Q_-^X} \left(1 - \frac{m_l^2}{q^2}\right)^2, \quad Q_\pm^X \equiv (m_B \pm m_X)^2 - q^2, \quad (3.1)$$

with q^2 being the invariant mass squared of the lepton-neutrino system and X the final-state hadron, we obtain the formulae for the differential decay rates as follows.

- For $B \rightarrow Pl\nu$ decays,

$$\begin{aligned} \frac{d\Gamma(B \rightarrow Pl\nu)}{dq^2} = \frac{N_B}{2} & \left\{ |1 + C_{V_L}^{ql} + C_{V_R}^{ql}|^2 [(2q^2 + m_l^2) (H_{V_+}^P)^2 + 3m_l^2 (H_{V_0}^P)^2] \right. \\ & + 3|C_{S_L}^{ql} + C_{S_R}^{ql}|^2 q^2 (H_S^P)^2 + 16|C_T^{ql}|^2 (q^2 + 2m_l^2) (H_T^P)^2 \\ & + 6\text{Re} \left[(1 + C_{V_L}^{ql} + C_{V_R}^{ql})(C_{S_L}^{ql*} + C_{S_R}^{ql*}) \right] m_l \sqrt{q^2} H_{V_0}^P H_S^P \\ & \left. - 24\text{Re} \left[(1 + C_{V_L}^{ql} + C_{V_R}^{ql}) C_T^{ql*} \right] m_l \sqrt{q^2} H_{V_+}^P H_T^P \right\}, \quad (3.2) \end{aligned}$$

with the helicity amplitudes given by

$$H_{V_+}^P \equiv \frac{\sqrt{Q_+^P Q_-^P}}{\sqrt{q^2}} f_+^P(q^2), \quad H_{V_0}^P \equiv \frac{m_B^2 - m_P^2}{\sqrt{q^2}} f_0^P(q^2), \quad (3.3)$$

$$H_S^P \equiv \frac{m_B^2 - m_P^2}{m_b - m_q} f_0^P(q^2), \quad H_T^P \equiv -\frac{\sqrt{Q_+^P Q_-^P}}{m_B + m_P} f_T^P(q^2), \quad (3.4)$$

where $f_{+,0}^P$ and f_T^P are the $B \rightarrow P$ transition form factors for the vector and tensor currents, respectively. Here we follow their definitions as given in Refs. [69, 73, 78].

- For $B \rightarrow Vl\nu$ decays,

$$\begin{aligned} \frac{d\Gamma(B \rightarrow Vl\nu)}{dq^2} = \frac{N_B}{2} & \left\{ (|1 + C_{V_L}^{ql}|^2 + |C_{V_R}^{ql}|^2) [(2q^2 + m_l^2) ((H_{V_+}^V)^2 + (H_{V_-}^V)^2 \right. \\ & + (H_{V_0}^V)^2) + 3m_l^2 (H_{V_t}^V)^2] + 3|C_{S_L}^{ql} - C_{S_R}^{ql}|^2 q^2 (H_S^V)^2 \\ & + 16|C_T^{ql}|^2 (q^2 + 2m_l^2) ((H_{T_+}^V)^2 + (H_{T_-}^V)^2 + (H_{T_0}^V)^2) \\ & - 2\text{Re} \left[(1 + C_{V_L}^{ql}) C_{V_R}^{ql*} \right] [(2q^2 + m_l^2) (2H_{V_+}^V H_{V_-}^V + (H_{V_0}^V)^2) + 3m_l^2 (H_{V_t}^V)^2] \\ & - 6\text{Re} \left[(1 + C_{V_L}^{ql} - C_{V_R}^{ql})(C_{S_L}^{ql*} - C_{S_R}^{ql*}) \right] m_l \sqrt{q^2} H_{V_t}^V H_S^V \\ & \left. - 24\text{Re} \left[(1 + C_{V_L}^{ql}) C_T^{ql*} \right] m_l \sqrt{q^2} (H_{T_0}^V H_{V_0}^V + H_{T_+}^V H_{V_+}^V - H_{T_-}^V H_{V_-}^V) \right\} \end{aligned}$$

$$+ 24\text{Re} \left[C_{V_R}^{ql} C_T^{ql*} \right] m_l \sqrt{q^2} \left(H_{T_0}^V H_{V_0}^V + H_{T_+}^V H_{V_-}^V - H_{T_-}^V H_{V_+}^V \right) \Big\}, \quad (3.5)$$

with the helicity amplitudes given by

$$H_{V_\pm}^V \equiv (m_B + m_V) A_1^V(q^2) \mp \frac{\sqrt{Q_+^V Q_-^V}}{m_B + m_V} V^V(q^2), \quad (3.6)$$

$$H_{V_0}^V \equiv \frac{m_B + m_V}{2m_V \sqrt{q^2}} \left[\frac{Q_+^V Q_-^V}{(m_B + m_V)^2} A_2^V(q^2) - (m_B^2 - m_V^2 - q^2) A_1^V(q^2) \right], \quad (3.7)$$

$$H_{V_t}^V \equiv -\frac{\sqrt{Q_+^V Q_-^V}}{\sqrt{q^2}} A_0^V(q^2), \quad H_S^V \equiv -\frac{\sqrt{Q_+^V Q_-^V}}{m_b + m_q} A_0^V(q^2), \quad (3.8)$$

$$H_{T_\pm}^V \equiv \frac{1}{\sqrt{q^2}} \left[\sqrt{Q_+^V Q_-^V} T_1^V(q^2) \pm (m_B^2 - m_V^2) T_2^V(q^2) \right], \quad (3.9)$$

$$H_{T_0}^V \equiv \frac{1}{2m_V} \left[-(m_B^2 + 3m_V^2 - q^2) T_2^V(q^2) + \frac{Q_+^V Q_-^V}{m_B^2 - m_V^2} T_3^V(q^2) \right], \quad (3.10)$$

where V^V , $A_{0,1,2}^V$, and $T_{1,2,3}^V$ are the $B \rightarrow V$ transition form factors for the vector, axial-vector, and tensor currents, respectively. We refer to Refs. [69, 79, 80] for their explicit definitions.

- For $\Lambda_b \rightarrow H l \nu$ decays,

$$\begin{aligned} \frac{d\Gamma(\Lambda_b \rightarrow H l \nu)}{dq^2} &= \frac{N_{\Lambda_b}}{4} \left\{ \left(|1 + C_{V_L}^{ql}|^2 + |C_{V_R}^{ql}|^2 \right) \left[(m_l^2 + 2q^2) \left((H_{V_+}^{H+})^2 \right. \right. \right. \\ &\quad \left. \left. \left. + (H_{V_+}^{H-})^2 + 2(H_{V_\perp}^{H+})^2 + 2(H_{V_\perp}^{H-})^2 \right) + 3m_l^2 \left((H_{V_0}^{H+})^2 + (H_{V_0}^{H-})^2 \right) \right] \right. \\ &\quad \left. + 3q^2 \left[|C_{S_L}^{ql} H_S^{H+} + C_{S_R}^{ql} H_S^{H-}|^2 + |C_{S_L}^{ql} H_S^{H-} + C_{S_R}^{ql} H_S^{H+}|^2 \right] \right. \\ &\quad \left. + 16|C_T^{ql}|^2 (q^2 + 2m_l^2) \left((H_{T_+}^{H+})^2 + (H_{T_+}^{H-})^2 + 2(H_{T_\perp}^{H+})^2 + 2(H_{T_\perp}^{H-})^2 \right) \right. \\ &\quad \left. + 4\text{Re} \left[(1 + C_{V_L}^{ql}) C_{V_R}^{ql*} \right] \left[(m_l^2 + 2q^2) \left(H_{V_+}^{H+} H_{V_+}^{H-} + 2H_{V_\perp}^{H+} H_{V_\perp}^{H-} \right) \right. \right. \\ &\quad \left. \left. + 3m_l^2 H_{V_0}^{H+} H_{V_0}^{H-} \right] + 6\text{Re} \left[(1 + C_{V_L}^{ql}) C_{S_L}^{ql*} + C_{V_R}^{ql} C_{S_R}^{ql*} \right] m_l \sqrt{q^2} \right. \\ &\quad \left. \times \left(H_{V_0}^{H+} H_S^{H+} + H_{V_0}^{H-} H_S^{H-} \right) + 6\text{Re} \left[(1 + C_{V_L}^{ql}) C_{S_R}^{ql*} + C_{V_R}^{ql} C_{S_L}^{ql*} \right] \right. \\ &\quad \left. \times m_l \sqrt{q^2} \left(H_{V_0}^{H+} H_S^{H-} + H_{V_0}^{H-} H_S^{H+} \right) + 24\text{Re} \left[(1 + C_{V_L}^{ql}) C_T^{ql*} \right] m_l \sqrt{q^2} \right. \\ &\quad \left. \times \left(H_{V_+}^{H+} H_{T_+}^{H+} + H_{V_+}^{H-} H_{T_+}^{H-} + 2H_{V_\perp}^{H+} H_{T_\perp}^{H+} + 2H_{V_\perp}^{H-} H_{T_\perp}^{H-} \right) + 24\text{Re} \left[C_{V_R}^{ql} C_T^{ql*} \right] \right. \\ &\quad \left. \times m_l \sqrt{q^2} \left(H_{V_+}^{H+} H_{T_+}^{H-} + H_{V_+}^{H-} H_{T_+}^{H+} + 2H_{V_\perp}^{H+} H_{T_\perp}^{H-} + 2H_{V_\perp}^{H-} H_{T_\perp}^{H+} \right) \right\}, \quad (3.11) \end{aligned}$$

with the helicity amplitudes given by

$$H_{V_+}^{H\pm} \equiv \frac{1}{\sqrt{q^2}} \left[(m_{\Lambda_b} + m_H) F_+^H \sqrt{Q_-^H} \mp (m_{\Lambda_b} - m_H) G_+^H \sqrt{Q_+^H} \right], \quad (3.12)$$

$$H_{V_0}^{H\pm} \equiv \frac{1}{\sqrt{q^2}} \left[(m_{\Lambda_b} - m_H) F_0^H \sqrt{Q_+^H} \mp (m_{\Lambda_b} + m_H) G_0^H \sqrt{Q_-^H} \right], \quad (3.13)$$

$$H_{V_\perp}^{H\pm} \equiv F_\perp^H \sqrt{Q_-^H} \mp G_\perp^H \sqrt{Q_+^H}, \quad (3.14)$$

$$H_S^{H\pm} \equiv \frac{m_{\Lambda_b} - m_H}{m_b - m_q} F_0^H \sqrt{Q_+^H} \pm \frac{m_{\Lambda_b} + m_H}{m_b + m_q} G_0^H \sqrt{Q_-^H}, \quad (3.15)$$

$$H_{T_+}^{H\pm} \equiv h_+^H \sqrt{Q_-^H} \pm \tilde{h}_+^H \sqrt{Q_+^H}, \quad (3.16)$$

$$H_{T_\perp}^{H\pm} \equiv \frac{1}{\sqrt{q^2}} \left[(m_{\Lambda_b} + m_H) h_\perp^H \sqrt{Q_-^H} \pm (m_{\Lambda_b} - m_H) \tilde{h}_\perp^H \sqrt{Q_+^H} \right], \quad (3.17)$$

where the expression of N_{Λ_b} is the same as that of N_B defined by Eq. (3.1), but now with the meson mass m_B replaced by the baryon mass m_{Λ_b} . The form factors $F_{+,0,\perp}^H$, $G_{+,0,\perp}^H$, $h_{+,\perp}^H$ and $\tilde{h}_{+,\perp}^H$ for the vector, axial-vector, and tensor currents are defined as in Refs. [81–84].

The form factors introduced as above need to be extracted from experimental data and/or evaluated by non-perturbative methods like lattice QCD and LCSR. Concerning the q^2 dependence of these form factors, it is now standard to use the z parametrization that satisfies unitarity, analyticity and perturbativity [85–87]. To this end, it is convenient to introduce the conformal mapping variable

$$z(q^2) \equiv \frac{\sqrt{t_+ - q^2} - \sqrt{t_+ - t_0}}{\sqrt{t_+ - q^2} + \sqrt{t_+ - t_0}}, \quad (3.18)$$

which maps the q^2 -plane cut for $q^2 > t_+$ onto the disk $|z(q^2)| < 1$ in the z complex plane, with $z(t_+) = -1$, $z(\infty) = 1$, and $z(t_0) = 0$, where t_+ is the threshold parameter and t_0 determines the point q^2 mapped onto the origin in the z plane. The values of t_+ and t_0 are fixed for each form factor depending on the individual setup of the analysis. In this way, the q^2 dependence of the form factors is given as a Taylor expansion in the variable $z(q^2)$, where the expansion coefficients are free parameters to be fitted. Explicit definitions are different for each form factor analysis, which will be described in the next two subsections. We will summarize recent updates of the form factor inputs and indicate what will be used in our analysis.

3.2 $B \rightarrow D$, $B \rightarrow D^*$, and $\Lambda_b \rightarrow \Lambda_c$ form factors

The $B \rightarrow D$ and $B \rightarrow D^*$ form factors have been studied for various purposes, as they affect both the $|V_{cb}|$ determinations and the $R_{D^{(*)}}$ evaluations. Theoretical

	Lattice		LCSR		Lattice + LCSR
	SM	Tensor	SM	Tensor	SM
$B \rightarrow D$	Refs. [88, 89]	no data	Ref. [93, 94]	Ref. [93]	Ref. [94]**)
$B \rightarrow D^*$	Refs. [90–92]	no data ^(*)	Ref. [93, 94]	Ref. [93]	Ref. [94]**)
$\Lambda_b \rightarrow \Lambda_c$	Ref. [83]	Ref. [95]	no data	no data	–

Table 1. Summary of recent theoretical evaluations of the $B \rightarrow D$, $B \rightarrow D^*$, and $\Lambda_b \rightarrow \Lambda_c$ form factors from lattice QCD and/or LCSR approaches. ^(*) The $B \rightarrow D^*$ tensor form factor is obtained in Ref. [92] only under the heavy quark symmetry. ^(**) The lattice QCD results of Refs. [88, 89] and [90] are taken to provide their Lattice + LCSR combined fit [94] for the $B \rightarrow D$ and $B \rightarrow D^*$ form factors, respectively.

studies have been done mainly by the lattice QCD and LCSR approaches. The lattice results are available for $B \rightarrow D$ in Refs. [88, 89] while for $B \rightarrow D^*$ in Refs. [90–92]. In particular, the latter has been recently reported for the first time but, for the moment, we do not have a conclusive combined fit for these results. Our purpose in this paper is to highlight the significance of uncertainties from the theoretical inputs, which is useful once a conclusive form factor evaluation (or fit) is available in the future. Here let us also point out that the lattice result of the tensor form factor is only available for $B \rightarrow D^*$ by HPQCD [92], which is however based on the heavy quark symmetry. Hence, it can be concluded that we have no direct lattice point for the tensor form factor in the so-called Boyd-Grinstein-Lebed (BGL) parametrization [86]. The LCSR calculation has been done in Ref. [93], and then updated by another group in Ref. [94] by including the next-to-leading-order QCD corrections and the various power-suppressed contributions. It should be clarified that the former study includes the tensor form factor, while the latter study provides a combined fit to their LCSR result and the lattice data point from Ref. [90] for the SM currents.

We list the current situation on the form factor evaluations in Table 1, where the columns labelled by “SM” indicate the vector and axial-vector form factors. As can be seen from the above summary table, the form factor inputs for $B \rightarrow D$ and $B \rightarrow D^*$ transitions have different sources and the lattice data points are still incoherent for the moment. Concerning our purpose, however, it is sufficient to simply choose the results from Ref. [94] for the vector ($f_{+,0}^D$, V^{D^*}) and axial-vector ($A_{0,1,2}^{D^*}$) and from Ref. [93] for the tensor (f_T^D and $T_{1,2,3}^{D^*}$) form factors. It is also noted that the BGL form factors for $B \rightarrow D^*$ transition are usually given, instead of V^{D^*} and $A_{0,1,2}^{D^*}$ themselves, by [94, 96]

$$f(q^2) = (m_B + m_{D^*})A_1^{D^*}(q^2), \quad g(q^2) = \frac{2V^{D^*}(q^2)}{m_B + m_{D^*}}, \quad F_2(q^2) = 2A_0^{D^*}(q^2), \quad (3.19)$$

$$F_1(q^2) = \frac{m_B + m_{D^*}}{2m_{D^*}} \left[(m_B^2 - m_{D^*}^2 - q^2) A_1^{D^*}(q^2) - \frac{Q_+^{D^*} Q_-^{D^*}}{(m_B + m_{D^*})^2} A_2^{D^*}(q^2) \right]. \quad (3.20)$$

These form factors can be schematically parametrized as [86, 97]

$$F(z) = \frac{1}{P_F(z)\phi_F(z)} \sum_{n=0}^{N_F} a_n^F z(q^2)^n, \quad (3.21)$$

in terms of the BGL series coefficients a_n^F , where N_F stands for the truncation order and the z expansion variable is defined as in Eq. (3.18) with the choice of

$$t_+ = (m_B + m_{D^*})^2, \quad t_0 = (m_B - m_{D^*})^2. \quad (3.22)$$

The prefactors $P_F(z)$ and ϕ_F are introduced to control the convergence of the form factors; $P_F(z)$ are the Blaschke factors served to account for the explicit poles in the variable q^2 that are associated with the on-shell productions of B_c^* bound states for $q^2 < t_+$, and $\phi_F(z)$ are the outer functions that guarantee the form factors to satisfy the unitarity bounds. In practice, they are just functions of the variable $z \equiv z(q^2)$. The outer functions are individually written as [97]

$$\phi_{f_+^D}(z) = \chi_{f_+^D} (1+z)^2 (1-z)^{1/2} [(1+r)(1-z) + 2\sqrt{r}(1+z)]^{-5}, \quad (3.23)$$

$$\phi_{f_0^D}(z) = \chi_{f_0^D} (1+z)(1-z)^{3/2} [(1+r)(1-z) + 2\sqrt{r}(1+z)]^{-4}, \quad (3.24)$$

$$\phi_g(z) = \chi_g (1+z)^2 (1-z)^{-1/2} [(1+r)(1-z) + 2\sqrt{r}(1+z)]^{-4}, \quad (3.25)$$

$$\phi_f(z) = \chi_f (1+z)(1-z)^{3/2} [(1+r)(1-z) + 2\sqrt{r}(1+z)]^{-4}, \quad (3.26)$$

$$\phi_{F_1}(z) = \chi_{F_1} (1+z)(1-z)^{5/2} [(1+r)(1-z) + 2\sqrt{r}(1+z)]^{-5}, \quad (3.27)$$

$$\phi_{F_2}(z) = \chi_{F_2} (1+z)^2 (1-z)^{-1/2} [(1+r)(1-z) + 2\sqrt{r}(1+z)]^{-4}, \quad (3.28)$$

where $r \equiv m_{D^*}/m_B$ is the mass ratio, and the prefactors χ_F can be numerically given as [98–100]

$$\chi_{f_+^D} = 12.43, \quad \chi_{f_0^D} = 10.11, \quad \chi_g = 53.79, \quad (3.29)$$

$$\chi_f = 1.454, \quad \chi_{F_1} = 0.195, \quad \chi_{F_2} = 10.71. \quad (3.30)$$

The Blaschke factors are given in the following form:

$$P_F(z) = \prod_n \frac{z - z_n^F}{1 - z z_n^F}, \quad (3.31)$$

where each form factor F has its own z_n^F that account for the resonance poles. We do not exhibit their explicit definitions, but only quote their numerical values as [98–100]

$$z_1^{f_+^D} = -0.433, \quad z_2^{f_0^D} = -0.819, \quad (3.32)$$

$$z_1^{f^D} = -0.308, \quad z_2^{f^D} = -0.555, \quad z_3^{f^D} = -0.646, \quad (3.33)$$

$$z_1^{F_2} = -0.274, \quad z_2^{F_2} = -0.443, \quad z_3^{F_2} = -0.791, \quad (3.34)$$

$$z_1^g = -0.286, \quad z_2^g = -0.479, \quad z_3^g = -0.537, \quad z_4^g = -0.890, \quad (3.35)$$

$$z_1^{f,F_1} = -0.402, \quad z_2^{f,F_1} = -0.406, \quad z_3^{f,F_1} = -0.637, \quad z_4^{f,F_1} = -0.642. \quad (3.36)$$

Based on the above setup, the BGL series coefficients a_n^F have been fitted to the lattice QCD and LCSR evaluations with $N_F = 2$ for the SM currents in Ref. [94]. They are given explicitly as

$$\begin{aligned} & \{a_0^{f^D}, a_1^{f^D}, a_2^{f^D}, a_1^{f_0^D}, a_2^{f_0^D}, a_0^g, a_1^g, a_2^g, a_0^f, a_1^f, a_2^f, a_1^{F_1}, a_2^{F_1}, a_1^{F_2}, a_2^{F_2}\} \\ & = \{0.0137(1), -0.0417(33), 0.0415(1124), -0.2072(147), 0.1880(5330), \\ & \quad 0.0256(9), -0.1005(456), 0.2587(6564), 0.0109(2), 0.0081(101), \\ & \quad 0.0693(2140), -0.0024(20), -0.0155(388), -0.2097(581), 0.5667(8789)\}, \quad (3.37) \end{aligned}$$

while the remaining coefficients $a_0^{f_0^D}$, $a_0^{F_1}$, and $a_0^{F_2}$ are determined by the kinematic conditions of $f_0^D(q^2 = 0) = f_+^D(q^2 = 0)$, $f(z = 0) = F_1(z = 0)/(m_B - m_{D^*})$, and $F_1(q^2 = 0) = (m_B^2 - m_{D^*}^2) F_2(q^2 = 0)/2$. That is

$$a_0^{f_0^D} = 4.945 a_0^{f^D} + 0.319 a_1^{f^D} + 0.021 a_2^{f^D} - 0.064 a_1^{f_0^D} - 0.004 a_2^{f_0^D}, \quad (3.38)$$

$$a_0^{F_1} = 0.167 a_0^f, \quad (3.39)$$

$$a_0^{F_2} = 3.563 a_0^f + 1.193 a_1^{F_1} + 0.067 a_2^{F_1} - 0.056 a_1^{F_2} - 0.003 a_2^{F_2}. \quad (3.40)$$

We will also take into account the correlation matrices for the BGL expansion coefficients in Eq. (3.37), as provided in Ref. [94], when evaluating the error propagations in the observables.

For the $B \rightarrow D^{(*)}$ tensor form factors, we follow Ref. [93] and adopt their fitted expansion parameters obtained by incorporating the LCSR data points. Here the form factors are parametrized in the Bharucha-Straub-Zwicky (BSZ) pattern [80] as

$$F(q^2) = \frac{1}{1 - q^2/M_F^2} \sum_{n=0}^{N_F} a_n^F [z(q^2) - z(0)]^n, \quad (3.41)$$

where the z variable takes the same form as in Eq. (3.18) but now with the choice of

$$t_+ \equiv (m_B + m_{D^{(*)}})^2, \quad t_0 \equiv (m_B + m_{D^{(*)}})(\sqrt{m_B} - \sqrt{m_{D^{(*)}}})^2. \quad (3.42)$$

The resonance masses M_F are given numerically as

$$M_{f_T^D} = M_{T_1^{D^*}} = 6.330 \text{ GeV}, \quad M_{T_2^{D^*}} = M_{T_{23}^{D^*}} = 6.767 \text{ GeV}, \quad (3.43)$$

for $F = f_T^D, T_1^{D*}, T_2^{D*}$, and T_{23}^{D*} , where T_{23}^{D*} is fitted instead of T_3^{D*} itself and related to T_3^{D*} via

$$T_{23}^{D*}(q^2) = \frac{T_2^{D*}(q^2)(m_B^2 + 3m_{D^*}^2 - q^2)(m_B^2 - m_{D^*}^2) - T_3^{D*}(q^2)Q_+^{D*}Q_-^{D*}}{8m_B m_{D^*}^2(m_B - m_{D^*})}. \quad (3.44)$$

Then, the fit results for the tensor form factors are given as [93]

$$\{a_0^{f_T^D}, a_1^{f_T^D}, a_2^{f_T^D}\} = \{0.565(36), -2.5(2.2), 10.6(31.8)\}, \quad (3.45)$$

$$\begin{aligned} & \{a_0^{T_1^{D*}, T_2^{D*}}, a_1^{T_1^{D*}}, a_2^{T_1^{D*}}, a_1^{T_2^{D*}}, a_2^{T_2^{D*}}, a_0^{T_{23}^{D*}}, a_1^{T_{23}^{D*}}, a_2^{T_{23}^{D*}}\} \\ & = \{0.630(78), -1.418(2.630), -0.688(39.922), 1.523(3.097), 0.007(47.537), \\ & \quad 0.806(93), 0.586(3.644), 4.667(57.422)\}, \end{aligned} \quad (3.46)$$

where $a_0^{T_2^{D*}} = a_0^{T_1^{D*}}$ is determined from the kinematic relation of $T_2^{D*}(q^2 = 0) = T_1^{D*}(q^2 = 0)$. In addition, the correlations among these expansion coefficients, provided in the same reference, are also taken into account in our analysis.

On the other hand, the $\Lambda_b \rightarrow \Lambda_c$ form factors have been evaluated by lattice QCD in Ref. [83] for the vector and axial-vector currents, and then in Ref. [95] for the tensor current. Their q^2 dependence is now parametrized as [87]

$$F(q^2) = \frac{1}{1 - q^2/M_F^2} \sum_{n=0}^{N_F} a_n^F z(q^2)^n, \quad (3.47)$$

for $F = F_+^{\Lambda_c}, F_0^{\Lambda_c}, F_\perp^{\Lambda_c}, G_+^{\Lambda_c}, G_0^{\Lambda_c}, G_\perp^{\Lambda_c}, h_+^{\Lambda_c}, h_\perp^{\Lambda_c}, \tilde{h}_+^{\Lambda_c}$, and $\tilde{h}_\perp^{\Lambda_c}$, where the z variable is also defined as in Eq. (3.18) with

$$t_+ \equiv M_F^2, \quad t_0 \equiv (m_{\Lambda_b} - m_{\Lambda_c})^2, \quad (3.48)$$

and

$$M_{F_+^{\Lambda_c}} = M_{F_\perp^{\Lambda_c}} = M_{h_+^{\Lambda_c}} = M_{h_\perp^{\Lambda_c}} = 6.332 \text{ GeV}, \quad M_{F_0^{\Lambda_c}} = 6.725 \text{ GeV}, \quad (3.49)$$

$$M_{G_+^{\Lambda_c}} = M_{G_\perp^{\Lambda_c}} = M_{\tilde{h}_+^{\Lambda_c}} = M_{\tilde{h}_\perp^{\Lambda_c}} = 6.768 \text{ GeV}, \quad M_{G_0^{\Lambda_c}} = 6.276 \text{ GeV}. \quad (3.50)$$

Equipped with the above setup of the parameterization as well as the endpoint constraints on the form factors,² $F_0^{\Lambda_c}(q^2 = 0) = F_+^{\Lambda_c}(q^2 = 0)$, $G_0^{\Lambda_c}(q^2 = 0) = G_+^{\Lambda_c}(q^2 = 0)$, $G_\perp^{\Lambda_c}(q^2 = t_0) = G_+^{\Lambda_c}(q^2 = t_0)$, and $\tilde{h}_\perp^{\Lambda_c}(q^2 = t_0) = \tilde{h}_+^{\Lambda_c}(q^2 = t_0)$, we can

²To be more precise, the endpoint constraints are imposed on the lattice spacing, while the final fit results in the physical limit are obtained by extrapolations from the lattice fit. Due to this procedure, the endpoint constraints $F_0^{\Lambda_c}(q^2 = 0) = F_+^{\Lambda_c}(q^2 = 0)$ and $G_0^{\Lambda_c}(q^2 = 0) = G_+^{\Lambda_c}(q^2 = 0)$ are not exact in their fit results but consistent within the errors.

obtain the series coefficients a_n^F with $N_F = 1$ by fitting to the lattice data points, which read [83, 95]

$$\begin{aligned} & \{a_0^{F_+^{\Lambda c}}, a_1^{F_+^{\Lambda c}}, a_0^{F_0^{\Lambda c}}, a_1^{F_0^{\Lambda c}}, a_0^{F_\perp^{\Lambda c}}, a_1^{F_\perp^{\Lambda c}}, a_0^{G_+^{\Lambda c}, G_\perp^{\Lambda c}}, a_1^{G_+^{\Lambda c}, G_\perp^{\Lambda c}}, a_0^{G_0^{\Lambda c}}, a_1^{G_0^{\Lambda c}}, a_0^{G_\perp^{\Lambda c}}, a_1^{G_\perp^{\Lambda c}}\} \\ & = \{0.8146(167), -4.8988(5425), 0.7439(125), -4.6477(6083), 1.0780(256), \\ & \quad -6.4171(8480), 0.6847(86), -4.4312(3572), 0.7396(143), -4.3665(3314), \\ & \quad -4.4634(3613)\}, \end{aligned} \quad (3.51)$$

$$\begin{aligned} & \{a_0^{\tilde{h}_+^{\Lambda c}}, a_1^{\tilde{h}_+^{\Lambda c}}, a_0^{\tilde{h}_0^{\Lambda c}}, a_1^{\tilde{h}_0^{\Lambda c}}, a_0^{\tilde{h}_\perp^{\Lambda c}}, a_1^{\tilde{h}_\perp^{\Lambda c}}, a_0^{\tilde{h}_+^{\Lambda c}, \tilde{h}_\perp^{\Lambda c}}, a_1^{\tilde{h}_+^{\Lambda c}, \tilde{h}_\perp^{\Lambda c}}\} = \{0.9752(303), -5.5000(1.2361), \\ & \quad 0.7054(137), -4.3578(5114), 0.6728(88), -4.4322(3882), -4.4928(3584)\}, \end{aligned} \quad (3.52)$$

where the covariance matrix of the fit results is explicitly given in the same references and will be taken into account in our study. Although this nominal fit is supposed to be the fundamental result of Refs. [83, 95], the authors have also provided a procedure to calculate the ‘‘systematic’’ uncertainty associated with a different choice of the expansion order N_F (the so-called higher-order fit). In our study, we follow exactly the same procedure proposed in Ref. [83] to calculate this additional uncertainty, and the total uncertainty is then obtained by adding the statistical and systematic ones in quadrature. For further details, we refer the readers to Eqs. (82)–(84) in Ref. [83].

3.3 $B \rightarrow \pi$, $B \rightarrow \rho$, and $\Lambda_b \rightarrow p$ form factors

In contrast to the extensively investigated $b \rightarrow c$ case, the current explorations of the semi-leptonic $b \rightarrow ul\nu$ decays are less studied both experimentally and theoretically. Regarding the experimental measurements, only the light-lepton modes have been observed for the moment, as mentioned in Sec. 1. On the other hand, several theoretical evaluations are available for the $B \rightarrow \pi$, $B \rightarrow \rho$, and $\Lambda_b \rightarrow p$ form factors, but not for all kinds of methods and currents. For example, the $B \rightarrow \pi$ form factors have been widely studied using both the lattice QCD [101–104] and LCSR [93, 105–109] approaches, with which the semi-leptonic $B \rightarrow \pi l\nu$ decay has been used to determine the CKM matrix element $|V_{ub}|$ exclusively. The $B \rightarrow \rho$ form factors are provided only by the LCSR calculations [80, 93, 110] for both the SM (vector and axial-vector) and NP (tensor) currents.

In Table 2, we list the recent theoretical evaluations of the form factors. At first, we follow Ref. [109] to parametrize the q^2 dependence of the $B \rightarrow \pi$ form factors through a modified BGL scenario, the so-called Bourrely-Caprini-Lellouch (BCL) form [87] that combines the pole factorization with an expansion in powers of the conformal mapping variable and simplifies the BGL unitarity requirement. The BCL parametrization of the vector and tensor form factors reads [87]

$$F(q^2) = \frac{1}{1 - q^2/M_F^2} \sum_{n=0}^{N_F-1} b_n^F \left[z(q^2)^n - (-1)^{n-N_F} \frac{n}{N_F} z(q^2)^{N_F} \right], \quad (3.53)$$

	Lattice		LCSR		Lattice + LCSR
	SM	Tensor	SM	Tensor	SM + Tensor
$B \rightarrow \pi$	Refs. [101–103]	Ref. [104]	Refs. [93, 106–108]		Ref. [109]
$B \rightarrow \rho$	no data	no data	Refs. [80, 93, 110]		–
$\Lambda_b \rightarrow p$	Ref. [83]	no data	Ref. [111]	no data	–

Table 2. Summary of recent theoretical estimations of the $B \rightarrow \pi$, $B \rightarrow \rho$, and $\Lambda_b \rightarrow p$ form factors from lattice QCD and/or LCSR approaches. Note that Ref. [105] provides the LCSR fit result for $B \rightarrow \pi$ as well, but only for the SM currents.

with the sub-threshold resonance masses given by [16]

$$M_{f_+^\pi} = M_{f_T^\pi} = 5.325 \text{ GeV}, \quad (3.54)$$

while for the scalar form factor we have

$$f_0^\pi(q^2) = \sum_{n=0}^{N_{f_0^\pi}-1} b_n^{f_0^\pi} z(q^2)^n, \quad (3.55)$$

where the disappearance of the pole factor is due to the fact that the lowest-lying resonance in the $J^P = 0^+$ channel is located above the $B\pi$ production threshold. The conformal mapping variable $z(q^2)$ is given as in Eq. (3.18), with

$$t_+ \equiv (m_B + m_\pi)^2, \quad t_0 \equiv (m_B + m_\pi)(\sqrt{m_B} - \sqrt{m_\pi})^2. \quad (3.56)$$

Then, the fit results for the BCL series coefficients from Ref. [109] are exhibited as

$$\begin{aligned} & \{b_0^{f_+^\pi}, b_1^{f_+^\pi}, b_2^{f_+^\pi}, b_0^{f_0^\pi}, b_1^{f_0^\pi}\} \\ & = \{0.404(13), -0.618(63), -0.473(215), 0.496(19), -1.537(56)\}, \end{aligned} \quad (3.57)$$

$$\{b_0^{f_T^\pi}, b_1^{f_T^\pi}, b_2^{f_T^\pi}\} = \{0.396(15), -0.553(73), -0.248(235)\}, \quad (3.58)$$

for the truncation order $N_F = 3$, where the remaining coefficient $b_2^{f_0^\pi}$ is related to the others as

$$b_2^{f_0^\pi} = 12.78(b_0^{f_+^\pi} - b_0^{f_0^\pi}) + 3.48b_1^{f_+^\pi} + 1.19b_2^{f_+^\pi} - 3.58b_1^{f_0^\pi}, \quad (3.59)$$

from the kinematic condition of $f_+^\pi(q^2 = 0) = f_0^\pi(q^2 = 0)$. In addition, the correlation matrix is provided by Table 2 in the same reference.

Regarding the $B \rightarrow \rho$ form factors, we employ the LCSR results provided in Ref. [80], although Refs. [93, 110] have also provided the fit results. This is a reasonable choice because, compared to the results obtained with the B -meson light-cone

distribution amplitude, the form factors can be currently evaluated with better accuracy by using the light-meson light-cone distribution amplitude [80], as analyzed in Ref. [93].³ This choice results in smaller uncertainties in the LCSR form factor fits and, consequently, in the $B \rightarrow \rho l \nu$ decay amplitudes. The form factors of our concern can be parametrized in the BSZ form as

$$F(q^2) = \frac{1}{1 - q^2/M_F^2} \sum_{n=0}^{N_F} a_n^F (z(q^2) - z(0))^n, \quad (3.60)$$

with the z variable given by Eq. (3.18) and

$$t_+ \equiv (m_B + m_\rho)^2, \quad t_0 \equiv (m_B + m_\rho) (\sqrt{m_B} - \sqrt{m_\rho})^2. \quad (3.61)$$

The resonance masses now read

$$M_{A_0^\rho} = 5.279 \text{ GeV}, \quad M_{V^\rho} = M_{T_1^\rho} = 5.325 \text{ GeV}, \quad (3.62)$$

$$M_{A_1^\rho} = M_{A_{12}^\rho} = M_{T_2^\rho} = M_{T_{23}^\rho} = 5.724 \text{ GeV}, \quad (3.63)$$

for $F = A_0^\rho, V^\rho, A_1^\rho, A_{12}^\rho, T_1^\rho, T_2^\rho$, and T_{23}^ρ , where A_{12}^ρ and T_{23}^ρ are fitted, instead of A_2^ρ and T_3^ρ themselves, with the following relations [80]:

$$A_{12}^\rho(q^2) = \frac{A_1^\rho(q^2) (m_B^2 - m_\rho^2 - q^2) (m_B + m_\rho)^2 - A_2^\rho(q^2) Q_+^\rho Q_-^\rho}{16 m_B m_\rho^2 (m_B + m_\rho)}, \quad (3.64)$$

$$T_{23}^\rho(q^2) = \frac{T_2^\rho(q^2) (m_B^2 + 3m_\rho^2 - q^2) (m_B^2 - m_\rho^2) - T_3^\rho(q^2) Q_+^\rho Q_-^\rho}{8 m_B m_\rho^2 (m_B - m_\rho)}. \quad (3.65)$$

Then, the fit results are imported from Ref. [80] such that

$$\begin{aligned} & \{a_1^{A_0^\rho}, a_2^{A_0^\rho}, a_0^{A_1^\rho}, a_1^{A_1^\rho}, a_2^{A_1^\rho}, a_0^{A_{12}^\rho}, a_1^{A_{12}^\rho}, a_2^{A_{12}^\rho}, a_0^{V^\rho}, a_1^{V^\rho}, a_2^{V^\rho}\} \\ &= \{-0.833(204), 1.331(1.050), 0.262(26), 0.393(139), 0.163(408), 0.297(35), \\ & \quad 0.759(197), 0.465(756), 0.327(31), -0.860(183), 1.802(965)\}, \end{aligned} \quad (3.66)$$

$$\begin{aligned} & \{a_0^{T_1^\rho}, a_1^{T_1^\rho}, a_2^{T_1^\rho}, a_1^{T_2^\rho}, a_2^{T_2^\rho}, a_0^{T_{23}^\rho}, a_1^{T_{23}^\rho}, a_2^{T_{23}^\rho}\} \\ &= \{0.272(26), -0.742(143), 1.453(773), 0.471(134), 0.576(465), 0.747(76), \\ & \quad 1.896(428), 2.930(1.807)\}, \end{aligned} \quad (3.67)$$

for $N_F = 2$, and the full correlation matrices are also provided as ancillary files in the same reference. The rest of the expansion coefficients, $a_0^{A_0^\rho}$ and $a_0^{T_2^\rho}$, are given as

$$a_0^{T_2^\rho} = a_0^{T_1^\rho}, \quad a_0^{A_0^\rho} = 1.201 a_0^{A_{12}^\rho}, \quad (3.68)$$

³Notice that the modern evaluations of the $B \rightarrow D^*$ form factors in the LCSR approach are only available with the former setup [93, 94, 112].

from the kinematic relations of $T_1^\rho(q^2 = 0) = T_2^\rho(q^2 = 0)$ and $A_{12}^\rho(q^2 = 0) = (m_B^2 - m_\rho^2) / (8m_B m_\rho) A_0^\rho(q^2 = 0)$, respectively.

For the baryonic $\Lambda_b \rightarrow p l \nu$ process, detailed computations of the relevant form factors have been carried out by both the lattice QCD [83] and LCSR [111, 113] approaches for the vector and axial-vector currents. Here we simply take the lattice QCD results, in which the q^2 dependence of the form factors is represented as [83]

$$F(q^2) = \frac{1}{1 - q^2/M_F^2} \sum_{n=0}^{N_F} a_n^F z(q^2)^n, \quad (3.69)$$

for $F = F_+, F_0, F_\perp, G_+, G_0, \text{ and } G_\perp$. It is noted that t_+ and t_0 involved in the $z(q^2)$ variable defined by Eq. (3.18) is now given by [83]

$$t_+ \equiv (m_B + m_\pi)^2, \quad t_0 \equiv (m_{\Lambda_b} - m_p)^2. \quad (3.70)$$

The resonance masses are taken as

$$M_{F_+^p} = M_{F_\perp^p} = 5.325 \text{ GeV}, \quad M_{F_0^p} = 5.656 \text{ GeV}, \quad (3.71)$$

$$M_{G_+^p} = M_{G_\perp^p} = 5.706 \text{ GeV}, \quad M_{G_0^p} = 5.279 \text{ GeV}. \quad (3.72)$$

Then, the lattice fit results are given as

$$\begin{aligned} & \{a_0^{F_+^p}, a_1^{F_+^p}, a_0^{F_0^p}, a_1^{F_0^p}, a_0^{F_\perp^p}, a_1^{F_\perp^p}, a_0^{G_+^p, G_\perp^p}, a_1^{G_+^p, G_\perp^p}, a_0^{G_0^p}, a_1^{G_0^p}, a_0^{G_\perp^p}, a_1^{G_\perp^p}\} \\ & = \{0.438(31), -0.645(209), 0.419(26), -0.786(204), 0.539(44), -0.807(304), \\ & \quad 0.391(20), -0.817(175), 0.453(29), -0.782(189), -0.906(196)\}, \end{aligned} \quad (3.73)$$

for the nominal fit with $N_F = 1$ and their covariances are also provided in the same reference. Similar to the case of the $\Lambda_b \rightarrow \Lambda_c$ form factors, we will also consider in our analysis the systematic uncertainty caused by their assumptions [83].

At present, we have no lattice QCD nor LCSR results for the $\Lambda_b \rightarrow p$ tensor form factors $h_{+,\perp}^p$ and $\tilde{h}_{+,\perp}^p$. However, we can infer the following approximations when taking into account the J^P properties of the $\Lambda_b \rightarrow p$ transition:

$$h_{+,\perp}^p \equiv R_{+,\perp} F_{+,\perp}^p, \quad \tilde{h}_{+,\perp}^p \equiv \tilde{R}_{+,\perp} G_{+,\perp}^p, \quad (3.74)$$

where $R_{+,\perp}$ and $\tilde{R}_{+,\perp}$ indicate some real constant parameters that need to be estimated. According to the preliminary analysis made in Ref. [114], we have $R_+ \approx 1.2$, $R_\perp \approx 0.7$, $\tilde{R}_+ \approx 1.0$, and $\tilde{R}_\perp \approx 1.0$, with an about 10% accuracy. Based on this observation, we will take these estimations as input, with a conservative uncertainty of 20% for each tensor form factor. The status of ongoing next-generation calculations of these form factors can be found in Ref. [115].

3.4 Numerical results

We are now ready to evaluate the appropriate propagation of the form factor uncertainties on the general R_X formulae. Taking into account all the form factor inputs summarized in Sec. 3.2, we obtain the following values of the coefficients a_X^{ij} defined in Eqs. (2.3)–(2.5):

$$\begin{aligned} \frac{R_D}{R_D^{\text{SM}}} : \quad & a_D^{SS} = 1.070 \pm 0.006, & a_D^{TT} &= 0.721 \pm 0.341, \\ & a_D^{VS} = 1.528 \pm 0.006, & a_D^{VT} &= 1.015 \pm 0.233, \end{aligned} \quad (3.75)$$

$$\begin{aligned} \frac{R_{D^*}}{R_{D^*}^{\text{SM}}} : \quad & a_{D^*}^{SS} = 0.043 \pm 0.002, & a_{D^*}^{TT} &= 17.76 \pm 9.37, \\ & a_{D^*}^{V_L V_R} = -1.797 \pm 0.015, & a_{D^*}^{VS} &= -0.113 \pm 0.004, \\ & a_{D^*}^{V_L T} = -5.470 \pm 1.717, & a_{D^*}^{V_R T} &= 7.098 \pm 1.944, \end{aligned} \quad (3.76)$$

$$\begin{aligned} \frac{R_{\Lambda_c}}{R_{\Lambda_c}^{\text{SM}}} : \quad & a_{\Lambda_c}^{SS} = 0.321 \pm 0.005 \pm 0.013, & a_{\Lambda_c}^{TT} &= 10.44 \pm 0.21 \pm 0.91, \\ & a_{\Lambda_c}^{V_L V_R} = -0.722 \pm 0.027 \pm 0.060, & a_{\Lambda_c}^{S_L S_R} &= 0.513 \pm 0.011 \pm 0.029, \\ & a_{\Lambda_c}^{VS_1} = 0.334 \pm 0.009 \pm 0.022, & a_{\Lambda_c}^{VS_2} &= 0.497 \pm 0.008 \pm 0.019, \\ & a_{\Lambda_c}^{V_L T} = -3.110 \pm 0.065 \pm 0.211, & a_{\Lambda_c}^{V_R T} &= 4.880 \pm 0.053 \pm 0.215, \end{aligned} \quad (3.77)$$

for the semi-leptonic $b \rightarrow c$ decays, where the third terms in $a_{\Lambda_c}^{ij}$ account for the systematic uncertainties obtained by following the same procedure as in Ref. [83]. Combining all these results, we finally obtain the R ratio sum rule,

$$\frac{R_{\Lambda_c}}{R_{\Lambda_c}^{\text{SM}}} = (0.272 \pm 0.015) \frac{R_D}{R_D^{\text{SM}}} + (0.728 \mp 0.015) \frac{R_{D^*}}{R_{D^*}^{\text{SM}}} + \delta_{\Lambda_c}, \quad (3.78)$$

with the shift factor given by

$$\begin{aligned} \delta_{\Lambda_c} = & (-0.001 \pm 0.005) (|C_{S_L}^{c\tau}|^2 + |C_{S_R}^{c\tau}|^2) + (-0.007 \pm 0.005) \text{Re} (C_{S_L}^{c\tau} C_{S_R}^{c\tau*}) \\ & + (-2.681 \pm 6.907) |C_T^{c\tau}|^2 + (-0.561 \pm 1.439) \text{Re} (C_{V_R}^{c\tau} C_T^{c\tau*}) \\ & + \text{Re} [(1 + C_{V_L}^{c\tau}) \{(0.041 \pm 0.034) C_{V_R}^{c\tau*} + (0.594 \pm 1.274) C_T^{c\tau*}\}] \\ & + (-0.002 \pm 0.009) \text{Re} [(1 + C_{V_L}^{c\tau}) C_{S_R}^{c\tau*} + C_{S_L}^{c\tau} C_{V_R}^{c\tau*}] . \end{aligned} \quad (3.79)$$

We observe a fluctuation of ± 0.015 from the central values for the R_X ratio coefficients. It can also be seen that the vector and scalar terms do not generally have considerable uncertainties in δ_{Λ_c} , while the terms involving the tensor WC $C_T^{c\tau}$ receive non-negligible uncertainties, which stem from the LCSR results for the $B \rightarrow D^{(*)}$ tensor form factors [93]. Once future precise lattice QCD results are confirmed with

a good consistency and a combined fit is available, it is expected that these terms can be evaluated at a similar level of accuracy with that of the vector and scalar terms. Let us remind that the recent lattice QCD results of Refs. [90–92] are not conclusive yet, and making a private combined fit with detailed correlations taken into account is beyond the scope of our work. Since our purpose is to exhibit how the R ratio sum rule is violated by the uncertainties of the theoretical inputs, our setup is rather informative.

It is also noted that the R ratio sum rule and the shift factor δ_{Λ_c} in Ref. [50] were obtained by taking their combined fits to the theoretical/experimental inputs and a unique form factor parametrization based on the heavy quark effective theory. This causes a difference from our results that are based on the well-known z -expansion parametrizations of the q^2 dependence of the form factors, although they are well consistent with each other within the uncertainty. The suppression of the numerical coefficients in δ_{Λ_c} can be obviously confirmed in both cases.

Similarly, we obtain the following numerical results for the $b \rightarrow u$ case, where our inputs are summarized in Sec. 3.3 and the additional conservative errors are imposed on the tensor form factors, $R_+ \simeq 1.20 \pm 0.24$, $R_\perp \simeq 0.70 \pm 0.14$, and $\tilde{R}_{+,\perp} \simeq 1.00 \pm 0.20$:

$$\begin{aligned} \frac{R_\pi}{R_\pi^{\text{SM}}} : \quad & a_\pi^{SS} = 1.497 \pm 0.094, & a_\pi^{TT} &= 3.804 \pm 0.238, \\ & a_\pi^{VS} = 1.239 \pm 0.073, & a_\pi^{VT} &= 2.511 \pm 0.088, \end{aligned} \quad (3.80)$$

$$\begin{aligned} \frac{R_\rho}{R_\rho^{\text{SM}}} : \quad & a_\rho^{SS} = 0.276 \pm 0.030, & a_\rho^{TT} &= 12.75 \pm 1.32, \\ & a_\rho^{V_L V_R} = -1.294 \pm 0.081, & a_\rho^{VS} &= -0.349 \pm 0.037, \\ & a_\rho^{V_L T} = -2.327 \pm 0.189, & a_\rho^{V_R T} &= 5.172 \pm 0.332, \end{aligned} \quad (3.81)$$

$$\begin{aligned} \frac{R_p}{R_p^{\text{SM}}} : \quad & a_p^{SS} = 0.533 \pm 0.029 \pm 0.022, & a_p^{TT} &= 9.304 \pm 2.108 \pm 0.544, \\ & a_p^{V_L V_R} = -0.190 \pm 0.095 \pm 0.130, & a_p^{S_L S_R} &= 0.266 \pm 0.056 \pm 0.065, \\ & a_p^{V_S1} = 0.101 \pm 0.033 \pm 0.037, & a_p^{V_S2} &= 0.523 \pm 0.029 \pm 0.024, \\ & a_p^{V_L T} = -0.583 \pm 0.528 \pm 0.306, & a_p^{V_R T} &= 4.214 \pm 0.453 \pm 0.124, \end{aligned} \quad (3.82)$$

where the systematic errors shown by the third terms of a_p^{ij} are obtained by following Ref. [83] as well as $a_{\Lambda_c}^{ij}$. In the end, we arrive at the following R ratio sum rule:

$$\frac{R_p}{R_p^{\text{SM}}} = (0.284 \pm 0.037) \frac{R_\pi}{R_\pi^{\text{SM}}} + (0.716 \mp 0.037) \frac{R_\rho}{R_\rho^{\text{SM}}} + \delta_p, \quad (3.83)$$

with

$$\begin{aligned}
\delta_p = & (-0.090 \pm 0.059) (|C_{S_L}^{u\tau}|^2 + |C_{S_R}^{u\tau}|^2) + (-0.185 \pm 0.038) \text{Re} (C_{S_L}^{u\tau} C_{S_R}^{u\tau*}) \\
& + (-0.913 \pm 2.403) |C_T^{u\tau}|^2 + (-0.203 \pm 0.538) \text{Re} (C_{V_R}^{u\tau} C_T^{u\tau*}) \\
& + \text{Re} [(1 + C_{V_L}^{u\tau}) \{(0.169 \pm 0.158) C_{V_R}^{u\tau*} + (0.370 \pm 0.632) C_T^{u\tau*}\}] \\
& + (-0.079 \pm 0.056) \text{Re} [(1 + C_{V_L}^{u\tau}) C_{S_R}^{u\tau*} + C_{S_L}^{u\tau} C_{V_R}^{u\tau*}] . \tag{3.84}
\end{aligned}$$

We can find that, compared with δ_{Λ_c} , the shift factor δ_p has larger (smaller) numerical coefficients for the scalar (tensor) terms. This could indicate that (i) the R ratio sum rule for $b \rightarrow u$ is more (less) sensitive to the scalar (tensor) NP contribution, or (ii) there is another different setup so that the NP effect on δ_p is changed. However, such a setup can be checked only when the evaluation of the $\Lambda_b \rightarrow p$ tensor form factors is well-developed. As pointed out in Sec. 3.3, the tensor terms in $B \rightarrow \rho\tau\nu$ are evaluated with a better accuracy than in $B \rightarrow D^*\tau\nu$, thanks to the precise light-meson inputs in the LCSR study. For the tensor terms in $\Lambda_b \rightarrow p\tau\nu$, on the other hand, they are currently obtained based on the estimate of the tensor form factors as detailed in Sec. 3.3. Although a direct lattice QCD calculation of the $\Lambda_b \rightarrow p$ tensor form factors is still missing, our result is already well informative for the moment: one can see that the tensor (scalar) NP contribution is less (more) sensitive in the $b \rightarrow u$ than in the $b \rightarrow c$ case.

For complementary, the SM predictions of the LFU ratios R_X^{SM} with the use of our form factor setup are summarized as

$$\begin{aligned}
R_D^{\text{SM}} = 0.302 \pm 0.008, \quad R_{D^*}^{\text{SM}} = 0.257 \pm 0.005, \quad R_{\Lambda_c}^{\text{SM}} = 0.332 \pm 0.010, \\
R_\pi^{\text{SM}} = 0.719 \pm 0.028, \quad R_\rho^{\text{SM}} = 0.532 \pm 0.011, \quad R_p^{\text{SM}} = 0.688 \pm 0.064. \tag{3.85}
\end{aligned}$$

These values are well consistent with that found in the literature at the 1σ level; see, *e.g.*, Refs. [32, 47, 116] and [37, 77, 108, 117] for the semi-leptonic $b \rightarrow c$ and $b \rightarrow u$ decays, respectively. As suggested in Refs. [33, 118], it would also be advantageous to define the ratio

$$\tilde{R}_M = \int_{m_\tau^2}^{q_{\text{max}}^2} \frac{d\Gamma(B, \Lambda_b \rightarrow M\tau\nu)}{dq^2} dq^2 \bigg/ \int_{m_\tau^2}^{q_{\text{max}}^2} \frac{d\Gamma(B, \Lambda_b \rightarrow M\ell\nu)}{dq^2} dq^2, \tag{3.86}$$

in which the range of q^2 integration in the numerator is the same as in the denominator. This observable has a nice advantage for the lattice inputs, because the lattice study of the form factors has to be performed at around the zero recoil point ($q^2 \sim q_{\text{max}}^2 = (m_{B,\Lambda_b} - m_M)^2$), and the resulting form factors extrapolated to the large recoil region ($q^2 \sim 0$) usually contain large uncertainties. Thus, the uncertainties of the theoretical predictions can be further reduced if we employ the ratio \tilde{R}_M . We can apply the same description of the R ratio sum rule shown above to the

ratio \tilde{R}_M by the replacement $R_M \rightarrow \tilde{R}_M$. Compared to the R_M/R_M^{SM} case, the NP contributions to $\tilde{R}_M/\tilde{R}_M^{\text{SM}}$ do not change, while the SM predictions are obtained as

$$\begin{aligned} \tilde{R}_D^{\text{SM}} &= 0.575 \pm 0.005, & \tilde{R}_{D^*}^{\text{SM}} &= 0.339 \pm 0.003, & \tilde{R}_{\Lambda_c}^{\text{SM}} &= 0.424 \pm 0.006, \\ \tilde{R}_\pi^{\text{SM}} &= 0.814 \pm 0.023, & \tilde{R}_\rho^{\text{SM}} &= 0.605 \pm 0.007, & \tilde{R}_p^{\text{SM}} &= 0.728 \pm 0.038. \end{aligned} \quad (3.87)$$

One can see the efficient reduction of the uncertainties compared to the numerical results given in Eq. (3.85). In the future, the lattice studies could provide the form factor inputs with much better precision than the LCSR evaluations, which is the reason that the ratio \tilde{R}_X can be significant for testing the LFU in these processes.

4 Phenomenological implications

Based on our numerical results, we will discuss phenomenological implications of the R ratio sum rules and make some NP investigations in light of the current experimental measurements.

4.1 The $b \rightarrow c$ mode

In this paper, we do not proceed with the NP investigation in the $b \rightarrow c$ decays, since it has been extensively studied in both theoretical and experimental aspects in the literature (see Refs. [5–8] for recent reviews). Instead, we simply employ the recent fit results for the $R_{D^{(*)}}$ measurements as well as the constraints from the B_c lifetime and the collider searches, analyzed in Ref. [47].

4.1.1 Sum rule predictions and shift factor

The R ratio sum rule introduced in Eq. (2.7) is valid in any tau-philic NP scenario described by the effective weak Hamiltonian in Eq. (2.1). One of its significant points is that we can obtain a unique prediction of the baryonic counterpart from the two semi-leptonic mesonic decays in a model-independent way. This provides a critical consistency check of the experimental measurements among the relevant decay processes, with the theoretical estimations encoded in the sum rule coefficients b and c , as well as the shift factor δ_H . For the present case of the semi-leptonic $b \rightarrow c$ decays, assuming a negligible δ_{Λ_c} and taking the latest world averages of R_D^{exp} and $R_{D^*}^{\text{exp}}$ summarized in Sec. 2.2, we find

$$R_{\Lambda_c}^{\text{SR}} = 0.372 \pm 0.017 \Big|_{R_X^{\text{SM, exp}}} \pm (< 0.001) \Big|_{\text{SR}}, \quad (\text{precise}) \quad (4.1)$$

where the first uncertainty comes from the $R_{D, D^*, \Lambda_c}^{\text{SM, exp}}$ inputs, whereas the second one from the sum rule coefficients and “(< 0.001)” means that the uncertainty is less than 0.001. Thus, we can see that the current form factor uncertainties are actually negligible with respect to the sum rule prediction for R_{Λ_c} . Such a suppression is

caused by the condition $b + c = 1$ of Eq. (2.8), which leads to a perfectly negative correlation between the coefficients b and c . This means that the sum rule prediction relies mainly on the central values of the theoretical inputs. For instance, even if we put a 100% uncertainty in the sum rule coefficients by hand, it still gives a sufficiently small uncertainty of $\pm 0.001|_{\text{SR}}$, which may sound incongruous. Just to be sure, we also take the conservative error estimation without considering the correlation between b and c , which results in

$$R_{\Lambda_c}^{\text{SR}} = 0.372 \pm 0.017|_{R_X^{\text{SM}, \text{exp}}} \pm 0.008|_{\text{SR}}. \quad (\text{conservative}) \quad (4.2)$$

This exercise demonstrates, besides trying to improve the theoretical calculations of the form factors, importance of properly considering the correlation among the form factor parameters when calculating the R ratio sum rule.

It is well-known that the current experimental measurements of R_D and R_{D^*} have discrepancies from the corresponding SM predictions, which is usually referred to as the $R_{D^{(*)}}$ anomalies. A recent NP fit study by two of us in Ref. [47] points out some NP solutions. For instance, a tensor NP scenario with $C_{T,\text{sol}}^{ct} \approx 0.02 \pm i 0.13$ can address the anomalies, which is also allowed by the collider search [65]. If we take this NP scenario, it induces a non-zero shift factor for the R ratio sum rule such as

$$\delta_{\Lambda_c}(C_{T,\text{sol}}^{ct}) = -0.035 \pm 0.096. \quad (4.3)$$

The previous study made in Ref. [50], based just on the central values, concludes that this effect is negligible. As one can see, however, it includes a large uncertainty for the moment and thus the R ratio sum rule relation can be shifted by $\delta_{\Lambda_c} \approx -0.1$ at the 1σ level. This can be compared with $\delta_{\Lambda_c}^{\text{SR/LHCb}} = -0.39 \pm 0.23$ as shown in Eq. (2.15), indicating a discrepancy between the sum rule fit $R_{\Lambda_c}^{\text{SR}}$ and the measured $R_{\Lambda_c}^{\text{LHCb}}$. It also implies that this discrepancy may be compensated with the tensor NP contribution, consistent with the NP solution to $R_{D^{(*)}}^{\text{exp}}$, within the current uncertainty. Therefore, reducing further the uncertainties from the form factor inputs is crucial to test the R_{Λ_c} measurement in comparison with the $R_{\Lambda_c}^{\text{SR}}$ prediction.

4.1.2 Relations to $R_{J/\psi}$ and R_{X_c}

The quark-level $b \rightarrow cl\nu$ transition also gives rise to other hadronic processes that can be measured. In particular, the $B_c \rightarrow J/\psi l\nu$ decays have been observed [16], and the first measurement of $R_{J/\psi}$ has been reported by the LHCb [44] and CMS [45, 46] collaborations. Indeed, it is pointed out that the model-independent NP contribution to $R_{J/\psi}/R_{J/\psi}^{\text{SM}}$ and $R_{D^*}/R_{D^*}^{\text{SM}}$ described by Eq. (2.1) has an interesting relation [119]

$$\frac{R_{J/\psi}}{R_{J/\psi}^{\text{SM}}} \simeq \frac{R_{D^*}}{R_{D^*}^{\text{SM}}}. \quad (4.4)$$

This can also be regarded as a sum rule with $b \simeq 0$ and $c \simeq 1$. By taking the recent experimental measurements as introduced in Sec. 1, we see that

$$\frac{R_{J/\psi}^{\text{exp}}}{R_{J/\psi}^{\text{SM}}} - \frac{R_{D^*}^{\text{exp}}}{R_{D^*}^{\text{SM}}} = 1.2 \pm 0.7, \quad (4.5)$$

where we refer to $R_{J/\psi}^{\text{SM}} = 0.258 \pm 0.004$ from Ref. [120] whereas $R_{D^*}^{\text{SM}}$ from our result of Eq. (3.85). Although the data of $R_{J/\psi}^{\text{exp}}$ still includes a large uncertainty, the relation of Eq. (4.4) is satisfied within 2σ for the moment. We do not go into further detail on this relation, but this is also a good point to be checked and will become significant once the $R_{J/\psi}$ measurement is improved.

There is another counterpart for the exclusive semi-leptonic $b \rightarrow c$ decay, *i.e.* the inclusive process $B \rightarrow X_c l \nu$. The NP contribution to $R_{X_c}/R_{X_c}^{\text{SM}}$ has been studied in Refs. [75, 121–130]. Since the numerical analysis of the inclusive decay depends on the expansion order and the scheme for the bottom-quark mass m_b , evaluating the uncertainties of the numerical coefficients associated with the NP WCs is not straightforward and is beyond the scope of this paper. Thus, we simply refer to the numerical result obtained with the $1S$ scheme for m_b in Ref. [130], which reads

$$\begin{aligned} \frac{R_{X_c}}{R_{X_c}^{\text{SM}}} \simeq & |1 + C_{V_L}^{c\tau}|^2 + |C_{V_R}^{c\tau}|^2 + 0.354(|C_{S_L}^{c\tau}|^2 + |C_{S_R}^{c\tau}|^2) + 11.194 |C_T^{c\tau}|^2 \\ & + 0.360 \text{Re} [(1 + C_{V_L}^{c\tau})C_{S_L}^{c\tau*} + C_{V_R}^{c\tau}C_{S_R}^{c\tau*}] - 0.511 \text{Re} [(1 + C_{V_L}^{c\tau})C_{V_R}^{c\tau*}] \\ & + 0.553 \text{Re} [C_{S_L}^{c\tau}C_{S_R}^{c\tau*}] + 0.564 \text{Re} [(1 + C_{V_L}^{c\tau})C_{S_R}^{c\tau*} + C_{V_R}^{c\tau}C_{S_L}^{c\tau*}] \\ & - 2.705 \text{Re} [(1 + C_{V_L}^{c\tau})C_T^{c\tau*}] + 1.939 \text{Re} [C_{V_R}^{c\tau}C_T^{c\tau*}], \end{aligned} \quad (4.6)$$

where the $\mathcal{O}(1/m_b^2)$ power and the $\mathcal{O}(\alpha_s)$ perturbative corrections to both the SM and NP terms have been properly taken into account. Furthermore, the SM prediction of $R_{X_c}^{\text{SM}}$ including the theoretical uncertainty has been already given in the literature (see, *e.g.*, Refs. [131, 132]), and we refer to $R_{X_c}^{\text{SM}} = 0.220 \pm 0.001$ again from Ref. [130]. One can find that the structure of the NP terms for $R_{X_c}/R_{X_c}^{\text{SM}}$ is the same as that for the baryonic decay $R_{\Lambda_c}/R_{\Lambda_c}^{\text{SM}}$ given by Eq. (2.5). Therefore, it is possible to construct the R ratio sum rule among R_D , R_{D^*} , and R_{X_c} . As an illustration with the central values of the inputs, we have

$$\frac{R_{X_c}}{R_{X_c}^{\text{SM}}} \simeq 0.288 \frac{R_D}{R_D^{\text{SM}}} + 0.712 \frac{R_{D^*}}{R_{D^*}^{\text{SM}}} + \delta_{X_c}, \quad (4.7)$$

with

$$\begin{aligned} \delta_{X_c} \simeq & 0.015 (|C_{S_L}^{c\tau}|^2 + |C_{S_R}^{c\tau}|^2) - 0.003 \text{Re} (C_{S_L}^{c\tau}C_{S_R}^{c\tau*}) - 1.655 |C_T^{c\tau}|^2 \\ & + \text{Re} [(1 + C_{V_L}^{c\tau}) \{0.192C_{V_R}^{c\tau*} + 0.896C_T^{c\tau*}\}] - 3.405 \text{Re} (C_{V_R}^{c\tau}C_T^{c\tau*}) \\ & + 0.043 \text{Re} [(1 + C_{V_L}^{c\tau})C_{S_R}^{c\tau*} + C_{S_L}^{c\tau}C_{V_R}^{c\tau*}]. \end{aligned} \quad (4.8)$$

Then, following the same argument that gives the prediction of $R_{\Lambda_c}^{\text{SR}}$ from the R ratio sum rule as in the previous subsection, we immediately obtain

$$R_{X_c}^{\text{SR}} \simeq 0.247 \pm 0.008 \Big|_{R_X^{\text{SM, exp}}}, \quad (4.9)$$

where only the uncertainties from the SM predictions and the experimental measurements are taken into account, while those from the sum rule coefficients are ignored. It can be seen that the sum rule prediction is consistent with the current experimental measurement, $R_{X_c}^{\text{exp}} = 0.228 \pm 0.039$ [34], after taking into account the large experimental uncertainty. In a similar way, we also find that

$$\delta_{X_c}(C_{T,\text{sol}}^{c\tau}) \simeq -0.011, \quad (4.10)$$

where $C_{T,\text{sol}}^{c\tau} \approx 0.02 \pm i 0.13$ denotes one of the NP solutions to the $R_{D^{(*)}}$ anomalies, as already introduced. Then, we can see that $\delta_{X_c}(C_{T,\text{sol}}^{c\tau})$ has a similar (central) value with that of Eq. (4.3). This can be understood from the fact that the numerical formulae of $R_{X_c}/R_{X_c}^{\text{SM}}$ and $R_{\Lambda_c}/R_{\Lambda_c}^{\text{SM}}$ have similar values and signs. To obtain a more conclusive result, however, we need to evaluate the uncertainties of the NP contributions in the inclusive decay, which is beyond the scope of the present work and will be explored in Ref. [130].

As the inclusive branching fraction corresponds to a sum over that of all the possible exclusive final states, the sum over the decay rates of all these exclusive processes should saturate the inclusive rate. Specific to the $b \rightarrow c$ case, the degree of saturation can be explored by comparing the inclusive branching ratio of $B \rightarrow X_c l \nu$ with the sum over that of $B \rightarrow D^{(*)} l \nu$ and $B \rightarrow D^{**} l \nu$ [7, 33, 132], where D^{**} denote the lightest orbitally excited D states. Our sum rule relation given by Eq. (4.7) could provide another complementary test of the dynamics behind these decays.

4.2 The $b \rightarrow u$ mode

Regarding the semi-leptonic $b \rightarrow u$ decays, we start with the NP investigations. At first, it is noted that parts of the NP WCs $C_i^{u\tau}$ relevant to the $b \rightarrow u\tau\nu$ transition can be constrained from the measured branching ratio of the purely leptonic decay, $\mathcal{B}(B \rightarrow \tau\nu)^{\text{exp}} = (1.09 \pm 0.24) \times 10^{-4}$ [16]. The theoretical prediction including both the SM and NP contributions can be written as

$$\mathcal{B}(B \rightarrow \tau\nu) = \frac{\tau_{B^-} G_F^2 |V_{ub}|^2 f_{B^-}^2}{8\pi} m_{B^-} m_\tau^2 \left(1 - \frac{m_\tau^2}{m_{B^-}^2}\right)^2 |1 + r_{\text{NP}}^{u\tau}|^2, \quad (4.11)$$

where τ_{B^-} and f_{B^-} are the lifetime and decay constant of the charged B meson, and $r_{\text{NP}}^{u\tau}$ represents the NP effect given by

$$r_{\text{NP}}^{u\tau} = C_{V_L}^{u\tau} - C_{V_R}^{u\tau} + \frac{m_{B^-}^2}{m_b m_\tau} (C_{S_R}^{u\tau} - C_{S_L}^{u\tau}). \quad (4.12)$$

Note that the tensor-type NP operator does not contribute to this decay at all. Taking the experimental value of $\mathcal{B}(B \rightarrow \tau\nu)^{\text{exp}} = (1.09 \pm 0.24) \times 10^{-4}$ [16], together with the theoretical inputs of $\tau_{B^-} = (1.638 \pm 0.004)$ ps, $f_{B^-} = (190.0 \pm 1.3)$ MeV and $|V_{ub}| = (3.82 \pm 0.20) \times 10^{-3}$ (the average over the direct determinations of $|V_{ub}|$ from exclusive and inclusive B decays) [16], we have

$$|1 + r_{\text{NP}}^{u\tau}| = 1.08 \pm 0.13, \quad (4.13)$$

which immediately leads to⁴

$$C_{V_L}^{u\tau} \in [-0.05, 0.21], \quad C_{V_R}^{u\tau} \in [-0.21, 0.05], \quad (4.14)$$

$$C_{S_L}^{u\tau} \in [-0.06, 0.01] \cup [0.52, 0.59], \quad C_{S_R}^{u\tau} \in [-0.59, -0.52] \cup [-0.01, 0.06], \quad (4.15)$$

at the 1σ level by assuming the presence of a single and real WC. Although the R_π measurement is currently available [39] as well, it gives mild bounds on $C_i^{u\tau}$ at present due to the large experimental uncertainty. Thus, we do not combine it in the following discussions but check the consistency below.

4.2.1 Correlations among R_X in the presence of NP

In Fig. 1, we show the correlation between R_π and R_ρ in the presence of a single NP contribution within its allowed range as specified in Eqs. (4.14) and (4.15). Regarding the tensor contribution, we just assume a real $C_T^{u\tau}$. The dashed curves represent the trajectories for the central values of R_π and R_ρ , while the cross bars indicate the uncertainties at the benchmark points as illustrations. The black cross bar shows the SM prediction together with its uncertainty. The 1σ lower value of R_π^{exp} is put as the black dashed line, and the upper one is out of the plot range. The effects of the scalar contributions in the vicinity of $C_{S_{L,R}}^{u\tau} \approx 0$ (corresponding to the gray rectangle in the left panel) are separately shown in the upper-right panel for better visibility. The S_R (S_L) effect in the other allowed range of Eq. (4.15) is in the very limited range shown as the cross bar (out of the plot range) in the left panel. Furthermore, we show in Fig. 2 the correlation between R_π and R_ρ , where the prescriptions of the lines, cross bars, and colors are the same as in Fig. 1. From these figures, we can see that (i) the NP effects projected onto the R_π - R_ρ and R_π - R_p planes look similar, (ii) the NP contributions to R_π and R_ρ are well distinctive from the corresponding SM predictions with the present accuracy of the form factor inputs, and (iii) R_p is less predictive due to the large uncertainty from the form factor inputs for the moment. One can also realize that the R ratio sum rule for the $b \rightarrow u$ case is not explicitly readable from these figures.

⁴Here we keep only those solutions with $|C_i^{u\tau}| < 1$, as generally expected from the perturbativity requirement.

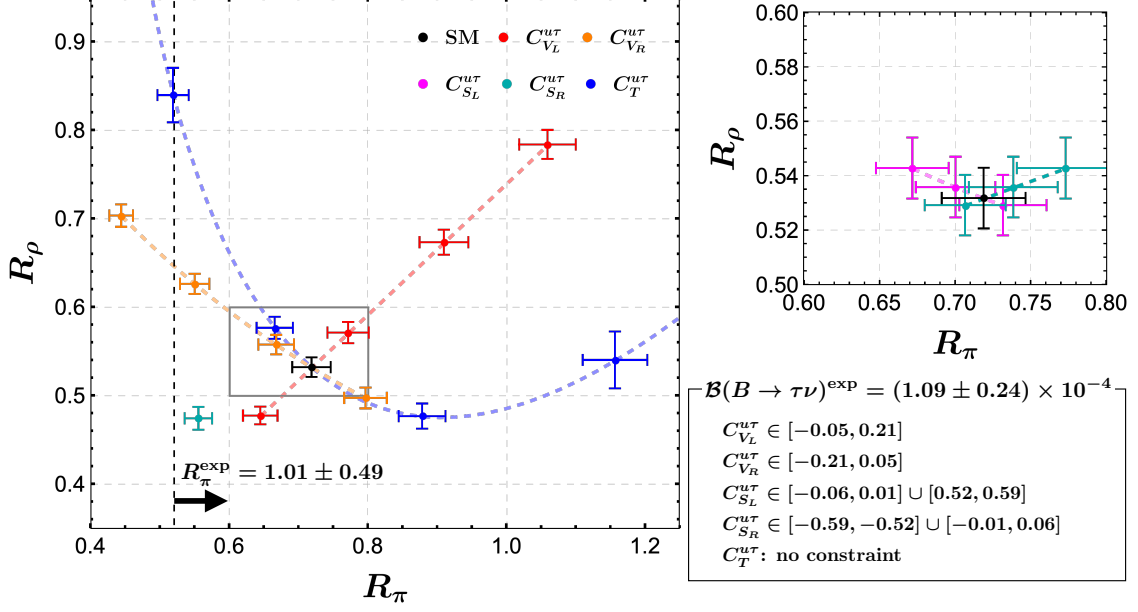


Figure 1. The correlation between R_π and R_ρ in the presence of a single NP contribution indicated on the plot. The SM prediction together with its uncertainty is indicated by the black cross bar, while the NP benchmark points by the cross bars in color, which give the uncertainties as illustrations. See the main text for the other descriptions in detail.

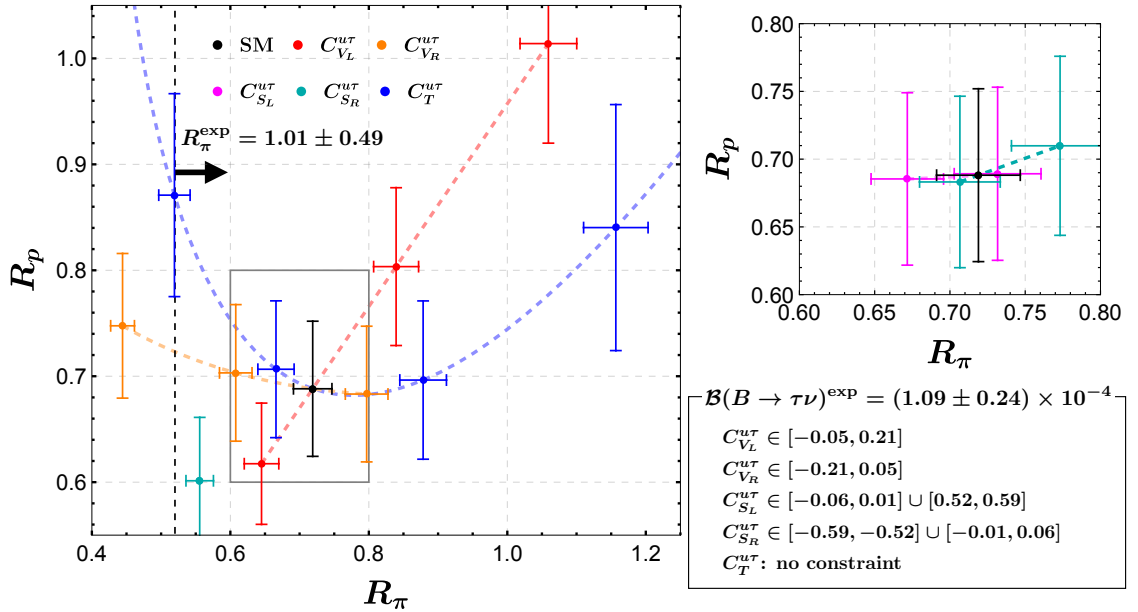


Figure 2. The correlation between R_π and R_ρ in the presence of a single NP contribution. The other captions are the same as in Fig. 1.

Apart from the less predictive R_p , the NP constraints as given by Eqs. (4.14) and (4.15) also lead to the predictions on R_π and R_ρ in the following ranges:

$$V_L : \quad 0.62 \lesssim R_\pi \lesssim 1.10, \quad 0.47 \lesssim R_\rho \lesssim 0.80, \quad (4.16)$$

$$V_R : \quad 0.43 \lesssim R_\pi \lesssim 0.82, \quad 0.72 \gtrsim R_\rho \gtrsim 0.49, \quad (4.17)$$

$$S_L : \quad 0.65 \lesssim R_\pi \lesssim 0.76, \quad 0.55 \gtrsim R_\rho \gtrsim 0.52, \quad (4.18)$$

$$(1.38 \lesssim R_\pi \lesssim 1.73, \quad 0.49 \gtrsim R_\rho \gtrsim 0.46), \quad (4.19)$$

$$S_R : \quad 0.68 \lesssim R_\pi \lesssim 0.81, \quad 0.52 \lesssim R_\rho \lesssim 0.55, \quad (4.20)$$

$$0.59 \gtrsim R_\pi \gtrsim 0.53, \quad 0.46 \lesssim R_\rho \lesssim 0.49, \quad (4.21)$$

where the correlation is aligned with the direction of the inequality signs, and the range in the parenthesis means that this region is out of the plot in Fig. 1. Regarding the NP prediction from the tensor contribution, we need the R_X measurement to study its effect. The bound from the present R_π^{exp} measurement [39] gives a very loose allowed range of $C_T^{u\tau} \in [-0.14, 0.30]$,⁵ and it leads to

$$T : \quad 0.50 \lesssim R_\pi \lesssim 1.57, \quad 0.46 \lesssim R_\rho \lesssim 0.87. \quad (4.22)$$

4.2.2 Sum rule predictions and shift factor

Since the $b \rightarrow u$ case has two missing measurements of $B \rightarrow \rho\tau\nu$ and $\Lambda_b \rightarrow p\tau\nu$, the sum rule prediction is only available for the combination of R_ρ and R_p . This can be represented with a vanishing δ_p as

$$R_p^{\text{SR}} - (0.926 \pm 0.088 |_{R_X^{\text{SM, exp}}} \mp 0.048 |_{\text{SR}}) R_\rho^{\text{SR}} = 0.274 \pm 0.136 |_{R_X^{\text{SM, exp}}} \pm 0.036 |_{\text{SR}}. \quad (4.23)$$

Due to the currently large experimental uncertainty of R_π^{exp} , the sum rule is less predictive at present. Within the SM, the branching ratios of the two missing decay modes, $\bar{B}^0 \rightarrow \rho^+\tau^-\nu$ and $\Lambda_b^0 \rightarrow p\tau^-\nu$, are both predicted to be of $\mathcal{O}(10^{-4})$ [37, 117]. Explicitly, with the updated form factor inputs, we obtain the SM predictions

$$\mathcal{B}(\bar{B}^0 \rightarrow \rho^+\tau^-\nu)_{\text{SM}} = (2.12 \pm 0.43) \times 10^{-4}, \quad (4.24)$$

$$\mathcal{B}(\Lambda_b^0 \rightarrow p\tau^-\nu)_{\text{SM}} = (3.80 \pm 0.44) \times 10^{-4}. \quad (4.25)$$

They should be measurable at the ongoing LHCb run-3 [1, 2] and/or Belle II [3, 4] experiments. In addition, when R_p and R_ρ are measured for the first time, the ratio R_π is also expected to be measured more precisely. Therefore, we believe that our above study offers another good motivation to perform precise measurements of these decays at the future experiments.

⁵Another range of $C_T^{u\tau} \in [-0.96, -0.52]$ is also allowed by R_π^{exp} , but excluded by the collider search, which gives $|C_T^{u\tau}| < 0.42$; see Ref. [65] for further details. Note that the allowed ranges for the other NP scenarios shown in the main text satisfy the collider bound.

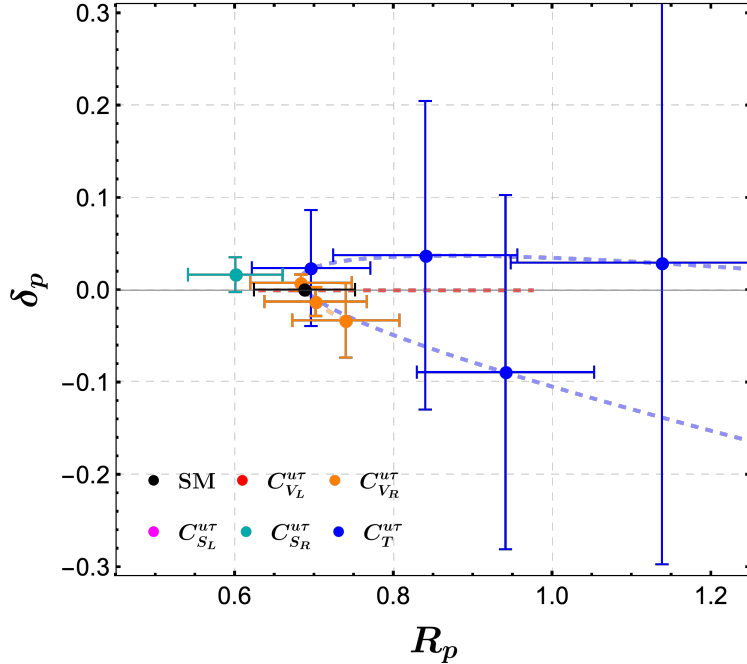


Figure 3. The relation between R_p and δ_p in the presence of a single NP contribution. The V_L scenario gives $\delta_p = 0$ by definition. The $S_{L,R}$ scenarios with $C_{S_L}^{u\tau} \in [-0.06, 0.01]$, $C_{S_R}^{u\tau} \in [-0.01, 0.06]$ give $\delta_p \approx 0$, and thus they are both omitted in the plot. The color prescription for the figure is the same as in Fig. 1.

In Fig. 3, we show the correlation between R_p and δ_p in the presence of a single NP contribution, where the prescription is again the same as in Fig. 1. Note that the V_L scenario gives $\delta_p = 0$ by definition. The $S_{L,R}$ scenarios with $C_{S_L}^{u\tau} \in [-0.06, 0.01]$ and $C_{S_R}^{u\tau} \in [-0.01, 0.06]$ are also omitted in the figure, since they give a negligible value of δ_p even with the form factor uncertainties taken into account. We can see from the figure that the V_R (S_R) scenario could have $\delta_p \approx -0.07$ ($+0.03$) at most, while the T scenario could reach $\delta_p \approx \pm 0.3$ due to the large uncertainty. If a future measurement of R_p has a different value from the corresponding SM prediction, we can then check how large the shift factor δ_p could be from this figure for each NP scenario. As an illustration, we take the T scenario as an example and represent the numerical values of the shift factor δ_p at some representative points of $C_T^{u\tau}$:

$$\delta_p(C_T^{u\tau} = -0.14) = -0.07 \pm 0.11, \quad (4.26)$$

$$\delta_p(C_T^{u\tau} = +0.30) = 0.03 \pm 0.25, \quad (4.27)$$

$$\delta_p(C_T^{u\tau} = -0.41) = -0.31 \pm 0.53, \quad (4.28)$$

where the first two correspond to the 1σ allowed range of $C_T^{u\tau}$ obtained from the measured R_π^{exp} , while the last one to the upper bound set by the collider search [65],

as mentioned in the last subsection. Concerning the scale of the branching ratio and the future statistics of the measurement of this baryonic process, we expect that a shift factor of $|\delta_p| \approx O(0.1)$ can be tested. Recalling that the $\Lambda_b \rightarrow p$ tensor form factor inputs in our analysis are only preliminary [114], a precise evaluation of the tensor form factors, especially with the aid of the next-generation lattice QCD techniques [115], is also necessary.

4.3 Combined study: SMEFT explanation

Finally, we perform a combined study of the $b \rightarrow cl\nu$ and $b \rightarrow ul\nu$ decays in the framework of SMEFT [51–54] with specific flavor symmetries [55, 56]. We begin with the so-called minimal flavor violation (MFV) hypothesis [133–135] and discuss its validity and possible extensions.

4.3.1 Brief description of SMEFT and $U(3)^5$ symmetry

In the case where the NP particles are much heavier than the electroweak scale and the electroweak symmetry breaking is realized linearly, the SMEFT is known to provide a model-independent framework to systematically study such kinds of NP effects, which are encoded in the short-distance WCs of a tower of higher-dimensional operators invariant under the SM gauge group. Following the same conventions as in Ref. [52], we can write the SMEFT Lagrangian as

$$\mathcal{L}_{\text{SMEFT}} = \mathcal{L}_{\text{SM}} + \frac{1}{\Lambda} \sum_i c_i^{(5)} \mathcal{Q}_i^{(5)} + \frac{1}{\Lambda^2} \sum_i c_i^{(6)} \mathcal{Q}_i^{(6)} + \dots, \quad (4.29)$$

where \mathcal{L}_{SM} is the renormalizable SM Lagrangian before the electroweak spontaneous symmetry breaking, whereas $\mathcal{Q}_i^{(n)}$ are the dimension- n operators induced by integrating out the heavy new particles and constructed solely in terms of the SM fields, with $c_i^{(n)}$ the corresponding dimensionless WCs normalized by the NP scale Λ . The ellipsis represents the terms with dimension higher than six.

Below the electroweak scale, the heavy SM particles of the top quark and the W^\pm , Z , Higgs bosons are all decoupled. The resulting theory is then described by the low-energy effective field theory (LEFT) [63, 64] invariant under the strong and electromagnetic gauge groups, which is our starting point of consideration as in Eq. (2.1) for the semi-leptonic $b \rightarrow ql\nu$ transitions. The WCs C_i^{ql} of the LEFT operators in Eq. (2.2) encode all the physics related to the heavy SM and NP degrees of freedom. In principle, these low-energy WCs are independent of $c_i^{(n)}$ in Eq. (4.29). However, if we start with the SMEFT, we can fix the former in terms of the latter by performing a matching between these two effective theories at the electroweak scale [63, 136]. This is our motivation to discuss the SMEFT framework. In practice, the WCs C_i^{ql} are usually evaluated at a low-energy scale μ_{low} characteristic of the process considered (*e.g.*, $\mu_{\text{low}} \simeq m_b$ for $b \rightarrow ql\nu$ decays) to avoid additional large corrections to the matrix elements of the LEFT operators. The connection between

the electroweak and the low-energy scale in LEFT is realized by the renormalization group [137, 138]. Such a standard procedure will be followed in our study.

In a bottom-up approach of the SMEFT, where the underlying ultraviolet-complete NP model is unknown, the flavor structure of the operators $\mathcal{Q}_i^{(n)}$ in Eq. (4.29) is generally not specified. In this case, the corresponding WCs $c_i^{(n)}$ will be flavor dependent, and must be taken as independent free parameters for different flavors. This causes a significant increase in the number of independent terms in the SMEFT Lagrangian, when all the possible flavors are taken into account. The flavor structures of the SMEFT operators can be probed on the basis of the flavor symmetries satisfied by the SM gauge sector. In particular, from the known structure of the SM Yukawa couplings indicated by the observed hierarchies among the SM fermion masses and mixings, we have already known that flavor is highly non-generic. It is therefore natural to employ specific hypotheses about the flavor symmetries on the whole SMEFT, such that the number of independent parameters in $c_i^{(n)}$ can be significantly reduced (see Refs. [53, 54] for reviews). In this paper, we consider first the $U(3)^5$ symmetry [133, 139], which is the maximal flavor symmetry compatible with the SM gauge group. It also allows us to implement the most restrictive hypothesis of MFV that can be utilized to suppress non-standard contributions to the various flavor violating observables [54, 55]. To this end, let us start with the $U(3)^5$ global symmetry transformation of the SM fermions [133, 139]

$$\mathcal{G}_F \equiv U(3)^5 = U(3)_Q \otimes U(3)_U \otimes U(3)_D \otimes U(3)_L \otimes U(3)_E = SU(3)^5 \otimes U(1)^5, \quad (4.30)$$

where the lepton and quark $SU(2)_L$ doublets are written as L and Q respectively, while the right-handed $SU(2)_L$ singlets are denoted by U (up-type quark), D (down-type quark), and E (charged lepton). Here, each $SU(3)$ subgroup acts on the flavor indices of the corresponding fermion field characterized by the subscript. Regarding the $U(1)$ transformations, each fundamental/anti-fundamental representation has a charge ± 1 under the associated Abelian subgroup.

4.3.2 Application to the semi-leptonic $b \rightarrow ql\nu$ processes

Here, let us apply the above formalism to the case of semi-leptonic $b \rightarrow ql\nu$ transitions. We assume that the NP preserves both the baryon and lepton numbers, which is the present case and thus the dimension-five operators $\mathcal{Q}_i^{(5)}$ will be irrelevant. Then, the most relevant dimension-six terms for $b \rightarrow ql\nu$ can be written as [52, 64]

$$\begin{aligned} \sum_i c_i^{(6)} \mathcal{Q}_i^{(6)} \Big|_{b \rightarrow ql\nu} &= c_{H_\ell}^{ij} \left(H^\dagger_i \overleftrightarrow{D}_\mu^I H \right) \left(\bar{L}^i \gamma^\mu \tau^I L^j \right) + c_{H_q}^{mn} \left(H^\dagger_i \overleftrightarrow{D}_\mu^I H \right) \left(\bar{Q}^m \gamma^\mu \tau^I Q^n \right) \\ &+ c_V^{mni j} \left(\bar{Q}^m \gamma^\mu \tau^I Q^n \right) \left(\bar{L}^i \gamma_\mu \tau^I L^j \right) + \left\{ c_{H_{\bar{q}}}^{mn} \left(\tilde{H}^\dagger_i D_\mu H \right) \left(\bar{U}^m \gamma^\mu D^n \right) \right. \\ &\left. + c_{S_d}^{mni j} \left(\bar{L}^i E^j \right) \left(\bar{D}^m Q^n \right) + c_{S_u}^{mni j} \left(\bar{L}^{a,i} E^j \right) \epsilon_{ab} \left(\bar{Q}^{b,m} U^n \right) \right\} \end{aligned}$$

$$+ c_T^{mni j} (\bar{L}^{a,i} \sigma_{\mu\nu} E^j) \epsilon_{ab} (\bar{Q}^{b,m} \sigma^{\mu\nu} U^n) + \text{h.c.} \Big\}, \quad (4.31)$$

where m, n and i, j are the quark and lepton flavor indices respectively, ϵ_{ab} is the anti-symmetric tensor for the $SU(2)_L$ doublet indices a, b , and H is the $SU(2)_L$ Higgs doublet with

$$H^\dagger i \overleftrightarrow{D}_\mu H \equiv i H^\dagger \left(\tau^I D_\mu - \overleftarrow{D}_\mu \tau^I \right) H, \quad \tilde{H} \equiv i \tau^2 H^*. \quad (4.32)$$

We do not consider the operators with dimension $n > 6$, because their effects will be further suppressed by the NP scale Λ . It should be noted that the operators associated with c_{H_ℓ} , c_{H_q} , and $c_{H_{\bar{q}}}$ contribute to the $b \rightarrow ql\nu$ transitions only by modifying the left-handed W couplings with fermions and the right-handed W coupling with quarks, respectively. The first two operators can also modify the Z couplings with the left-handed fermions. However, these modified couplings undergo severe constraints from other processes [140]. For example, global and/or individual fits of the SMEFT WCs to the available experimental data, especially to the electroweak precision observables, have demonstrated that a rough bound of $|c_{H_{\ell,q,\bar{q}}}^{ij,mn}|/\Lambda^2 < \mathcal{O}(10^{-2}) \text{ TeV}^{-2}$ is valid for any lepton and quark flavors [141–143]. This implies that these terms do not give rise to a sizable LFU violating contribution to the $b \rightarrow ql\nu$ transitions of our interest, and we will therefore neglect them in the following discussion.

To establish possible correlations between the $b \rightarrow cl\nu$ and $b \rightarrow ul\nu$ decays within the SMEFT, we now resort to the MFV hypothesis [133, 134]. According to the description presented in App. A, the MFV hypothesis in the quark sector allows us to write the flavor structure of the WC c_V , for instance, as

$$c_V^{mni j} = \delta_{mn} c_{V\ell}^{ij}, \quad (4.33)$$

where the lepton sector is separately represented as $c_{V\ell}^{ij}$ for later convenience. Applying the MFV hypothesis to the lepton sector and requiring the generation of the desired LFU violation between the first two lepton generations and the third one, we have the form of flavor structure

$$c_{V\ell}^{ij} = (Y_E Y_E^\dagger)_{ij} c_V^0, \quad (4.34)$$

where Y_E is the SM Yukawa matrix for lepton, and c_V^0 denotes a flavor universal coupling. Such a structure can naturally generate a τ -philic interaction. A detailed argument to get the above form, together with its comparison with that of a flavor-changing neutral current (FCNC), can be found in App. A. By adopting the same argument to the other terms in Eq. (4.31), we find the following MFV-based flavor structures of the WCs:

$$c_{S_d}^{mni j} = (Y_D^\dagger)_{mn} (Y_E)_{ij} c_{S_d}^0, \quad c_{S_u}^{mni j} = (Y_U)_{mn} (Y_E)_{ij} c_{S_u}^0, \quad (4.35)$$

$$c_T^{mij} = (Y_U)_{mn}(Y_E)_{ij}c_T^0, \quad (4.36)$$

where Y_U and Y_D are the SM Yukawa matrices for up- and down-type quarks, whereas $c_{S_d}^0$, $c_{S_u}^0$ and c_T^0 are flavor universal as well as c_V^0 . Then, matching the SMEFT Lagrangian of Eq. (4.31) to the LEFT one of Eq. (2.2) at the tree level, we obtain the following relations between the WCs of these two effective theories:

$$C_{V_L}^{q\tau} = -\frac{2m_\tau^2}{\Lambda^2}c_V^0, \quad C_{V_R}^{q\tau} = 0, \quad (4.37)$$

$$C_{S_L}^{q\tau} = -\frac{m_\tau m_q}{\Lambda^2}c_{S_u}^{0*}, \quad C_{S_R}^{q\tau} = -\frac{m_\tau m_b}{\Lambda^2}c_{S_d}^{0*}, \quad (4.38)$$

$$C_T^{q\tau} = -\frac{m_\tau m_q}{\Lambda^2}c_T^{0*}, \quad (4.39)$$

for $q = u, c$ at the electroweak scale. Let us remind the normalization factor of $2\sqrt{2}G_F V_{qb}$ in Eq. (2.2) when getting the above matching relations. It should also be noted that the dimension-six terms in SMEFT have no LFU-violating contribution to the right-handed WC $C_{V_R}^{ql}$ in LEFT, and the minimum dimension of the operators to generate such kinds of contributions is found to be $n = 8$, which implies that their effects are further suppressed by the NP scale Λ . See also footnote 1. Finally, we have the following exact relations between the $b \rightarrow c$ and $b \rightarrow u$ sectors:

$$C_{V_L}^{c\tau} = C_{V_L}^{c\tau}, \quad C_{S_R}^{c\tau} = C_{S_R}^{c\tau}, \quad C_{S_L}^{c\tau} = \frac{m_u}{m_c}C_{S_L}^{c\tau} \approx 0, \quad C_T^{c\tau} = \frac{m_u}{m_c}C_T^{c\tau} \approx 0. \quad (4.40)$$

Thus, only the V_L and S_R types of NP are of importance for the $b \rightarrow u\tau\nu$ processes in the framework of SMEFT with MFV. To get sizable contributions of our interest, however, the parameters c_V^0 and $c_{S_d}^0$ are required to be large. This is due to the fact that the insertion of $Y_E Y_E^\dagger$ introduces the large suppression of $m_\tau^2/v^2 \approx 5 \times 10^{-5}$. For instance, the best-fit point from the $R_{D^{(*)}}$ measurements for the V_L -type NP is $C_{V_L}^{c\tau} \approx 0.079$ [47], which leads to $c_V^0/\Lambda^2 \approx -1.25 \times 10^4 \text{ TeV}^{-2}$. Since the parameter c_V^0 itself is not physical, such a large number is not an issue by the way.

4.3.3 Third generation-philic interaction and $U(2)^5$ symmetry

To be more general, Eq. (4.40) can be realized by taking the MFV hypothesis only in the quark sector and simply assuming a τ -philic interaction in the lepton sector. For instance, it is sufficient to just consider $c_{V_\ell}^{\tau\tau}$ defined in Eq. (4.33) as a free parameter while assuming that the other components are all zero, with which we obtain $c_{V_\ell}^{\tau\tau}/\Lambda^2 \approx -1.31 \text{ TeV}^{-2}$ from the combined fit analysis to the $R_{D^{(*)}}$ measurements [47]. For later purpose, we also present its 2σ allowed range

$$-1.83 \text{ TeV}^{-2} < c_{V_\ell}^{\tau\tau}/\Lambda^2 < -0.78 \text{ TeV}^{-2}. \quad (4.41)$$

In any case, the MFV-based parameterization for the lepton sector is not indispensable for our analysis, and hence we may use $c_{V_\ell}^{\tau\tau}$ in the following discussion.

As explained around Eq. (A.10), the leading term generating the quark FCNC interaction is different from the one generating the flavor-changing charged current (FCCC) $b \rightarrow q\tau\nu$ transition. Hence, all the FCNC constraints are actually irrelevant to our analysis. The serious concern is indeed the flavor diagonal part of the $q\bar{q} \rightarrow \tau^+\tau^-$ processes, which is affected by the SMEFT operators of Eq. (4.31). Under the MFV hypothesis in the quark sector, all the quark flavors q have the same WCs for this diagonal part, *e.g.*, $c_V^{1133} = c_V^{2233} = c_V^{3333} = c_V^{\tau\tau}$. This immediately leads to a severe constraint by the $\tau^+\tau^-$ search at the LHC [144, 145]. From a recent study of Ref. [146], we see that

$$-0.0099 \text{ TeV}^{-2} < c_V^{1133}/\Lambda^2 < 0.0040 \text{ TeV}^{-2}, \quad (4.42)$$

$$-0.13 \text{ TeV}^{-2} < c_V^{2233}/\Lambda^2 < 0.040 \text{ TeV}^{-2}, \quad (4.43)$$

$$-0.80 \text{ TeV}^{-2} < c_V^{3333}/\Lambda^2 < 0.53 \text{ TeV}^{-2}, \quad (4.44)$$

for the individual WCs in the SMEFT with the most general flavor structure at 95% CL.⁶ Thus, the LHC bound on $c_V^{\tau\tau}$ has (almost) no overlap with the range given by Eq. (4.41) that is obtained from the $R_{D^{(*)}}$ measurements. This might indicate that the MFV hypothesis of Eq. (4.33) does not work at all.

The problematic LHC bounds of Eqs. (4.42) and (4.43) can be avoided if we start with the third generation-philic WC of the form

$$c_V^{mij} \equiv \delta_{m3}\delta_{n3}\delta_{i3}\delta_{j3}c_V^{\tau\tau}, \quad (4.45)$$

with which we can also produce $C_{V_L}^{u\tau} = C_{V_L}^{c\tau}$, as obtained in Eq. (4.40). In this case, we only need to concern the bound for the third generation WC of Eq. (4.44) for $c_V^{3333} = c_V^{\tau\tau}$. Indeed, such a specific structure can be realized by imposing the $U(2)^5$ flavor symmetry [55, 56, 147–150] on the SMEFT Lagrangian, which distinguishes operators acting on the third generation from that on the first two ones, and constitutes an excellent approximate symmetry of the SM that is broken only at the level of $\mathcal{O}(10^{-2})$. A detailed description can be found in App. A. It is still concerned that the $R_{D^{(*)}}$ bound of Eq. (4.41) is already on the edge of the LHC bound of Eq. (4.44). However, let us point out that there is a loophole in the analysis of Ref. [146]: only the ATLAS search [144] has been taken into account to obtain Eq. (4.44), even though the CMS search is also available [145]. Especially, we would like to mention that the CMS collaboration observed an excess, which could result in a milder bound on c_V^{3333} , and hence the ATLAS and CMS measurements are not yet conclusive. It would be, therefore, reasonable to take Eq. (4.44) only as a reference bound for now, and a

⁶Two points should be noted here: (i) our notation of the SMEFT WCs corresponds to the well-known convention [52], such as $c_V^{1133} = [\mathcal{C}_q^{(3)}]_{3311}$; (ii) to be precise, the MFV case needs to take into account all the quark generations for the $\tau^+\tau^-$ production in the analysis, which is different from the individual constraints and should obtain a much stronger bound [146].

further improved search for the $\tau^+\tau^-$ final state is expected. In addition, the ratio $R_{\Upsilon(3S)} = \Gamma(\Upsilon(3S) \rightarrow \tau^+\tau^-)/\Gamma(\Upsilon(3S) \rightarrow \ell^+\ell^-)$ can also provide a viable constraint

$$-37.1 \text{ TeV}^{-2} < c_{V\ell}^{\tau\tau}/\Lambda^2 < 3.2 \text{ TeV}^{-2}, \quad (4.46)$$

at the 2σ level, by taking the analytic formula and the experimental data taken from Refs. [47, 151, 152]. We can clearly see that the $R_{D^{(*)}}$ bound of Eq. (4.41) lies within the range obtained from the $R_{\Upsilon(3S)}$ measurement.

The LHC bounds are also crucial in the case of $c_{S_d}^{mni j}$ with MFV. Again, the third generation-philic scenario of

$$c_{S_d}^{mni j} \equiv \delta_{m3}\delta_{n3}\delta_{i3}\delta_{j3}c_{S\ell}^{\tau\tau}, \quad (4.47)$$

works for the semi-leptonic $b \rightarrow ql\nu$ decays, and hence it is viable as a good approximation of the $U(2)^5$ flavor symmetry that generates $C_{S_R}^{u\tau} = C_{S_R}^{c\tau}$, as illustrated in App. A. In this case, the LHC bound on $c_{S_d}^{3333} = c_{S\ell}^{\tau\tau}$, read from Ref. [146], can be obtained as

$$-0.92 \text{ TeV}^{-2} < c_{S\ell}^{\tau\tau}/\Lambda^2 < 0.92 \text{ TeV}^{-2}, \quad (4.48)$$

at 95% CL, after running from the scale $\Lambda = 1 \text{ TeV}$ down to the m_b scale [47, 153]. This is the only relevant constraint, while the $R_{\Upsilon(3S)}$ measurement is not affected by the operator associated with $c_{S_d}^{mni j}$. For the cases of $c_{S_u}^{mni j}$ and $c_T^{mni j}$, on the other hand, although the $U(2)^5$ flavor symmetry also supports the third generation-philic setup, it induces negligible and hierarchical contributions to the semi-leptonic $b \rightarrow c$ and $b \rightarrow u$ decays; see App. A for further details.

To summarize, the relation of Eq. (4.40) is still valid in this third generation-philic setup and also consistent with the relevant experimental constraints. Finally, one should note that renormalization group running from the electroweak to the B -meson scale does not change the relations between $C_X^{u\tau}$ and $C_X^{c\tau}$ specified in Eq. (4.40). Thus, we can adopt these relations in the following numerical analysis.

4.3.4 Numerical analysis

With the above setup, the measured branching ratio of $\mathcal{B}(B \rightarrow \tau\nu)^{\text{exp}}$ [16], the latest $R_D-R_{D^*}$ fit [47], and the LHC bounds [146] are most relevant to our combined analysis. In Fig. 4, we put projections on the R_D-R_π and $R_{D^*}-R_\rho$ planes, allowed/favored by these three considerations for the V_L and S_R types of NP scenarios. Here, the red and dark-cyan dashed lines, indicating the resulting central values of the ratios R_X , are obtained under the constraint of $\mathcal{B}(B \rightarrow \tau\nu)^{\text{exp}}$ for V_L and S_R , respectively. The red and blue regions are favored by the $R_D-R_{D^*}$ fit results within 2σ for V_L and S_R , respectively. The measured $R_{D^{(*)}}^{\text{exp}}$ are also shown by the gray bands, with the dashed (solid) vertical lines at the 1σ (2σ) level. It should be noted that the current best-fit solution of the S_R -type NP scenario cannot reproduce the central

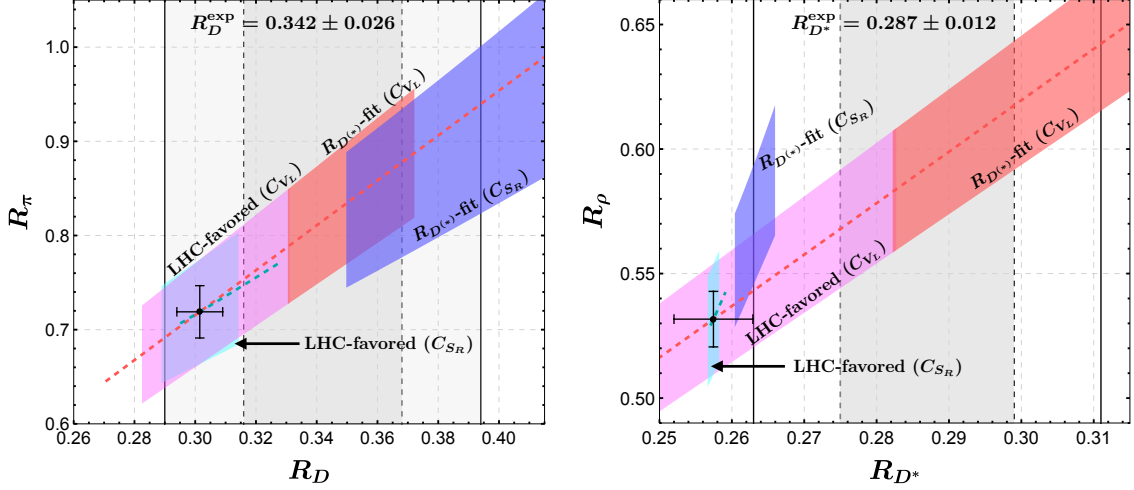


Figure 4. Projections on the R_D - R_π and R_{D^*} - R_ρ planes evaluated from the measured $\mathcal{B}(B \rightarrow \tau\nu)^{\text{exp}}$, the latest R_D - R_{D^*} fit, and the LHC bounds. The individual measurements of $R_{D^{(*)}}^{\text{exp}}$ are also shown at the 1σ (2σ) level, as indicated by the dashed (solid) vertical lines. The red and dark-cyan dashed lines are obtained by the $\mathcal{B}(B \rightarrow \tau\nu)$ measurement for the V_L and S_R types of NP scenarios, respectively. The allowed/favored regions from the R_D - R_{D^*} fit and the LHC bounds are shown in different colors as described in the figure.

values $R_{D^{(*)}}^{\text{exp}}$, although the scenario improves the fit to the $R_{D^{(*)}}$ data [47]. We also show the 2σ favored regions resulting from the LHC bounds in light-magenta and light-cyan for V_L and S_R , respectively. However, let us repeat that the LHC bounds are not conclusive yet and taken only as illustrations. From Fig. 4, we can see that the R_D - R_{D^*} fit is (not) consistent with the $\mathcal{B}(B \rightarrow \tau\nu)^{\text{exp}}$ constraint in the V_L (S_R)-type NP scenario. Hence, the S_R -type NP scenario is excluded as long as the relation of $C_{S_R}^{u\tau} = C_{S_R}^{c\tau}$ is assumed. This is a significant outcome of our combined analysis.

We can also *predict* the ratio R_p in our combined analysis with the specific flavor symmetries. The relation of $C_{V_L}^{u\tau} = C_{V_L}^{c\tau}$ leads to

$$V_L\text{-type NP: } R_p = \frac{R_p^{\text{SM}}}{R_{\Lambda_c}^{\text{SM}}} R_{\Lambda_c}. \quad (4.49)$$

Hence, the sum rule fit result of $R_{\Lambda_c}^{\text{SR}}$ given in Eq. (2.13) and the LHCb measurement of $R_{\Lambda_c}^{\text{LHCb}}$ in Eq. (2.14), respectively, imply

$$R_{\Lambda_c}^{\text{SR}} : 0.69 \lesssim R_p \lesssim 0.85, \quad (4.50)$$

$$R_{\Lambda_c}^{\text{LHCb}} : 0.34 \lesssim R_p \lesssim 0.67. \quad (4.51)$$

Although these predictions are still quite uncertain, the former is more consistent with the SM value than the latter. Therefore, we see that the discrepancy between $R_{\Lambda_c}^{\text{SR}}$ and $R_{\Lambda_c}^{\text{LHCb}}$ can be tested once the ratio R_p is observed. To conclude, we expect

that measuring the ratios R_π , R_ρ and R_p for the $b \rightarrow u$ sector can provide another check of the R ratio sum rule for the $b \rightarrow c$ sector implied from the $R_{D^{(*)}}$ anomalies. It can also test the third generation-philic NP scenario discussed here.

5 Summary

As a powerful tool to test the LFU of the SM, the ratios $R_{D^{(*)}}$ and R_{Λ_c} have recently received a lot of attention, because any significant deviations between the experimental measurements and the theoretical predictions of them would directly indicate the presence of NP beyond the SM. Interestingly enough, there exists a strong correlation among R_D , R_{D^*} and R_{Λ_c} , which is referred to as the R ratio sum rule that is almost independent of NP contributions to the processes. Therefore, the R ratio sum rule gives a crucial feedback to the experimental measurements. However, to be definitely conclusive, we need precise calculations of both the SM predictions and the NP contributions. On the other hand, although the same arguments can be applied to the ratios R_π , R_ρ , and R_p as above, we still have fewer measurements and/or theoretical studies of the semi-leptonic $b \rightarrow ul\nu$ decays. As such a situation will be significantly improved at the ongoing LHCb run-3 and Belle II experiments, it is also important to perform a precise study of both the SM and NP effects in the $b \rightarrow u$ sector.

Motivated by the above observations, we have in this paper performed a detailed study of all the aforementioned R_X ratios in the presence of model-independent NP contributions by using the available lattice QCD and/or LCSR fits to the $B \rightarrow P$ ($P = D, \pi$), $B \rightarrow V$ ($V = D^*, \rho$) and $\Lambda_b \rightarrow H$ ($H = \Lambda_c, p$) form factors. In particular, we have evaluated the uncertainties of the NP contributions to every R_X ratio, the R ratio sum rules, and the shift factor δ_H , inherited from the form factor fits for both the SM and NP currents. It is found that our result of δ_{Λ_c} (for the central value) is consistent with that obtained in the previous studies while our result gives the uncertainty for the first time. We have also obtained the R ratio sum rule among R_π , R_ρ , and R_p for the first time. To establish possible correlations between the $b \rightarrow cl\nu$ and $b \rightarrow ul\nu$ processes, we have also performed a combined study in the framework of SMEFT with specific flavor symmetries. Our main results can be summarized as below.

- In Sec. 4.1, we have obtained the explicit R_{Λ_c} prediction from the R ratio sum rule as in Eq. (4.1), namely,

$$R_{\Lambda_c}^{\text{SR}} = 0.372 \pm 0.017 \Big|_{R_X^{\text{SM, exp}}} \pm (< 0.001) \Big|_{\text{SR}}, \quad (5.1)$$

which indicates that the uncertainty stemming from the sum rule is negligible. This concludes that the current experimental measurement $R_{\Lambda_c}^{\text{LHCb}} = 0.242 \pm 0.076$ still shows a significant deviation from the sum rule prediction, implying $\delta_{\Lambda_c}^{\text{SR/LHCb}} = -0.39 \pm 0.23$ as in Eq. (2.15). On the other hand, we found that

the shift factor δ_{Λ_c} involves non-negligible uncertainties from the form factor inputs. For instance, it turned out that the tensor NP solution to the R_D - R_{D^*} fit generates $\delta_{\Lambda_c}(C_{T,\text{sol}}^{c\tau} \approx 0.02 \pm i 0.13) = -0.035 \pm 0.096$ as in Eq. (4.3), which may be compared with $\delta_{\Lambda_c}^{\text{SR/LHCb}}$. Thus, we found that this discrepancy may be compensated with the tensor NP contribution, consistent with the NP solution to $R_{D^{(*)}}^{\text{exp}}$, within the current uncertainty. This is one of the novel points of our study, which is available only by evaluating the uncertainties from the form factor inputs. Our result also offers an extensive motivation for reducing the uncertainties of the form factor inputs in the $b \rightarrow c$ sector.

- In Sec. 4.2, we have obtained, from the R ratio sum rule, the relation between R_ρ and R_p that have not been measured yet. To see a conclusive correlation, however, the precise measurements of R_π and R_ρ are necessary. Apart from the sum rule, we have additionally investigated the NP effects on the R_π - R_ρ and R_π - R_p relations, in which the uncertainties are also considered. It turned out that the NP type can be distinguished by the R_π - R_ρ plane even with the current uncertainty. On the other hand, it is difficult to see the specific relation on R_π - R_p distinct for each NP type since R_p includes the large uncertainties. It also shows a good motivation for evaluating the form factor inputs from the theoretical side and measuring R_X from the experimental side in the $b \rightarrow u$ sector.
- In addition, we have configured two significant R ratio sum rules by employing the ratios $R_{J/\psi}$ from $B_c \rightarrow J/\psi l \nu$ and R_{X_c} from $B \rightarrow X_c l \nu$ decays, respectively. The sum rule given by Eq. (4.4) would become significant once the $R_{J/\psi}$ measurement is improved, while the sum rule among R_{X_c} , R_D and R_{D^*} could provide another complementary test of the dynamics behind these decays.
- We have performed a combined study of the $b \rightarrow cl\nu$ and $b \rightarrow ul\nu$ decays based on the SMEFT with both $U(3)^5$ and $U(2)^5$ flavor symmetries. Under the assumption, the corresponding WCs can be correlated such as $C_{V_L}^{u\tau} = C_{V_L}^{c\tau}$ and $C_{S_R}^{u\tau} = C_{S_R}^{c\tau}$, resulting in the interesting correlations between the $b \rightarrow c$ and $b \rightarrow u$ decays. It is found that the R_D - R_{D^*} fit is (not) consistent with the $\mathcal{B}(B \rightarrow \tau\nu)^{\text{exp}}$ constraint in the $V_L(S_R)$ -type NP scenario. Hence, the S_R -type NP scenario is excluded as long as the relation of $C_{S_R}^{u\tau} = C_{S_R}^{c\tau}$ is assumed. On the other hand, the V_L -type NP gives the explicit relation as $R_p/R_p^{\text{SM}} = R_{\Lambda_c}/R_{\Lambda_c}^{\text{SM}}$. This could provide a further consistency check of $R_{\Lambda_c}^{\text{SR}}$ and $R_{\Lambda_c}^{\text{LHCb}}$ in such a flavor specific NP scenario, if R_p is observed by the future experiments.

With the successful running of Belle II and LHCb run-3, together with the progress of lattice QCD and LCSR calculations of the form factors, we will have more precise predictions of the R_X ratios and subsequently the R ratio sum rules, which

can be utilized to identify the potential NP scenarios responsible for the $b \rightarrow c\tau\nu$ anomaly and possible deviations in the $b \rightarrow u\tau\nu$ processes in the future.

Acknowledgement

We appreciate Takashi Kaneko for the fruitful discussion about the lattice results of the form factor inputs. We also thank Stefan Meinel for providing his preliminary evaluation of the $\Lambda_b \rightarrow p$ tensor form factors. This work is supported by the National Natural Science Foundation of China under Grant Nos. 12475094, 12135006 and 12075097, as well as by the Fundamental Research Funds for the Central Universities under Grant Nos. CCNU22LJ004 and CCNU24AI003. S.I. enjoys support from JSPS KAKENHI Grant Number 24K22879 and JPJSCCA20200002.

A Flavor symmetries for the semi-leptonic decays

A.1 MFV hypothesis

Within the SM, the Yukawa sector is the only breaking source of the symmetry group \mathcal{G}_F defined by Eq. (4.30). However, once we promote the SM Yukawa couplings $Y_{U,D,E}$ to become some *spurions*, *i.e.*, non-dynamical fields with the well-defined transformation properties under the non-Abelian part of \mathcal{G}_F ,

$$Y_U \sim (\mathbf{3}, \bar{\mathbf{3}}, \mathbf{1}, \mathbf{1}, \mathbf{1}), \quad Y_D \sim (\mathbf{3}, \mathbf{1}, \bar{\mathbf{3}}, \mathbf{1}, \mathbf{1}), \quad Y_E \sim (\mathbf{1}, \mathbf{1}, \mathbf{1}, \mathbf{3}, \bar{\mathbf{3}}), \quad (\text{A.1})$$

for each $SU(3)$ factor in the same order as in Eq. (4.30), the whole SM Lagrangian will be formally invariant under the global symmetry of \mathcal{G}_F . The above configuration can be adapted to the SMEFT Lagrangian as well. This means that all the higher-dimensional operators built out of the SM field contents and the Yukawa spurions $Y_{U,D,E}$ in the SMEFT can be made formally invariant under \mathcal{G}_F to all orders, and the breaking of the symmetry occurs only via the appropriate insertions of the spurions $Y_{U,D,E}$, which induces the flavor violating interactions below the electroweak scale [133, 134]. Notice that, with the MFV hypothesis, the dynamics of flavor violation is completely determined by the structure of the ordinary Yukawa couplings, both within the SM and beyond [54, 55].

As an illustration, let us discuss the term associated with c_V introduced in Eq. (4.31). The MFV criterion implies that the quark and lepton sectors are factorized such that $c_V^{mni j} = c_{Vq}^{mn} c_{V\ell}^{ij}$, where c_{Vq}^{mn} and $c_{V\ell}^{ij}$ transform as $(\mathbf{1} \oplus \mathbf{8}, \mathbf{1}, \mathbf{1})$ and $(\mathbf{1} \oplus \mathbf{8}, \mathbf{1})$ under the $SU(3)_Q \otimes SU(3)_U \otimes SU(3)_D$ and $SU(3)_L \otimes SU(3)_E$ subgroups of \mathcal{G}_F , respectively. The most general form of c_{Vq} can be represented in terms of the building blocks $Y_U Y_U^\dagger$ and $Y_D Y_D^\dagger$ as [154, 155]

$$c_{Vq}^{mn} = \left(b_0^{(q)} \mathbf{1} + b_1^{(q)} (Y_U Y_U^\dagger) + b_2^{(q)} (Y_D Y_D^\dagger) + \dots \right)_{mn}, \quad (\text{A.2})$$

where $b_k^{(q)}$ are undetermined but flavor-blind coefficients, and the ellipsis denotes other terms with any possible products of $Y_U Y_U^\dagger$ and $Y_D Y_D^\dagger$ with some finite powers. The complete expression can be found in Ref. [155], which is however not necessary for our case, as will be described below. Explicitly, the quark sector has the following contributions to the left-handed charged current of $\bar{u}_L^m \gamma^\mu d_L^n$:

$$\delta_{mn} (\bar{u}_L^m \gamma^\mu d_L^n) \rightarrow V_{u^m d^n} (\bar{u}_L^m \gamma^\mu d_L^n) , \quad (\text{A.3})$$

$$(Y_U Y_U^\dagger)_{mn} (\bar{u}_L^m \gamma^\mu d_L^n) \rightarrow \frac{2m_{u^m}^2}{v^2} V_{u^m d^n} (\bar{u}_L^m \gamma^\mu d_L^n) , \quad (\text{A.4})$$

$$(Y_D Y_D^\dagger)_{mn} (\bar{u}_L^m \gamma^\mu d_L^n) \rightarrow \frac{2m_{d^n}^2}{v^2} V_{u^m d^n} (\bar{u}_L^m \gamma^\mu d_L^n) , \quad (\text{A.5})$$

where the quark fields on the right-hand side are already transformed from the weak to the mass eigenstate basis, $f_L \rightarrow f'_L = W_f^\dagger f_L$, with W_f being the 3×3 unitary matrices in flavor space and the prime being omitted in the above equations. We can see that in the fermion mass eigenbasis, the FCCC transition induced by the $b_{k \neq 0}^{(q)}$ terms occurs via the elements of the CKM matrix $V = W_u^\dagger W_d$, together with the suppression factor $(m_q^2/v^2)^k$. Therefore, all the terms with $b_{k \neq 0}^{(q)}$ are negligible for $b \rightarrow (u, c)$ transitions as long as all the coefficients $b_k^{(q)}$ are assumed to be of the same order. As a consequence, we need only keep the term with $b_0^{(q)}$ for the quark sector and, up to here, the WC c_V can be expressed as

$$c_V^{mnij} = \delta_{mn} c_{V\ell}^{ij} . \quad (\text{A.6})$$

In the same way, the MFV hypothesis in the lepton sector allows us to represent the flavor structure of $c_{V\ell}^{ij}$ as [135, 155]

$$c_{V\ell}^{ij} = \left(\sum_{k=0} b_k^{(\ell)} (Y_E Y_E^\dagger)^k \right)_{ij} , \quad (\text{A.7})$$

and, after performing the necessary mass basis rotation, we have

$$(Y_E Y_E^\dagger)_{ij} (\bar{\ell}_L^i \gamma^\mu \nu_L^j) \rightarrow \frac{2m_{\ell^i}^2}{v^2} \delta_{ij} (\bar{\ell}_L^i \gamma^\mu \nu_L^j) . \quad (\text{A.8})$$

It is observed that the terms with $b_{k \neq 0}^{(\ell)}$ naturally induce a τ -philic interaction and $b_1^{(\ell)}$ gives the largest contribution, while $b_0^{(\ell)} = 0$ is necessary to obtain the desired LFU violation. To conclude, the natural setup of the WC c_V under the MFV hypothesis can finally be represented as

$$c_V^{mnij} = \delta_{mn} (Y_E Y_E^\dagger)_{ij} c_V^0 , \quad (\text{A.9})$$

where $c_V^0 \equiv b_0^{(q)} b_1^{(\ell)}$, and we have taken $b_0^{(\ell)} = 0$ in the lepton sector.

From the form of Eq. (A.2), we can also see that the quark flavor structures differ between the charged and neutral currents. For instance, the quark sector $\bar{Q}^m \gamma^\mu \tau^I Q^n$ of our interest also induces the neutral current $\bar{d}_L^m \gamma^\mu d_L^n$. In this case, the $b_{k \neq 0}^{(q)}$ terms provide the following dominant contribution from the mass basis rotation:

$$(Y_U Y_U^\dagger)_{mn} (\bar{d}_L^m \gamma^\mu d_L^n) \rightarrow \sum_l \frac{m_{u^l}^2}{v^2} V_{u^l d^m}^* V_{u^l d^n} (\bar{d}_L^m \gamma^\mu d_L^n) \approx \frac{m_t^2}{v^2} V_{td^m}^* V_{td^n} (\bar{d}_L^m \gamma^\mu d_L^n), \quad (\text{A.10})$$

which is different from Eq. (A.4) and generates a considerable effect on the FCNC process like $b \rightarrow s \ell \ell$. This is the original idea to introduce the MFV hypothesis to constrain the coefficients $b_{k \neq 0}^{(q)}$. Note also that the term with $b_0^{(q)}$ of Eq. (A.2), while producing the leading contribution to the semi-leptonic $b \rightarrow q l \nu$ transitions, does not induce the tree-level FCNC interactions.

A.2 Third generation-philic flavor structure

The $U(2)^5$ approach is somewhat similar to what has been discussed for the $U(3)^5$ flavor symmetry, with the only difference that we are now requiring the SMEFT Lagrangian to be invariant under the smaller group [147–149]

$$U(2)^5 = U(2)_Q \otimes U(2)_U \otimes U(2)_D \otimes U(2)_L \otimes U(2)_E. \quad (\text{A.11})$$

By construction, the symmetry acts on each of the five SM fermion species with different gauge quantum numbers, as indicated by the subscripts in Eq. (A.11). Within each of these species, the first two generations transform as a doublet, while the third one as a singlet, under the corresponding $U(2)$ subgroup. Explicitly, the $U(2)^5$ representations of the five SM fermion species can be written, respectively, as

$$Q = \begin{bmatrix} Q^a \sim (\mathbf{2}, \mathbf{1}, \mathbf{1}, \mathbf{1}, \mathbf{1}) \\ Q^3 \sim (\mathbf{1}, \mathbf{1}, \mathbf{1}, \mathbf{1}, \mathbf{1}) \end{bmatrix}, \quad L = \begin{bmatrix} L^a \sim (\mathbf{1}, \mathbf{1}, \mathbf{1}, \mathbf{2}, \mathbf{1}) \\ L^3 \sim (\mathbf{1}, \mathbf{1}, \mathbf{1}, \mathbf{1}, \mathbf{1}) \end{bmatrix}, \quad (\text{A.12})$$

and

$$U = \begin{bmatrix} U^a \sim (\mathbf{1}, \mathbf{2}, \mathbf{1}, \mathbf{1}, \mathbf{1}) \\ U^3 \sim (\mathbf{1}, \mathbf{1}, \mathbf{1}, \mathbf{1}, \mathbf{1}) \end{bmatrix}, D = \begin{bmatrix} D^a \sim (\mathbf{1}, \mathbf{1}, \mathbf{2}, \mathbf{1}, \mathbf{1}) \\ D^3 \sim (\mathbf{1}, \mathbf{1}, \mathbf{1}, \mathbf{1}, \mathbf{1}) \end{bmatrix}, E = \begin{bmatrix} E^a \sim (\mathbf{1}, \mathbf{1}, \mathbf{1}, \mathbf{1}, \mathbf{2}) \\ E^3 \sim (\mathbf{1}, \mathbf{1}, \mathbf{1}, \mathbf{1}, \mathbf{1}) \end{bmatrix}, \quad (\text{A.13})$$

with the flavor index $a = 1, 2$. To obtain the $U(2)^5$ invariant subset from the full SMEFT basis of Eq. (4.31), let us introduce the minimal set of spurions needed to reproduce the observed SM fermion masses and mixings [55, 56]

$$\begin{aligned} V_Q &\sim (\mathbf{2}, \mathbf{1}, \mathbf{1}, \mathbf{1}, \mathbf{1}), & V_L &\sim (\mathbf{1}, \mathbf{1}, \mathbf{1}, \mathbf{2}, \mathbf{1}), \\ \Delta_U &\sim (\mathbf{2}, \bar{\mathbf{2}}, \mathbf{1}, \mathbf{1}, \mathbf{1}), & \Delta_D &\sim (\mathbf{2}, \mathbf{1}, \bar{\mathbf{2}}, \mathbf{1}, \mathbf{1}), & \Delta_E &\sim (\mathbf{1}, \mathbf{1}, \mathbf{1}, \mathbf{2}, \bar{\mathbf{2}}), \end{aligned} \quad (\text{A.14})$$

where V_Q and V_L are two-dimensional complex vectors, while Δ_U , Δ_D and Δ_E are 2×2 complex matrices. In terms of these spurions, the 3×3 Yukawa couplings $Y_{U,D,E}$ can be decomposed, respectively, as [55, 56]

$$Y_U = y_t \begin{pmatrix} \Delta_U x_t V_Q \\ 0 & 1 \end{pmatrix}, \quad Y_D = y_b \begin{pmatrix} \Delta_D x_b V_Q \\ 0 & 1 \end{pmatrix}, \quad Y_E = y_\tau \begin{pmatrix} \Delta_E x_\tau V_L \\ 0 & 1 \end{pmatrix}, \quad (\text{A.15})$$

where $x_{t,b,\tau}$ and $y_{t,b,\tau}$ are free complex parameters that are all expected to be of $\mathcal{O}(1)$. Unlike the case of $U(3)^5$ symmetry, the spurions introduced here cannot be completely determined in terms of the fermion masses and mixings, and we can only estimate their sizes by requiring no fine-tuning in these $\mathcal{O}(1)$ parameters. This implies that $|V_{Q,L}| = \mathcal{O}(10^{-1})$, while the entries in $\Delta_{U,D,E}$ are significantly smaller than $|V_{Q,L}|$, with a maximal size of $\mathcal{O}(10^{-2})$ in the quark sector [156].⁷

If we consider the insertion of at most one power of the leading spurion V_Q and one power of the leading spurion V_L while neglecting all the sub-leading spurions $\Delta_{U,D,E}$, the $U(2)^5$ invariant form of the third term on the right-hand side of Eq. (4.31) can then be written as [156]

$$c_V^0 (\Gamma_L^\dagger)^{in} (\Gamma_L)^{mj} (\bar{Q}^m \gamma^\mu \tau^I Q^n) (\bar{L}^i \gamma_\mu \tau^I L^j), \quad (\text{A.16})$$

where c_V^0 determines the overall strength of the NP effect, and the flavor structure is parametrized by the product of two factorized tensors, $(\Gamma_L^\dagger)^{in} (\Gamma_L)^{mj}$. They are normalized by $(\Gamma_L^\dagger)^{33} (\Gamma_L)^{33} = 1$, which is the only term surviving in the exact $U(2)^5$ symmetric limit. The explicit expression of the tensor Γ_L^{mj} is given in the interaction basis by [156]

$$\Gamma_L^{mj} = \begin{pmatrix} x_{QL} V_Q^m (V_L^j)^* & x_Q V_Q^m \\ x_L (V_L^j)^* & 1 \end{pmatrix}, \quad (\text{A.17})$$

where x_Q , x_L and x_{QL} are $\mathcal{O}(1)$ coefficients and all the higher-order terms in $V_{Q,L}$ have been neglected. Transforming to the mass eigenstate bases of down-type quarks and charged leptons, with

$$Q_L^m = \begin{pmatrix} V_{nm}^* u_L^n \\ d_L^m \end{pmatrix}, \quad L_L^j = \begin{pmatrix} \nu_L^j \\ e_L^j \end{pmatrix}, \quad (\text{A.18})$$

we have $\Gamma_L \rightarrow \hat{\Gamma}_L = W_d^\dagger \Gamma_L W_e$, where W_d and W_e are the unitary transformations introduced to diagonalize the Yukawa couplings Y_D and Y_E , respectively. Making

⁷It should be noted that, in the limit of vanishing neutrino masses, the size of $|V_L|$ cannot be unambiguously determined, and the SM lepton Yukawa coupling Y_E can even be reproduced by setting $V_L = 0$. On the other hand, assuming a common structure for the three Yukawa couplings, as suggested by the similar hierarchies observed in their eigenvalues, it is natural to assume that $|V_Q| \sim |V_L|$. This in turn ensures the hypothesis of a common origin for the two leading $U(2)^5$ breaking terms in the quark and lepton sectors [54, 156].

use of the general forms of W_d and W_e given in Ref. [156] and neglecting the tiny terms suppressed by more than two powers of $V_{Q,L}$, we have [156]

$$\hat{\Gamma}_L = e^{i\phi_Q} \begin{pmatrix} \Delta_{QL}^{de} & \Delta_{QL}^{d\mu} & \lambda_Q^d \\ \Delta_{QL}^{se} & \Delta_{QL}^{s\mu} & \lambda_Q^s \\ \lambda_L^e & \lambda_L^\mu & x_{QL}^{b\tau} \end{pmatrix} \approx e^{i\phi_Q} \begin{pmatrix} 0 & 0 & \lambda_Q^d \\ 0 & \Delta_{QL}^{s\mu} & \lambda_Q^s \\ \lambda_L^e & \lambda_L^\mu & 1 \end{pmatrix}, \quad (\text{A.19})$$

with $x_{QL}^{b\tau} = \mathcal{O}(1)$, $\lambda_Q^s = \mathcal{O}(|V_Q|)$, $\lambda_L^\mu = \mathcal{O}(|V_L|)$, $\Delta_{QL}^{s\mu} = \mathcal{O}(\lambda_Q^s \lambda_L^\mu)$, and

$$\frac{\lambda_Q^d}{\lambda_Q^s} = \frac{\Delta_{QL}^{de}}{\Delta_{QL}^{se}} = \frac{\Delta_{QL}^{d\mu}}{\Delta_{QL}^{s\mu}} = \frac{V_{td}^*}{V_{ts}^*}, \quad \frac{\lambda_L^e}{\lambda_L^\mu} = \frac{\Delta_{QL}^{se}}{\Delta_{QL}^{s\mu}} = \frac{\Delta_{QL}^{de}}{\Delta_{QL}^{d\mu}} = s_e, \quad (\text{A.20})$$

where $s_e = \sin \theta_e$ denotes the sine of the mixing angle between the first two generations in lepton sector.

It is now ready to obtain the strength governing the $b \rightarrow q\tau\nu$ transition due to the third term on the right-hand side of Eq. (4.31),

$$C_{V_L}^{q\tau} = -\frac{v^2}{\Lambda^2} c_V^{\prime 0} \left[1 + \lambda_Q^s \left(\frac{V_{qs}}{V_{qb}} + \frac{V_{qd} V_{td}^*}{V_{qb} V_{ts}^*} \right) \right] \quad (\text{A.21})$$

$$= -\frac{v^2}{\Lambda^2} c_V^{\prime 0} \left(1 - \lambda_Q^s \frac{V_{tb}^*}{V_{ts}^*} \right), \quad (\text{A.22})$$

where the second line results from the unitarity of the CKM matrix. It is of particular interest to note that, relative to the SM, the $b \rightarrow u$ and $b \rightarrow c$ transitions share the same size of NP effects, which is a distinctive feature of the minimally broken $U(2)^5$ hypothesis [156]. On the other hand, the flavor diagonal strengths $C_{V_L}^{mmm33}$ governing the $q\bar{q} \rightarrow \tau^+\tau^-$ processes display the following hierarchical structures:

$$c_V^{1133} = |\lambda_Q^d|^2 c_V^{\prime 0} \leq c_V^{2233} = |\lambda_Q^s|^2 c_V^{\prime 0} \ll c_V^{3333} = c_V^{\prime 0}. \quad (\text{A.23})$$

Therefore, the LHC bounds given by Eqs. (4.42) and (4.43), once transformed into the constraint on $c_V^{\prime 0}$, can be safely avoided in the SMEFT with a minimally broken $U(2)^5$ hypothesis. Hence, the flavor structure of Eq. (4.45) can be regarded as a good approximation of the exact $U(2)^5$ hypothesis.

Similarly, we can apply the same setup to the remaining three terms in the third and fourth lines of Eq. (4.31). Guided by the $U(2)^5$ flavor symmetry and considering at most one power of V_Q and one power of V_L , we can decompose the flavor structures of these three terms as

$$c_{S_d}^{\prime 0} (\Gamma_L^\dagger)^{in} (\Gamma_R)^{mj} (\bar{L}^i E^j) (\bar{D}^m Q^n), \quad (\text{A.24})$$

$$c_{S_u}^{\prime 0} (\Gamma_L^\dagger)^{im} (\Gamma_R)^{nj} (\bar{L}^{a,i} E^j) \epsilon_{ab} (\bar{Q}^{b,m} U^n), \quad (\text{A.25})$$

$$c_T^{\prime 0} (\Gamma_L^\dagger)^{im} (\Gamma_R)^{nj} (\bar{L}^{a,i} \sigma_{\mu\nu} E^j) \epsilon_{ab} (\bar{Q}^{b,m} \sigma^{\mu\nu} U^n). \quad (\text{A.26})$$

Here, Γ_L is already defined in Eq. (A.17), with $V_{Q,L}$ given by [156]

$$V_{Q,L} = V_{Q,L}^* = \begin{pmatrix} 0 \\ |V_{Q,L}| \end{pmatrix}, \quad (\text{A.27})$$

while Γ_R is defined by

$$\Gamma_R \equiv \begin{pmatrix} 0 & 0 \\ 0 & 1 \end{pmatrix}. \quad (\text{A.28})$$

The matrices Γ_L and Γ_R are both given in the weak eigenbasis, and obtained by neglecting the $U(2)_{U,D,E}$ breaking spurions and making the only surviving term in the exact $U(2)^5$ limit normalized to one (*i.e.* $(\Gamma_L^\dagger)^{33}(\Gamma_R)^{33} = 1$). In addition, the overall strengths of the NP effects for the three terms are controlled by the prefactors $c_{S_d}^0$, $c_{S_u}^0$ and c_T^0 , respectively. After transforming to the fermion mass eigenbasis, the LEFT WCs governing the charged $b \rightarrow q\tau\nu$ transitions are derived, respectively, as

$$C_{S_R}^{q\tau} = -\frac{v^2}{2\Lambda^2} c_{S_u}^0 \left(1 - \lambda_Q^s \frac{V_{tb}^*}{V_{ts}^*} \right), \quad (\text{A.29})$$

and

$$C_{S_L}^{u\tau} = C_T^{u\tau} \simeq 0, \quad C_{S_L}^{c\tau} = C_T^{c\tau} \propto m_c/m_t, \quad (\text{A.30})$$

at the electroweak scale. From Eqs. (A.22) and (A.29), we can see that the left-handed vector (right-handed scalar) NP contribution has the same size in both $b \rightarrow u\tau\nu$ and $b \rightarrow c\tau\nu$ transitions, even though the original flavor structures of the corresponding operators may be independent from each other. For the left-handed scalar and tensor types of NP effects, on the other hand, we can find from Eq. (A.30) that their contributions to the $b \rightarrow u\tau\nu$ and $b \rightarrow c\tau\nu$ transitions show an obviously hierarchical structure, being proportional to the light up-type quark masses, although their effects are practically negligible. These relations among the LEFT WCs coincide with what we have derived in the SMEFT with MFV hypothesis, and they hold not only at the electroweak but also at the m_b scale when we consider the renormalization group running effects.

B Covariance tables for our results

In Tables 3 and 4, we provide covariance for all the coefficients of our numerical formulae for R_D and R_{D^*} along with their central values.

Here, we also give instructions on how to estimate the uncertainties of the ratio R_{Λ_c} and the shift factor δ_{Λ_c} . Besides the statistical uncertainty, we have also followed the recommended procedure of Ref. [83] to calculate the systematic uncertainty from the $\Lambda_b \rightarrow \Lambda_c$ form factor inputs. The total uncertainty is then obtained by adding the statistical and systematic ones in quadrature. The central values and statistical error covariance are obtained by their fit analysis for the $\Lambda_b \rightarrow \Lambda_c$ form factors,

Covariance	R_D^{SM}	a_D^{SS}	a_D^{TT}	a_D^{VS}	a_D^{VT}
R_D^{SM}	0.000057	0.000033	0.000081	0.000028	0.000058
a_D^{SS}	0.000033	0.000030	0.000061	0.000031	0.000037
a_D^{TT}	0.000081	0.000061	0.116347	0.000054	0.079300
a_D^{VS}	0.000028	0.000031	0.000054	0.000033	0.000030
a_D^{VT}	0.000058	0.000037	0.079300	0.000030	0.054057
Central value	0.3015	1.0698	0.7215	1.5276	1.0146

Table 3. Covariance and central values for the ratio R_D corresponding to Eq. (3.75).

Covariance	$R_{D^*}^{\text{SM}}$	$a_{D^*}^{SS}$	$a_{D^*}^{TT}$	$a_{D^*}^{V_L V_R}$	$a_{D^*}^{VS}$	$a_{D^*}^{V_L T}$	$a_{D^*}^{V_R T}$
$R_{D^*}^{\text{SM}}$	0.000030	-0.000003	0.001526	-0.000012	0.000009	-0.000292	0.000302
$a_{D^*}^{SS}$	-0.000003	0.000002	-0.000443	0.000001	-0.000007	0.000094	-0.000110
$a_{D^*}^{TT}$	0.001526	-0.000443	87.784597	0.001661	0.001310	-15.344725	18.095736
$a_{D^*}^{V_L V_R}$	-0.000012	0.000001	0.001661	0.000230	-0.000003	0.000403	0.000612
$a_{D^*}^{VS}$	0.000009	-0.000007	0.001310	-0.000003	0.000019	-0.000273	0.000320
$a_{D^*}^{V_L T}$	-0.000292	0.000094	-15.344725	0.000403	-0.000273	2.949721	-3.269753
$a_{D^*}^{V_R T}$	0.000302	-0.000110	18.095736	0.000612	0.000320	-3.269753	3.778571
Central value	0.2575	0.0427	17.7607	-1.7971	-0.1130	-5.4698	7.0979

Table 4. Covariance and central values for the ratio R_{D^*} corresponding to Eq. (3.76).

called the normal-order (NO) fit, which corresponds to the regular central values c_a and errors σ_a for each observable a . In addition, a similar fit analysis but with a different setup for the form factor parameters, called the higher-order (HO) fit, is also performed, which gives c_a^{HO} and σ_a^{HO} for the same observable a . Then, what they called the ‘‘systematic’’ error is defined as

$$\sigma_a^{\text{sys}} = \max \left[|c_a - c_a^{\text{HO}}|, \sqrt{|\sigma_a^2 - (\sigma_a^{\text{HO}})^2|} \right], \quad (\text{B.1})$$

and the total error is taken as $\sqrt{\sigma_a^2 + (\sigma_a^{\text{sys}})^2}$. This is how we evaluate the uncertainties of R_{Λ_c} and δ_{Λ_c} and also all the numerical results relevant to the $\Lambda_b \rightarrow \Lambda_c$ form factors. In Tables 5 and 6, we show the covariance tables of R_{Λ_c} and δ_{Λ_c} for the form factor inputs from the NO and HO fit results. Note that a_{SR}^{SS} , $a_{\text{SR}}^{S_L S_R}$, a_{SR}^{TT} , $a_{\text{SR}}^{V_R T}$, $a_{\text{SR}}^{V_L V_R}$, $a_{\text{SR}}^{V_L T}$, and a_{SR}^{VS} correspond to the coefficients of $|C_{S_L}^{c\tau}|^2 + |C_{S_R}^{c\tau}|^2$, $\text{Re}(C_{S_L}^{c\tau} C_{S_R}^{c\tau*})$, $|C_T^{c\tau}|^2$, $\text{Re}(C_{V_R}^{c\tau} C_T^{c\tau*})$, $\text{Re}[(1 + C_{V_L}^{c\tau}) C_{V_R}^{c\tau*}]$, $\text{Re}[(1 + C_{V_L}^{c\tau}) C_T^{c\tau*}]$, and $\text{Re}[(1 + C_{V_L}^{c\tau}) C_{S_R}^{c\tau*} + C_{S_L}^{c\tau} C_{V_R}^{c\tau*}]$ in Eq. (3.79), respectively. One can utilize these tables to take into account the correlation among the different terms of our numerical formulae for R_{Λ_c} and δ_{Λ_c} , with which the total uncertainties are finally obtained by the above prescription.

Covariance (NO)	$R_{\Lambda_c}^{\text{SM}}$	$a_{\Lambda_c}^{\text{SS}}$	$a_{\Lambda_c}^{\text{TT}}$	$a_{\Lambda_c}^{\text{V}_L\text{V}_R}$	$a_{\Lambda_c}^{\text{S}_L\text{S}_R}$	$a_{\Lambda_c}^{\text{VS}_1}$	$a_{\Lambda_c}^{\text{VS}_2}$	$a_{\Lambda_c}^{\text{V}_L\text{T}}$	$a_{\Lambda_c}^{\text{V}_R\text{T}}$
$R_{\Lambda_c}^{\text{SM}}$	0.000054	0.000005	0.000372	-0.000089	0.000010	-0.000004	-0.000008	-0.000220	0.000135
$a_{\Lambda_c}^{\text{SS}}$	0.000005	0.000025	-0.000014	0.000086	0.000053	0.000040	0.000035	0.000091	-0.000064
$a_{\Lambda_c}^{\text{TT}}$	0.000372	-0.000014	0.042716	-0.000818	0.000012	-0.000075	-0.000144	-0.005770	0.010311
$a_{\Lambda_c}^{\text{V}_L\text{V}_R}$	-0.000089	0.000086	-0.000818	0.000745	0.000186	0.000175	0.000158	0.001324	-0.000572
$a_{\Lambda_c}^{\text{S}_L\text{S}_R}$	0.000010	0.000053	0.000012	0.000186	0.000123	0.000096	0.000074	0.000153	-0.000117
$a_{\Lambda_c}^{\text{VS}_1}$	-0.000004	0.000040	-0.000075	0.000175	0.000096	0.000080	0.000060	0.000174	-0.000125
$a_{\Lambda_c}^{\text{VS}_2}$	-0.000008	0.000035	-0.000144	0.000158	0.000074	0.000060	0.000056	0.000217	-0.000145
$a_{\Lambda_c}^{\text{V}_L\text{T}}$	-0.000220	0.000091	-0.005770	0.001324	0.000153	0.000174	0.000217	0.004173	-0.001990
$a_{\Lambda_c}^{\text{V}_R\text{T}}$	0.000135	-0.000064	0.010311	-0.000572	-0.000117	-0.000125	-0.000145	-0.001990	0.002859
Central value (NO)	0.3318	0.3214	10.4377	-0.7218	0.5134	0.3339	0.4968	-3.1096	4.8800
Covariance (HO)	$R_{\Lambda_c}^{\text{SM}}$	$a_{\Lambda_c}^{\text{SS}}$	$a_{\Lambda_c}^{\text{TT}}$	$a_{\Lambda_c}^{\text{V}_L\text{V}_R}$	$a_{\Lambda_c}^{\text{S}_L\text{S}_R}$	$a_{\Lambda_c}^{\text{VS}_1}$	$a_{\Lambda_c}^{\text{VS}_2}$	$a_{\Lambda_c}^{\text{V}_L\text{T}}$	$a_{\Lambda_c}^{\text{V}_R\text{T}}$
$R_{\Lambda_c}^{\text{SM}}$	0.000104	0.000019	0.001093	-0.000106	0.000040	0.000011	0.000003	-0.000368	0.000321
$a_{\Lambda_c}^{\text{SS}}$	0.000019	0.000200	0.001571	0.000810	0.000427	0.000322	0.000286	0.000640	-0.000066
$a_{\Lambda_c}^{\text{TT}}$	0.001093	0.001571	0.868537	0.005756	0.003359	0.002285	0.001933	-0.156204	0.202509
$a_{\Lambda_c}^{\text{V}_L\text{V}_R}$	-0.000106	0.000810	0.005756	0.004394	0.001778	0.001398	0.001195	0.004539	-0.000638
$a_{\Lambda_c}^{\text{S}_L\text{S}_R}$	0.000040	0.000427	0.003359	0.001778	0.000950	0.000726	0.000601	0.001314	-0.000084
$a_{\Lambda_c}^{\text{VS}_1}$	0.000011	0.000322	0.002285	0.001398	0.000726	0.000565	0.000457	0.001077	-0.000137
$a_{\Lambda_c}^{\text{VS}_2}$	0.000003	0.000286	0.001933	0.001195	0.000601	0.000457	0.000421	0.001047	-0.000221
$a_{\Lambda_c}^{\text{V}_L\text{T}}$	-0.000368	0.000640	-0.156204	0.004539	0.001314	0.001077	0.001047	0.048578	-0.040611
$a_{\Lambda_c}^{\text{V}_R\text{T}}$	0.000321	-0.000066	0.202509	-0.000638	-0.000084	-0.000137	-0.000221	-0.040611	0.049201
Central value (HO)	0.3284	0.3193	10.6645	-0.7157	0.5085	0.3309	0.4946	-3.0972	4.9345

Table 5. Covariance and central values for the ratio R_{Λ_c} corresponding to Eq. (3.77) for the NO (upper panel) and HO (lower panel) parameter fits. The systematic errors are evaluated by means of Eq. (B.1) based on Ref. [83].

In principle, we can also provide similar tables for the $b \rightarrow u$ case. However, it is not much useful for now because we are still using the preliminary results for the $\Lambda_b \rightarrow p$ tensor form factors. In addition, we need more precise fit studies of the $B \rightarrow \rho$ form factors as well as the experimental measurements of the ratios R_π , R_ρ , and R_p . Otherwise, the correlation among the different NP contributions is less significant. Thus, we do not show these results here.

Covariance (NO)	a_{SR}^{SS}	$a_{\text{SR}}^{S_L S_R}$	a_{SR}^{TT}	$a_{\text{SR}}^{V_R T}$	$a_{\text{SR}}^{V_L V_R}$	$a_{\text{SR}}^{V_L T}$	a_{SR}^{VS}
a_{SR}^{SS}	0.000015	0.000012	-0.000775	-0.000209	0.000021	0.000186	0.000024
$a_{\text{SR}}^{S_L S_R}$	0.000012	0.000014	-0.000430	-0.000103	-0.000012	0.000062	0.000014
a_{SR}^{TT}	-0.000775	-0.000430	46.545257	9.602331	-0.002067	-8.128861	-0.001652
$a_{\text{SR}}^{V_R T}$	-0.000209	-0.000103	9.602331	2.008910	-0.000567	-1.730379	-0.000456
$a_{\text{SR}}^{V_L V_R}$	0.000021	-0.000012	-0.002067	-0.000567	0.000568	0.001674	0.000075
$a_{\text{SR}}^{V_L T}$	0.000186	0.000062	-8.128861	-1.730379	0.001674	1.570848	0.000442
a_{SR}^{VS}	0.000024	0.000014	-0.001652	-0.000456	0.000075	0.000442	0.000047
Central value (NO)	-0.0011	-0.0075	-2.6808	-0.5606	0.0408	0.5936	-0.0017
Covariance (HO)	a_{SR}^{SS}	$a_{\text{SR}}^{S_L S_R}$	a_{SR}^{TT}	$a_{\text{SR}}^{V_R T}$	$a_{\text{SR}}^{V_L V_R}$	$a_{\text{SR}}^{V_L T}$	a_{SR}^{VS}
a_{SR}^{SS}	0.000028	0.000022	-0.000902	-0.000287	0.000032	0.000259	0.000045
$a_{\text{SR}}^{S_L S_R}$	0.000022	0.000024	-0.000573	-0.000157	-0.000013	0.000110	0.000026
a_{SR}^{TT}	-0.000902	-0.000573	47.712307	9.871231	0.000090	-8.341200	-0.001835
$a_{\text{SR}}^{V_R T}$	-0.000287	-0.000157	9.871231	2.072108	-0.000232	-1.781711	-0.000601
$a_{\text{SR}}^{V_L V_R}$	0.000032	-0.000013	0.000090	-0.000232	0.001155	0.002406	0.000106
$a_{\text{SR}}^{V_L T}$	0.000259	0.000110	-8.341200	-1.781711	0.002406	1.623709	0.000579
a_{SR}^{VS}	0.000045	0.000026	-0.001835	-0.000601	0.000106	0.000579	0.000087
Central value (HO)	-0.0013	-0.0082	-2.4860	-0.5175	0.0541	0.6181	-0.0011

Table 6. Covariance and central values for the shift factor δ_{Λ_c} corresponding to Eq. (3.79) for the NO (upper panel) and HO (lower panel) parameter fits. The systematic errors are evaluated by means of Eq. (B.1) based on Ref. [83].

References

- [1] **LHCb** Collaboration, R. Aaij et al., *Physics case for an LHCb Upgrade II - Opportunities in flavour physics, and beyond, in the HL-LHC era*, [arXiv:1808.08865](https://arxiv.org/abs/1808.08865).
- [2] **LHCb** Collaboration, *Future physics potential of LHCb*, <https://cds.cern.ch/record/2806113/files/LHCbPUB-2022-012.pdf>.
- [3] **Belle-II** Collaboration, W. Altmannshofer et al., *The Belle II Physics Book*, *PTEP* **2019** (2019), no. 12 123C01, [[arXiv:1808.10567](https://arxiv.org/abs/1808.10567)]. [Erratum: *PTEP* **2020**, 029201 (2020)].
- [4] **Belle-II** Collaboration, L. Aggarwal et al., *Snowmass White Paper: Belle II physics reach and plans for the next decade and beyond*, [arXiv:2207.06307](https://arxiv.org/abs/2207.06307).
- [5] B. Capdevila, A. Crivellin, and J. Matias, *Review of semileptonic B anomalies*, *Eur. Phys. J. ST* **1** (2023) 20, [[arXiv:2309.01311](https://arxiv.org/abs/2309.01311)].
- [6] D. London and J. Matias, *B Flavour Anomalies: 2021 Theoretical Status Report*, *Ann. Rev. Nucl. Part. Sci.* **72** (2022) 37–68, [[arXiv:2110.13270](https://arxiv.org/abs/2110.13270)].

- [7] F. U. Bernlochner, M. F. Sevilla, D. J. Robinson, and G. Wormser, *Semitauponic b -hadron decays: A lepton flavor universality laboratory*, *Rev. Mod. Phys.* **94** (2022), no. 1 015003, [[arXiv:2101.08326](#)].
- [8] S. Bifani, S. Descotes-Genon, A. Romero Vidal, and M.-H. Schune, *Review of Lepton Universality tests in B decays*, *J. Phys. G* **46** (2019), no. 2 023001, [[arXiv:1809.06229](#)].
- [9] F. U. Bernlochner, M. T. Prim, and K. K. Vos, *$|V_{ub}|$ and $|V_{cb}|$ from exclusive semileptonic decays*, *Eur. Phys. J. ST* **233** (2024), no. 2 347–358.
- [10] **Belle** Collaboration, R. Glattauer et al., *Measurement of the decay $B \rightarrow D\ell\nu_\ell$ in fully reconstructed events and determination of the Cabibbo-Kobayashi-Maskawa matrix element $|V_{cb}|$* , *Phys. Rev. D* **93** (2016), no. 3 032006, [[arXiv:1510.03657](#)].
- [11] **Belle** Collaboration, E. Waheed et al., *Measurement of the CKM matrix element $|V_{cb}|$ from $B^0 \rightarrow D^{*-}\ell^+\nu_\ell$ at Belle*, *Phys. Rev. D* **100** (2019), no. 5 052007, [[arXiv:1809.03290](#)]. [Erratum: *Phys.Rev.D* 103, 079901 (2021)].
- [12] **Belle** Collaboration, M. T. Prim et al., *Measurement of differential distributions of $B \rightarrow D^*\ell\nu_\ell$ and implications on $|V_{cb}|$* , *Phys. Rev. D* **108** (2023), no. 1 012002, [[arXiv:2301.07529](#)].
- [13] **Belle-II** Collaboration, I. Adachi et al., *Determination of $|V_{cb}|$ using $\bar{B}^0 \rightarrow D^{*+}\ell^-\bar{\nu}_\ell$ decays with Belle II*, *Phys. Rev. D* **108** (2023), no. 9 092013, [[arXiv:2310.01170](#)].
- [14] **BaBar** Collaboration, J. P. Lees et al., *Extraction of form Factors from a Four-Dimensional Angular Analysis of $\bar{B} \rightarrow D^*\ell^-\bar{\nu}_\ell$* , *Phys. Rev. Lett.* **123** (2019), no. 9 091801, [[arXiv:1903.10002](#)].
- [15] **BaBar** Collaboration, J. P. Lees et al., *Model-independent extraction of form factors and $|V_{cb}|$ in $B^- \rightarrow D\ell^-\bar{\nu}_\ell$ with hadronic tagging at BABAR*, *Phys. Rev. D* **110** (2024), no. 3 032018, [[arXiv:2311.15071](#)].
- [16] **Particle Data Group** Collaboration, S. Navas et al., *Review of particle physics*, *Phys. Rev. D* **110** (2024), no. 3 030001.
- [17] W. I. Jay, R. van Tonder, and R. Watanabe, *Summary of the CKM 2023 Working Group on V_{ub} , V_{cb} and semileptonic/leptonic B decays including τ* , in *12th International Workshop on the CKM Unitarity Triangle*, 3, 2024. [[arXiv:2403.18175](#)].
- [18] **Belle** Collaboration, M. Huschle et al., *Measurement of the branching ratio of $\bar{B} \rightarrow D^{(*)}\tau^-\bar{\nu}_\tau$ relative to $\bar{B} \rightarrow D^{(*)}\ell^-\bar{\nu}_\ell$ decays with hadronic tagging at Belle*, *Phys. Rev. D* **92** (2015), no. 7 072014, [[arXiv:1507.03233](#)].
- [19] **Belle** Collaboration, Y. Sato et al., *Measurement of the branching ratio of $\bar{B}^0 \rightarrow D^{*+}\tau^-\bar{\nu}_\tau$ relative to $\bar{B}^0 \rightarrow D^{*+}\ell^-\bar{\nu}_\ell$ decays with a semileptonic tagging method*, *Phys. Rev. D* **94** (2016), no. 7 072007, [[arXiv:1607.07923](#)].

- [20] Belle Collaboration, S. Hirose et al., *Measurement of the τ lepton polarization and $R(D^*)$ in the decay $\bar{B} \rightarrow D^* \tau^- \bar{\nu}_\tau$* , *Phys. Rev. Lett.* **118** (2017), no. 21 211801, [[arXiv:1612.00529](#)].
- [21] Belle Collaboration, S. Hirose et al., *Measurement of the τ lepton polarization and $R(D^*)$ in the decay $\bar{B} \rightarrow D^* \tau^- \bar{\nu}_\tau$ with one-prong hadronic τ decays at Belle*, *Phys. Rev. D* **97** (2018), no. 1 012004, [[arXiv:1709.00129](#)].
- [22] Belle Collaboration, G. Caria et al., *Measurement of $\mathcal{R}(D)$ and $\mathcal{R}(D^*)$ with a semileptonic tagging method*, *Phys. Rev. Lett.* **124** (2020), no. 16 161803, [[arXiv:1910.05864](#)].
- [23] BaBar Collaboration, J. P. Lees et al., *Evidence for an excess of $\bar{B} \rightarrow D^{(*)} \tau^- \bar{\nu}_\tau$ decays*, *Phys. Rev. Lett.* **109** (2012) 101802, [[arXiv:1205.5442](#)].
- [24] BaBar Collaboration, J. P. Lees et al., *Measurement of an Excess of $\bar{B} \rightarrow D^{(*)} \tau^- \bar{\nu}_\tau$ Decays and Implications for Charged Higgs Bosons*, *Phys. Rev. D* **88** (2013), no. 7 072012, [[arXiv:1303.0571](#)].
- [25] LHCb Collaboration, R. Aaij et al., *Measurement of the ratio of branching fractions $\mathcal{B}(\bar{B}^0 \rightarrow D^{*+} \tau^- \bar{\nu}_\tau) / \mathcal{B}(\bar{B}^0 \rightarrow D^{*+} \mu^- \bar{\nu}_\mu)$* , *Phys. Rev. Lett.* **115** (2015), no. 11 111803, [[arXiv:1506.08614](#)]. [Erratum: *Phys.Rev.Lett.* 115, 159901 (2015)].
- [26] LHCb Collaboration, R. Aaij et al., *Measurement of the ratio of the $B^0 \rightarrow D^{*-} \tau^+ \nu_\tau$ and $B^0 \rightarrow D^{*-} \mu^+ \nu_\mu$ branching fractions using three-prong τ -lepton decays*, *Phys. Rev. Lett.* **120** (2018), no. 17 171802, [[arXiv:1708.08856](#)].
- [27] LHCb Collaboration, R. Aaij et al., *Test of Lepton Flavor Universality by the measurement of the $B^0 \rightarrow D^{*-} \tau^+ \nu_\tau$ branching fraction using three-prong τ decays*, *Phys. Rev. D* **97** (2018), no. 7 072013, [[arXiv:1711.02505](#)].
- [28] LHCb Collaboration, R. Aaij et al., *Measurement of the ratios of branching fractions $\mathcal{R}(D^*)$ and $\mathcal{R}(D^0)$* , *Phys. Rev. Lett.* **131** (2023) 111802, [[arXiv:2302.02886](#)].
- [29] LHCb Collaboration, R. Aaij et al., *Test of lepton flavor universality using $B^0 \rightarrow D^{*-} \tau^+ \nu_\tau$ decays with hadronic τ channels*, *Phys. Rev. D* **108** (2023), no. 1 012018, [[arXiv:2305.01463](#)].
- [30] LHCb Collaboration, R. Aaij et al., *Measurement of the branching fraction ratios $R(D^+)$ and $R(D^{*+})$ using muonic τ decays*, [arXiv:2406.03387](#).
- [31] Belle-II Collaboration, I. Adachi et al., *A test of lepton flavor universality with a measurement of $R(D^*)$ using hadronic B tagging at the Belle II experiment*, [arXiv:2401.02840](#).
- [32] HFLAV Collaboration. “Preliminary average of $R(D)$ and $R(D^*)$ for Moriond 2024” at <https://hflav-eos.web.cern.ch/hflav-eos/semi/moriond24/html/RDsDsstar/RDRDs.html>.
- [33] M. Freytsis, Z. Ligeti, and J. T. Ruderman, *Flavor models for $\bar{B} \rightarrow D^{(*)} \tau \bar{\nu}$* , *Phys. Rev. D* **92** (2015), no. 5 054018, [[arXiv:1506.08896](#)].

- [34] **Belle-II** Collaboration, I. Adachi et al., *First Measurement of $R(X_{\tau/\ell})$ as an Inclusive Test of the $b \rightarrow c\tau\nu$ Anomaly*, *Phys. Rev. Lett.* **132** (2024), no. 21 211804, [[arXiv:2311.07248](#)].
- [35] **Belle-II** Collaboration, I. Adachi et al., *Determination of $|V_{ub}|$ from simultaneous measurements of untagged $B^0 \rightarrow \pi^- \ell^+ \nu_\ell$ and $B^+ \rightarrow \rho^0 \ell^+ \nu_\ell$ decays*, [arXiv:2407.17403](#).
- [36] **HFLAV** Collaboration, Y. S. Amhis et al., *Averages of b -hadron, c -hadron, and τ -lepton properties as of 2021*, *Phys. Rev. D* **107** (2023), no. 5 052008, [[arXiv:2206.07501](#)].
- [37] F. U. Bernlochner, M. T. Prim, and D. J. Robinson, *$B \rightarrow \rho\nu$ and $\omega\nu$ in and beyond the Standard Model: Improved predictions and $|V_{ub}|$* , *Phys. Rev. D* **104** (2021), no. 3 034032, [[arXiv:2104.05739](#)].
- [38] D. Leljak, B. Melić, F. Novak, M. Reboud, and D. van Dyk, *Toward a complete description of $b \rightarrow u\ell^-\bar{\nu}$ decays within the Weak Effective Theory*, *JHEP* **08** (2023) 063, [[arXiv:2302.05268](#)].
- [39] **Belle** Collaboration, P. Hamer et al., *Search for $B^0 \rightarrow \pi^- \tau^+ \nu_\tau$ with hadronic tagging at Belle*, *Phys. Rev. D* **93** (2016), no. 3 032007, [[arXiv:1509.06521](#)].
- [40] **DELPHI** Collaboration, J. Abdallah et al., *Measurement of the $\Lambda_b^0(b)$ decay form-factor*, *Phys. Lett. B* **585** (2004) 63–84, [[hep-ex/0403040](#)].
- [41] **LHCb** Collaboration, R. Aaij et al., *Observation of the decay $\Lambda_b^0 \rightarrow \Lambda_c^+ \tau^- \bar{\nu}_\tau$* , *Phys. Rev. Lett.* **128** (2022), no. 19 191803, [[arXiv:2201.03497](#)].
- [42] F. U. Bernlochner, Z. Ligeti, M. Papucci, and D. J. Robinson, *Interpreting LHCb’s $\Lambda_b \rightarrow \Lambda_c \tau \bar{\nu}$ measurement and puzzles in semileptonic Λ_b decays*, *Phys. Rev. D* **107** (2023), no. 1 L011502, [[arXiv:2206.11282](#)].
- [43] **LHCb** Collaboration, R. Aaij et al., *Determination of the quark coupling strength $|V_{ub}|$ using baryonic decays*, *Nature Phys.* **11** (2015) 743–747, [[arXiv:1504.01568](#)].
- [44] **LHCb** Collaboration, R. Aaij et al., *Measurement of the ratio of branching fractions $\mathcal{B}(B_c^+ \rightarrow J/\psi \tau^+ \nu_\tau)/\mathcal{B}(B_c^+ \rightarrow J/\psi \mu^+ \nu_\mu)$* , *Phys. Rev. Lett.* **120** (2018), no. 12 121801, [[arXiv:1711.05623](#)].
- [45] **CMS** Collaboration, A. Hayrapetyan et al., *Test of lepton flavor universality in semileptonic B_c^+ meson decays in proton-proton collisions at $\sqrt{s} = 13$ TeV*, [arXiv:2408.00678](#).
- [46] **CMS** Collaboration, C. Rovelli, *Lepton flavour (universality) violation studies at CMS*, . <https://indico.cern.ch/event/1291157/contributions/5878345/>.
- [47] S. Iguro, T. Kitahara, and R. Watanabe, *Global fit to $b \rightarrow c\tau\nu$ anomalies as of Spring 2024*, *Phys. Rev. D* **110** (2024), no. 7 075005, [[arXiv:2405.06062](#)].
- [48] M. Blanke, A. Crivellin, S. de Boer, T. Kitahara, M. Moscati, U. Nierste, and I. Nišandžić, *Impact of polarization observables and $B_c \rightarrow \tau\nu$ on new physics*

- explanations of the $b \rightarrow c\tau\nu$ anomaly, *Phys. Rev. D* **99** (2019), no. 7 075006, [[arXiv:1811.09603](#)].
- [49] M. Blanke, A. Crivellin, T. Kitahara, M. Moscati, U. Nierste, and I. Nišandžić, *Addendum to “Impact of polarization observables and $B_c \rightarrow \tau\nu$ on new physics explanations of the $b \rightarrow c\tau\nu$ anomaly”*, [arXiv:1905.08253](#). [Addendum: *Phys.Rev.D* 100, 035035 (2019)].
- [50] M. Fedele, M. Blanke, A. Crivellin, S. Iguro, T. Kitahara, U. Nierste, and R. Watanabe, *Impact of $\Lambda_b \rightarrow \Lambda_c\tau\nu$ measurement on new physics in $b \rightarrow cl\nu$ transitions*, *Phys. Rev. D* **107** (2023), no. 5 055005, [[arXiv:2211.14172](#)].
- [51] W. Buchmuller and D. Wyler, *Effective Lagrangian Analysis of New Interactions and Flavor Conservation*, *Nucl. Phys. B* **268** (1986) 621–653.
- [52] B. Grzadkowski, M. Iskrzynski, M. Misiak, and J. Rosiek, *Dimension-Six Terms in the Standard Model Lagrangian*, *JHEP* **10** (2010) 085, [[arXiv:1008.4884](#)].
- [53] I. Brivio and M. Trott, *The Standard Model as an Effective Field Theory*, *Phys. Rept.* **793** (2019) 1–98, [[arXiv:1706.08945](#)].
- [54] G. Isidori, F. Wilsch, and D. Wyler, *The standard model effective field theory at work*, *Rev. Mod. Phys.* **96** (2024), no. 1 015006, [[arXiv:2303.16922](#)].
- [55] D. A. Faroughy, G. Isidori, F. Wilsch, and K. Yamamoto, *Flavour symmetries in the SMEFT*, *JHEP* **08** (2020) 166, [[arXiv:2005.05366](#)].
- [56] A. Greljo, A. Palavrić, and A. E. Thomsen, *Adding Flavor to the SMEFT*, *JHEP* **10** (2022) 010, [[arXiv:2203.09561](#)].
- [57] S. Iguro and Y. Omura, *Status of the semileptonic B decays and muon $g-2$ in general 2HDMs with right-handed neutrinos*, *JHEP* **05** (2018) 173, [[arXiv:1802.01732](#)].
- [58] D. J. Robinson, B. Shakya, and J. Zupan, *Right-handed neutrinos and $R(D^{(*)})$* , *JHEP* **02** (2019) 119, [[arXiv:1807.04753](#)].
- [59] K. S. Babu, B. Dutta, and R. N. Mohapatra, *A theory of $R(D^*, D)$ anomaly with right-handed currents*, *JHEP* **01** (2019) 168, [[arXiv:1811.04496](#)].
- [60] R. Mandal, C. Murgui, A. Peñuelas, and A. Pich, *The role of right-handed neutrinos in $b \rightarrow c\tau\bar{\nu}$ anomalies*, *JHEP* **08** (2020), no. 08 022, [[arXiv:2004.06726](#)].
- [61] N. Penalva, E. Hernández, and J. Nieves, *The role of right-handed neutrinos in $b \rightarrow c\tau(\pi\nu_\tau, \rho\nu_\tau, \mu\bar{\nu}_\mu\nu_\tau)\bar{\nu}_\tau$ from visible final-state kinematics*, *JHEP* **10** (2021) 122, [[arXiv:2107.13406](#)].
- [62] A. Datta, H. Liu, and D. Marfatia, *$\bar{B} \rightarrow D^{(*)}\ell\bar{X}$ decays in effective field theory with massive right-handed neutrinos*, *Phys. Rev. D* **106** (2022), no. 1 L011702, [[arXiv:2204.01818](#)].
- [63] E. E. Jenkins, A. V. Manohar, and P. Stoffer, *Low-Energy Effective Field Theory*

- below the Electroweak Scale: Operators and Matching, *JHEP* **03** (2018) 016, [[arXiv:1709.04486](#)]. [Erratum: *JHEP* **12**, 043 (2023)].
- [64] J. Aebischer, A. Crivellin, M. Fael, and C. Greub, *Matching of gauge invariant dimension-six operators for $b \rightarrow s$ and $b \rightarrow c$ transitions*, *JHEP* **05** (2016) 037, [[arXiv:1512.02830](#)].
- [65] S. Iguro, M. Takeuchi, and R. Watanabe, *Testing leptoquark/EFT in $\bar{B} \rightarrow D^{(*)}l\bar{\nu}$ at the LHC*, *Eur. Phys. J. C* **81** (2021), no. 5 406, [[arXiv:2011.02486](#)].
- [66] A. Greljo, J. Martin Camalich, and J. D. Ruiz-Álvarez, *Mono- τ Signatures at the LHC Constrain Explanations of B-decay Anomalies*, *Phys. Rev. Lett.* **122** (2019), no. 13 131803, [[arXiv:1811.07920](#)].
- [67] C.-H. Chen and C.-Q. Geng, *Charged Higgs on $B^- \rightarrow \tau\bar{\nu}_\tau$ and $\bar{B} \rightarrow P(V)l\bar{\nu}_\ell$* , *JHEP* **10** (2006) 053, [[hep-ph/0608166](#)].
- [68] A. Celis, M. Jung, X.-Q. Li, and A. Pich, *Sensitivity to charged scalars in $B \rightarrow D^{(*)}\tau\nu_\tau$ and $B \rightarrow \tau\nu_\tau$ decays*, *JHEP* **01** (2013) 054, [[arXiv:1210.8443](#)].
- [69] M. Tanaka and R. Watanabe, *New physics in the weak interaction of $\bar{B} \rightarrow D^{(*)}\tau\bar{\nu}$* , *Phys. Rev. D* **87** (2013), no. 3 034028, [[arXiv:1212.1878](#)].
- [70] S. Fajfer, J. F. Kamenik, and I. Nisandzic, *On the $B \rightarrow D^*\tau\bar{\nu}_\tau$ Sensitivity to New Physics*, *Phys. Rev. D* **85** (2012) 094025, [[arXiv:1203.2654](#)].
- [71] Y. Sakaki, M. Tanaka, A. Tayduganov, and R. Watanabe, *Testing leptoquark models in $\bar{B} \rightarrow D^{(*)}\tau\bar{\nu}$* , *Phys. Rev. D* **88** (2013), no. 9 094012, [[arXiv:1309.0301](#)].
- [72] F. U. Bernlochner, *$B \rightarrow \pi\tau\bar{\nu}_\tau$ decay in the context of type II 2HDM*, *Phys. Rev. D* **92** (2015), no. 11 115019, [[arXiv:1509.06938](#)].
- [73] M. Tanaka and R. Watanabe, *New physics contributions in $B \rightarrow \pi\tau\bar{\nu}$ and $B \rightarrow \tau\bar{\nu}$* , *PTEP* **2017** (2017), no. 1 013B05, [[arXiv:1608.05207](#)].
- [74] X.-Q. Li, Y.-D. Yang, and X. Zhang, *$\Lambda_b \rightarrow \Lambda_c\tau\bar{\nu}_\tau$ decay in scalar and vector leptoquark scenarios*, *JHEP* **02** (2017) 068, [[arXiv:1611.01635](#)].
- [75] Q.-Y. Hu, X.-Q. Li, and Y.-D. Yang, *$b \rightarrow c\tau\nu$ transitions in the standard model effective field theory*, *Eur. Phys. J. C* **79** (2019), no. 3 264, [[arXiv:1810.04939](#)].
- [76] Q.-Y. Hu, X.-Q. Li, Y.-D. Yang, and D.-H. Zheng, *The measurable angular distribution of $\Lambda_b^0 \rightarrow \Lambda_c^+ (\rightarrow \Lambda^0\pi^+) \tau^- (\rightarrow \pi^-\nu_\tau) \bar{\nu}_\tau$ decay*, *JHEP* **02** (2021) 183, [[arXiv:2011.05912](#)].
- [77] A. Biswas and S. Nandi, *A closer look at observables from exclusive semileptonic $B \rightarrow (\pi, \rho)l\nu_\ell$ decays*, *JHEP* **09** (2021) 127, [[arXiv:2105.01732](#)].
- [78] D. Du, A. X. El-Khadra, S. Gottlieb, A. S. Kronfeld, J. Laiho, E. Lunghi, R. S. Van de Water, and R. Zhou, *Phenomenology of semileptonic B-meson decays with form factors from lattice QCD*, *Phys. Rev. D* **93** (2016), no. 3 034005, [[arXiv:1510.02349](#)].

- [79] P. Ball and R. Zwicky, $B_{d,s} \rightarrow \rho, \omega, K^*, \phi$ decay form-factors from light-cone sum rules revisited, *Phys. Rev. D* **71** (2005) 014029, [[hep-ph/0412079](#)].
- [80] A. Bharucha, D. M. Straub, and R. Zwicky, $B \rightarrow V\ell^+\ell^-$ in the Standard Model from light-cone sum rules, *JHEP* **08** (2016) 098, [[arXiv:1503.05534](#)].
- [81] C.-H. Chen and C. Q. Geng, Baryonic rare decays of $\Lambda_b \rightarrow \Lambda\ell^+\ell^-$, *Phys. Rev. D* **64** (2001) 074001, [[hep-ph/0106193](#)].
- [82] T. Feldmann and M. W. Y. Yip, Form factors for $\Lambda_b \rightarrow \Lambda$ transitions in the soft-collinear effective theory, *Phys. Rev. D* **85** (2012) 014035, [[arXiv:1111.1844](#)]. [Erratum: *Phys.Rev.D* 86, 079901 (2012)].
- [83] W. Detmold, C. Lehner, and S. Meinel, $\Lambda_b \rightarrow p\ell^-\bar{\nu}_\ell$ and $\Lambda_b \rightarrow \Lambda_c\ell^-\bar{\nu}_\ell$ form factors from lattice QCD with relativistic heavy quarks, *Phys. Rev. D* **92** (2015), no. 3 034503, [[arXiv:1503.01421](#)].
- [84] W. Detmold and S. Meinel, $\Lambda_b \rightarrow \Lambda\ell^+\ell^-$ form factors, differential branching fraction, and angular observables from lattice QCD with relativistic b quarks, *Phys. Rev. D* **93** (2016), no. 7 074501, [[arXiv:1602.01399](#)].
- [85] I. Caprini, L. Lellouch, and M. Neubert, Dispersive bounds on the shape of $\bar{B} \rightarrow D^{(*)}\ell\bar{\nu}$ form-factors, *Nucl. Phys. B* **530** (1998) 153–181, [[hep-ph/9712417](#)].
- [86] C. G. Boyd, B. Grinstein, and R. F. Lebed, Model independent extraction of $|V_{cb}|$ using dispersion relations, *Phys. Lett. B* **353** (1995) 306–312, [[hep-ph/9504235](#)].
- [87] C. Bourrely, I. Caprini, and L. Lellouch, Model-independent description of $B \rightarrow \pi\ell\nu$ decays and a determination of $|V_{ub}|$, *Phys. Rev. D* **79** (2009) 013008, [[arXiv:0807.2722](#)]. [Erratum: *Phys.Rev.D* 82, 099902 (2010)].
- [88] MILC Collaboration, J. A. Bailey et al., $B \rightarrow D\ell\nu$ form factors at nonzero recoil and $|V_{cb}|$ from 2+1-flavor lattice QCD, *Phys. Rev. D* **92** (2015), no. 3 034506, [[arXiv:1503.07237](#)].
- [89] HPQCD Collaboration, H. Na, C. M. Bouchard, G. P. Lepage, C. Monahan, and J. Shigemitsu, $B \rightarrow D\ell\nu$ form factors at nonzero recoil and extraction of $|V_{cb}|$, *Phys. Rev. D* **92** (2015), no. 5 054510, [[arXiv:1505.03925](#)]. [Erratum: *Phys.Rev.D* 93, 119906 (2016)].
- [90] Fermilab Lattice, MILC, Fermilab Lattice, MILC Collaboration, A. Bazavov et al., Semileptonic form factors for $B \rightarrow D^*\ell\nu$ at nonzero recoil from 2 + 1-flavor lattice QCD: Fermilab Lattice and MILC Collaborations, *Eur. Phys. J. C* **82** (2022), no. 12 1141, [[arXiv:2105.14019](#)]. [Erratum: *Eur.Phys.J.C* 83, 21 (2023)].
- [91] JLQCD Collaboration, Y. Aoki, B. Colquhoun, H. Fukaya, S. Hashimoto, T. Kaneko, R. Kellermann, J. Koponen, and E. Kou, $B \rightarrow D^*\ell\nu\ell$ semileptonic form factors from lattice QCD with Möbius domain-wall quarks, *Phys. Rev. D* **109** (2024), no. 7 074503, [[arXiv:2306.05657](#)].
- [92] HPQCD, (HPQCD Collaboration)‡ Collaboration, J. Harrison and C. T. H. Davies, $B \rightarrow D^*$ and $B_s \rightarrow D_s^*$ vector, axial-vector and tensor form factors for the

- full q^2 range from lattice QCD, *Phys. Rev. D* **109** (2024), no. 9 094515, [[arXiv:2304.03137](#)].
- [93] N. Gubernari, A. Kokulu, and D. van Dyk, *B → P and B → V Form Factors from B-Meson Light-Cone Sum Rules beyond Leading Twist*, *JHEP* **01** (2019) 150, [[arXiv:1811.00983](#)].
- [94] B.-Y. Cui, Y.-K. Huang, Y.-M. Wang, and X.-C. Zhao, *Shedding new light on $R(D_{(s)}^{(*)})$ and $|V_{cb}|$ from semileptonic $\bar{B}_{(s)} \rightarrow D_{(s)}^{(*)} \ell \bar{\nu}_\ell$ decays*, *Phys. Rev. D* **108** (2023), no. 7 L071504, [[arXiv:2301.12391](#)].
- [95] A. Datta, S. Kamali, S. Meinel, and A. Rashed, *Phenomenology of $\Lambda_b \rightarrow \Lambda_c \tau \bar{\nu}_\tau$ using lattice QCD calculations*, *JHEP* **08** (2017) 131, [[arXiv:1702.02243](#)].
- [96] T. Kapoor, Z.-R. Huang, and E. Kou, *New physics search via angular distribution of $B \rightarrow D^* \ell \nu_\ell$ decay in the light of the new lattice data*, [[arXiv:2401.11636](#)].
- [97] C. G. Boyd, B. Grinstein, and R. F. Lebed, *Precision corrections to dispersive bounds on form-factors*, *Phys. Rev. D* **56** (1997) 6895–6911, [[hep-ph/9705252](#)].
- [98] D. Bigi and P. Gambino, *Revisiting $B \rightarrow D \ell \nu$* , *Phys. Rev. D* **94** (2016), no. 9 094008, [[arXiv:1606.08030](#)].
- [99] D. Bigi, P. Gambino, and S. Schacht, *A fresh look at the determination of $|V_{cb}|$ from $B \rightarrow D^* \ell \nu$* , *Phys. Lett. B* **769** (2017) 441–445, [[arXiv:1703.06124](#)].
- [100] D. Bigi, P. Gambino, and S. Schacht, *$R(D^*)$, $|V_{cb}|$, and the Heavy Quark Symmetry relations between form factors*, *JHEP* **11** (2017) 061, [[arXiv:1707.09509](#)].
- [101] J. M. Flynn, T. Izubuchi, T. Kawanai, C. Lehner, A. Soni, R. S. Van de Water, and O. Witzel, *$B \rightarrow \pi \ell \nu$ and $B_s \rightarrow K \ell \nu$ form factors and $|V_{ub}|$ from 2+1-flavor lattice QCD with domain-wall light quarks and relativistic heavy quarks*, *Phys. Rev. D* **91** (2015), no. 7 074510, [[arXiv:1501.05373](#)].
- [102] **Fermilab Lattice, MILC Collaboration**, J. A. Bailey et al., *$|V_{ub}|$ from $B \rightarrow \pi \ell \nu$ decays and (2+1)-flavor lattice QCD*, *Phys. Rev. D* **92** (2015), no. 1 014024, [[arXiv:1503.07839](#)].
- [103] **JLQCD Collaboration**, B. Colquhoun, S. Hashimoto, T. Kaneko, and J. Koponen, *Form factors of $B \rightarrow \pi \ell \nu$ and a determination of $|V_{ub}|$ with Möbius domain-wall fermions*, *Phys. Rev. D* **106** (2022), no. 5 054502, [[arXiv:2203.04938](#)].
- [104] **Fermilab Lattice, MILC Collaboration**, J. A. Bailey et al., *$B \rightarrow \pi \ell \ell$ form factors for new-physics searches from lattice QCD*, *Phys. Rev. Lett.* **115** (2015), no. 15 152002, [[arXiv:1507.01618](#)].
- [105] Y.-M. Wang and Y.-L. Shen, *QCD corrections to $B \rightarrow \pi$ form factors from light-cone sum rules*, *Nucl. Phys. B* **898** (2015) 563–604, [[arXiv:1506.00667](#)].
- [106] A. Khodjamirian and A. V. Rusov, *$B_s \rightarrow K \ell \nu_\ell$ and $B_{(s)} \rightarrow \pi(K) \ell^+ \ell^-$ decays at large recoil and CKM matrix elements*, *JHEP* **08** (2017) 112, [[arXiv:1703.04765](#)].
- [107] C.-D. Lü, Y.-L. Shen, Y.-M. Wang, and Y.-B. Wei, *QCD calculations of $B \rightarrow \pi, K$*

- form factors with higher-twist corrections, *JHEP* **01** (2019) 024, [[arXiv:1810.00819](#)].
- [108] D. Leljak, B. Melić, and D. van Dyk, *The $\bar{B} \rightarrow \pi$ form factors from QCD and their impact on $|V_{ub}|$* , *JHEP* **07** (2021) 036, [[arXiv:2102.07233](#)].
- [109] B.-Y. Cui, Y.-K. Huang, Y.-L. Shen, C. Wang, and Y.-M. Wang, *Precision calculations of $B_{d,s} \rightarrow \pi, K$ decay form factors in soft-collinear effective theory*, *JHEP* **03** (2023) 140, [[arXiv:2212.11624](#)].
- [110] J. Gao, C.-D. Lü, Y.-L. Shen, Y.-M. Wang, and Y.-B. Wei, *Precision calculations of $B \rightarrow V$ form factors from soft-collinear effective theory sum rules on the light-cone*, *Phys. Rev. D* **101** (2020), no. 7 074035, [[arXiv:1907.11092](#)].
- [111] Y.-M. Wang, Y.-L. Shen, and C.-D. Lu, *$\Lambda_b \rightarrow p, \Lambda$ transition form factors from QCD light-cone sum rules*, *Phys. Rev. D* **80** (2009) 074012, [[arXiv:0907.4008](#)].
- [112] S. Faller, A. Khodjamirian, C. Klein, and T. Mannel, *$B \rightarrow D^{(*)}$ Form Factors from QCD Light-Cone Sum Rules*, *Eur. Phys. J. C* **60** (2009) 603–615, [[arXiv:0809.0222](#)].
- [113] K.-S. Huang, W. Liu, Y.-L. Shen, and F.-S. Yu, *$\Lambda_b \rightarrow p, N^*(1535)$ form factors from QCD light-cone sum rules*, *Eur. Phys. J. C* **83** (2023), no. 4 272, [[arXiv:2205.06095](#)].
- [114] S. Meinel. Private conversation. To appear on arXiv.
- [115] S. Meinel, *Status of next-generation $\Lambda_b \rightarrow p, \Lambda, \Lambda_c$ form-factor calculations*, *PoS LATTICE2023* (2024) 275, [[arXiv:2309.01821](#)].
- [116] F. U. Bernlochner, Z. Ligeti, D. J. Robinson, and W. L. Sutcliffe, *Precise predictions for $\Lambda_b \rightarrow \Lambda_c$ semileptonic decays*, *Phys. Rev. D* **99** (2019), no. 5 055008, [[arXiv:1812.07593](#)].
- [117] R. Dutta, *$\Lambda_b \rightarrow (\Lambda_c, p) \tau \nu$ decays within standard model and beyond*, *Phys. Rev. D* **93** (2016), no. 5 054003, [[arXiv:1512.04034](#)].
- [118] M. Tanaka, *Charged Higgs effects on exclusive semitauonic B decays*, *Z. Phys. C* **67** (1995) 321–326, [[hep-ph/9411405](#)].
- [119] T. Yasmeen, I. Ahmed, S. Shafaq, M. Arslan, and M. J. Aslam, *Probing New Physics in Light of Recent Developments in $b \rightarrow c \ell \nu$ Transitions*, *PTEP* **2024** (2024), no. 7 073B07, [[arXiv:2401.02334](#)].
- [120] **LATTICE-HPQCD** Collaboration, J. Harrison, C. T. H. Davies, and A. Lytle, *$R(J/\psi)$ and $B_c^- \rightarrow J/\psi \ell^- \bar{\nu}_\ell$ Lepton Flavor Universality Violating Observables from Lattice QCD*, *Phys. Rev. Lett.* **125** (2020), no. 22 222003, [[arXiv:2007.06956](#)].
- [121] Y. Grossman and Z. Ligeti, *The Inclusive $\bar{B} \rightarrow \tau \bar{\nu} X$ decay in two Higgs doublet models*, *Phys. Lett. B* **332** (1994) 373–380, [[hep-ph/9403376](#)].
- [122] W. D. Goldberger, *Semileptonic B decays as a probe of new physics*, [hep-ph/9902311](#).

- [123] P. Colangelo and F. De Fazio, *Tension in the inclusive versus exclusive determinations of $|V_{cb}|$: a possible role of new physics*, *Phys. Rev. D* **95** (2017), no. 1 011701, [[arXiv:1611.07387](#)].
- [124] A. Celis, M. Jung, X.-Q. Li, and A. Pich, *Scalar contributions to $b \rightarrow c(u)\tau\nu$ transitions*, *Phys. Lett. B* **771** (2017) 168–179, [[arXiv:1612.07757](#)].
- [125] T. Mannel, A. V. Rusov, and F. Shahriaran, *Inclusive semitauonic B decays to order $\mathcal{O}(\Lambda_{QCD}^3/m_b^3)$* , *Nucl. Phys. B* **921** (2017) 211–224, [[arXiv:1702.01089](#)].
- [126] S. Kamali, A. Rashed, and A. Datta, *New physics in inclusive $B \rightarrow X_c \ell \bar{\nu}$ decay in light of $R(D^{(*)})$ measurements*, *Phys. Rev. D* **97** (2018), no. 9 095034, [[arXiv:1801.08259](#)].
- [127] S. Bhattacharya, S. Nandi, and S. Kumar Patra, *$b \rightarrow c\tau\nu_\tau$ Decays: a catalogue to compare, constrain, and correlate new physics effects*, *Eur. Phys. J. C* **79** (2019), no. 3 268, [[arXiv:1805.08222](#)].
- [128] S. Kamali, *New physics in inclusive semileptonic B decays including nonperturbative corrections*, *Int. J. Mod. Phys. A* **34** (2019), no. 06n07 1950036, [[arXiv:1811.07393](#)].
- [129] M. Fael, M. Rahimi, and K. K. Vos, *New physics contributions to moments of inclusive $b \rightarrow c$ semileptonic decays*, *JHEP* **02** (2023) 086, [[arXiv:2208.04282](#)].
- [130] L.-F. Lai, X.-Q. Li, Y.-Y. Li, and Y.-D. Yang. To appear on arXiv.
- [131] Z. Ligeti and F. J. Tackmann, *Precise predictions for $B \rightarrow X_c \tau \bar{\nu}$ decay distributions*, *Phys. Rev. D* **90** (2014), no. 3 034021, [[arXiv:1406.7013](#)].
- [132] M. Rahimi and K. K. Vos, *Standard Model predictions for lepton flavour universality ratios of inclusive semileptonic B decays*, *JHEP* **11** (2022) 007, [[arXiv:2207.03432](#)].
- [133] R. S. Chivukula and H. Georgi, *Composite Technicolor Standard Model*, *Phys. Lett. B* **188** (1987) 99–104.
- [134] G. D’Ambrosio, G. F. Giudice, G. Isidori, and A. Strumia, *Minimal flavor violation: An Effective field theory approach*, *Nucl. Phys. B* **645** (2002) 155–187, [[hep-ph/0207036](#)].
- [135] V. Cirigliano, B. Grinstein, G. Isidori, and M. B. Wise, *Minimal flavor violation in the lepton sector*, *Nucl. Phys. B* **728** (2005) 121–134, [[hep-ph/0507001](#)].
- [136] W. Dekens and P. Stoffer, *Low-energy effective field theory below the electroweak scale: matching at one loop*, *JHEP* **10** (2019) 197, [[arXiv:1908.05295](#)]. [Erratum: *JHEP* **11**, 148 (2022)].
- [137] E. E. Jenkins, A. V. Manohar, and P. Stoffer, *Low-Energy Effective Field Theory below the Electroweak Scale: Anomalous Dimensions*, *JHEP* **01** (2018) 084, [[arXiv:1711.05270](#)]. [Erratum: *JHEP* **12**, 042 (2023)].
- [138] L. Naterop and P. Stoffer, *Low-energy effective field theory below the electroweak*

- scale: one-loop renormalization in the 't Hooft-Veltman scheme, *JHEP* **02** (2024) 068, [[arXiv:2310.13051](#)].
- [139] J. M. Gerard, *FERMION MASS SPECTRUM IN $SU(2)_L \times U(1)$* , *Z. Phys. C* **18** (1983) 145.
- [140] A. Greljo, J. Salko, A. Smolkovič, and P. Stangl, *SMEFT restrictions on exclusive $b \rightarrow ul\nu$ decays*, *JHEP* **11** (2023) 023, [[arXiv:2306.09401](#)].
- [141] J. Ellis, C. W. Murphy, V. Sanz, and T. You, *Updated Global SMEFT Fit to Higgs, Diboson and Electroweak Data*, *JHEP* **06** (2018) 146, [[arXiv:1803.03252](#)].
- [142] S. Dawson and P. P. Giardino, *Electroweak and QCD corrections to Z and W pole observables in the standard model EFT*, *Phys. Rev. D* **101** (2020), no. 1 013001, [[arXiv:1909.02000](#)].
- [143] A. Efrati, A. Falkowski, and Y. Soreq, *Electroweak constraints on flavorful effective theories*, *JHEP* **07** (2015) 018, [[arXiv:1503.07872](#)].
- [144] **ATLAS** Collaboration, G. Aad et al., *Search for heavy Higgs bosons decaying into two tau leptons with the ATLAS detector using pp collisions at $\sqrt{s} = 13$ TeV*, *Phys. Rev. Lett.* **125** (2020), no. 5 051801, [[arXiv:2002.12223](#)].
- [145] **CMS** Collaboration, A. Tumasyan et al., *Searches for additional Higgs bosons and for vector leptoquarks in $\tau\tau$ final states in proton-proton collisions at $\sqrt{s} = 13$ TeV*, *JHEP* **07** (2023) 073, [[arXiv:2208.02717](#)].
- [146] L. Allwicher, D. A. Faroughy, F. Jaffredo, O. Sumensari, and F. Wilsch, *Drell-Yan tails beyond the Standard Model*, *JHEP* **03** (2023) 064, [[arXiv:2207.10714](#)].
- [147] R. Barbieri, G. Isidori, J. Jones-Perez, P. Lodone, and D. M. Straub, *$U(2)$ and Minimal Flavour Violation in Supersymmetry*, *Eur. Phys. J. C* **71** (2011) 1725, [[arXiv:1105.2296](#)].
- [148] R. Barbieri, D. Buttazzo, F. Sala, and D. M. Straub, *Flavour physics from an approximate $U(2)^3$ symmetry*, *JHEP* **07** (2012) 181, [[arXiv:1203.4218](#)].
- [149] G. Blankenburg, G. Isidori, and J. Jones-Perez, *Neutrino Masses and LFV from Minimal Breaking of $U(3)^5$ and $U(2)^5$ flavor Symmetries*, *Eur. Phys. J. C* **72** (2012) 2126, [[arXiv:1204.0688](#)].
- [150] L. Allwicher, C. Cornella, G. Isidori, and B. A. Stefanek, *New physics in the third generation. A comprehensive SMEFT analysis and future prospects*, *JHEP* **03** (2024) 049, [[arXiv:2311.00020](#)].
- [151] D. Aloni, A. Efrati, Y. Grossman, and Y. Nir, *Υ and ψ leptonic decays as probes of solutions to the $R_D^{(*)}$ puzzle*, *JHEP* **06** (2017) 019, [[arXiv:1702.07356](#)].
- [152] **BaBar** Collaboration, J. P. Lees et al., *Precision measurement of the $\mathcal{B}(\Upsilon(3S) \rightarrow \tau^+\tau^-)/\mathcal{B}(\Upsilon(3S) \rightarrow \mu^+\mu^-)$ ratio*, *Phys. Rev. Lett.* **125** (2020) 241801, [[arXiv:2005.01230](#)].
- [153] M. González-Alonso, J. Martin Camalich, and K. Mimouni, *Renormalization-group*

- evolution of new physics contributions to (semi)leptonic meson decays*, *Phys. Lett. B* **772** (2017) 777–785, [[arXiv:1706.00410](#)].
- [154] B. Grinstein, X. Lu, L. Merlo, and P. Quilés, *Hilbert series for covariants and their applications to minimal flavor violation*, *JHEP* **2024** (2024) 154, [[arXiv:2312.13349](#)].
- [155] B.-F. Hou, X.-Q. Li, M. Shen, Y.-D. Yang, and X.-B. Yuan, *Deciphering the Belle II data on $B \rightarrow K\nu\bar{\nu}$ decay in the (dark) SMEFT with minimal flavour violation*, *JHEP* **06** (2024) 172, [[arXiv:2402.19208](#)].
- [156] J. Fuentes-Martín, G. Isidori, J. Pagès, and K. Yamamoto, *With or without $U(2)$? Probing non-standard flavor and helicity structures in semileptonic B decays*, *Phys. Lett. B* **800** (2020) 135080, [[arXiv:1909.02519](#)].